NOTE TO USERS

Université d'Ottawa · University of Ottawa

Université d'Ottawa · University of Ottawa

FACULTÉ DES ÉTUDES SUPÉRIEURES ET POSTDOCTORALES

FACULTY OF GRADUATE AND POSTDOCTORAL STUDIES

Sherine RAHAL

AUTEUR DE LA THÈSE - AUTHOR OF THESIS

M. Sc. (Cellular and Molecular Medicine)

GRADE - DEGREE

Department of Cellular and Molecular Medicine

FACULTÉ, ÉCOLE, DÉPARTEMENT - FACULTY, SCHOOL, DEPARTMENT

TITRE DE LA THÈSE - TITLE OF THE THESIS

The Role of Prostaglandin EP Receptors in a Model of Glomerulonephritis

C. Kennedy

DIRECTEUR DE LA THÈSE - THESIS SUPERVISOR

CO-DIRECTEUR DE LA THÈSE - THESIS CO-SUPERVISOR

EXAMINATEURS DE LA THÈSE - THESIS EXAMINERS

S. Gee

R. Hebert

J.-M. De Koninck, Ph.D.

LE DOYEN DE LA FACULTÉ DES ÉTUDES SUPÉRIEURES ET POSTDOCTORALES

DEAN OF THE FACULTY OF GRADUATE AND POSTDOCTORAL STUDIES

THE ROLE OF PROSTAGLANDIN EP RECEPTORS IN A MODEL OF GLOMERULONEPHRITIS

Sherine S. Rahal

Thesis submitted to the Department of Cellular and Molecular Medicine in partial fulfillment of the requirements for the degree of Master of Science

Faculty of Medicine
University of Ottawa
Ottawa, Ontario, Canada
August 2004

Your file Votre référence
ISBN: 0-494-01585-3
Our file Notre référence
ISBN: 0-494-01585-3

ABSTRACT

Prostaglandin E_2 (PGE_2) interacts with four E-Prostanoid (EP) receptor subtypes - designated EP_{1-4}. In glomerulonephritis (GN), a renal inflammatory disease, inhibition of enhanced renal PGE_2 synthesis by nonsteroidal-anti-inflammatory drugs (NSAIDs), results in both beneficial anti-proteinuric effects and deleterious side effects on renal blood flow (RBF) and Na^+ homeostasis, implying that one or more EP subtypes may mediate these actions. We set out to investigate the role of the EP_1 receptor in GN since it localizes to the collecting duct, where it may regulate Na^+ homeostasis, in podocytes and mesangial cells, where it could alter the permeability of the glomerulus, and in arterioles, where EP_1 receptors may induce vasoconstriction thereby reducing RBF. A mouse model of GN was induced in wildtype (wt) and $EP_1^{-/-}$ mice using an anti-rat-glomerular basement membrane (anti-GBM) antibody. Proteinuria was similar in GN wt and GN EP $_1^{-/-}$ groups thereby negating a role for this subtype in modulating filtration barrier permeability. However, the severity of renal impairment was more profound in GN EP $_1^{-/-}$ mice as compared to GN wt animals, as serum creatinine, urea, and K^+ levels were each significantly greater in GN EP $_1^{-/-}$ mice. GN $EP_1^{-/-}$ mice exhibited higher cortical EP_4 receptor mRNA expression levels (a subtype that promotes afferent vasodilatation) compared to GN wt mice, suggesting that this subtype might temper reduced RBF in GN. In contrast, GN wt but not GN $EP_1^{-/-}$ mice exhibited elevated EP_4 receptor mRNA levels in the papilla (where it contributes to water reabsorption) being reflected in a more

pronounced reduction in urine osmolality and greater body weight loss for GN $EP_1^{-/-}$ mice. Increased severity of renal impairment seen in GN $EP_1^{-/-}$ mice suggests that the EP_1 receptor subtype tempers GN progression, and that it may be a downstream target of NSAID-induced renal side effects manifested during the course of this disease.

DEDICATION

To my parents, Samih and Thérèse, my brother and sisters,
Nissreen, Ramsey, Rana, and Lara and also to my dear friends whose support,
interest and enthusiasm has motivated me to do my best.

ACKNOWLEDGMENTS

I would like to thank my supervisor Dr. Chris Kennedy for his ongoing support, advice, and encouragement throughout my research. I could not have been more fortunate in finding such a mentor. Thank you.

In addition, I am grateful to Dr. Richard Hébert and Dr. William Staines for serving as members of my advisory committee. Their insightful suggestions were valuable in helping to focus my research.

Also, a special thanks to Dr. Wissam Faour, Jean-Louis Michaud and Lyne McVeigh, whose assistance was deeply appreciated and whose presence in the lab made the work more enjoyable.

I would also like to thank the Animal Care staff, especially Kim and Eileen for their individual help.

Finally, I would like to thank the entire Kidney group for their ongoing support.

DECLARATION

I certify that this thesis does not incorporate without acknowledgement any material previously submitted for a degree in any university. To the best of my knowledge this thesis does not contain material previously written by another except where due reference is made in the text.

I authorize the University of Ottawa to reproduce this thesis in whole or in part at the request of another institution for the purpose of academic research.

Shérine S. Rahal

TABLE OF CONTENTS

LIST OF FIGURES

LIST OF TABLES

LIST OF ABBREVIATIONS

AA	arachidonic acid
ACE	angiotensin-converting enzyme
AChE	aldosterone-acetylcholinesterase
ADH	antidiuretic hormone
Ang	angiotensin
ANOVA	ANalysis Of VAriance
ANP	atrial natriuretic peptide
AQP2	aquaporin-2
AVP	arginine vasopressin
BP	blood pressure
°C	degree celsius
cAMP	cyclic adenosine monophosphate
COX	cyclooxygenase
cPLA2	cytoplasmic phospholipase A2
Cr	creatinine
CT	threshold cycle
ECFV	extracellular fluid volume
EIA	enzyme immunoassays
ELISA	enzyme-linked immunoassay
EP	E-Prostanoid

$EP_1^{-/-}$	EP_1 knockout
$EP_2^{-/-}$	EP_2 knockout
$EP_3^{-/-}$	EP_3 knockout
$EP_4^{-/-}$	EP_4 knockout
ESRD	end stage renal disease
FITC	fluorescein isothiocyanate
FSGS	focal segmental glomerular sclerosis
g	gram
GAPDH	glyseraldehyde-3-phosphate dehydrogenase
GBM	glomerular basement membrane
GFR	glomerular filtration rate
G_i	inhibitory G protein
GN	glomerulonephritis
G-Protein	guanine nucleotide binding proteins
GPCR	G- protein coupled receptor
G_s	stimulatory G protein
H&E	hematoxylin and eosin
HRP	horse radish peroxidase
Hrs	hours
HS	high salt
IL-1	interleukin-1
IM	inner medullary
JGA	juxtaglomerular apparatus

L	liter
log	logarithm
LPS	lipopolysaccharide
LS	low salt
mg	milligram
min	minute
ml	milliliter
mmHg	millimeters of mercury
mmol	millimolar
mRNA	messenger ribo-nucleic acid
Mx1-Cre	myxovirus resistance-1-Cre
nm	nanometer
NSAIDs	non-steroidal anti-inflammatory drugs
OM	outer medullary
PAS	periodic acid schiff
PBS	phosphate buffered saline
PFA	paraformaldeyde
pg	picograms
PGD_2	prostaglandin D_2
PGE_2	prostaglandin E_2
PGF_{2_α}	prostaglandin F_{2_α}
PGG	prostaglandin G
PGH_2	prostaglandin H_2

RBF	renal blood flow
rpm	revolutions per minute
RT-PCR	reverse transcription-polymerase chain reaction
sec	second
S.E.M	standard error mean
SDS	sodium dodecyl sulphate
TxA_2	thromboxane A_2
µg	microgram
µl	microlitier
µm	micrometer
µmol	micromolar
WD	water deprived
wt	wild type

1 INTRODUCTION

Over a century ago the French physiologist Claude Bernard (1813-1878) first proposed that cells of multicellular organisms flourish because they live in the relative constancy of "*le milieu interieur*" (the internal environment) despite changing conditions in the external environment. The ability of cells, tissues and organs to maintain an internal balance (that is, *homeostasis*) is achieved, in part, through communication by auto-, para –, and endocrine signaling.

The kidney (Figure 1.1) is one such organ that contributes to the regulation of the internal environment. This complex collection of tissue and cells is responsible for regulating blood pressure, extracellular fluid volume as well as its electrolyte composition in a way that can be adjusted according to the body's needs. Homeostasis is maintained in large part through the kidney's functional units known as nephrons (Figure 1.1). Each kidney contains on average, 1-1.5 million nephrons. Blood vessels and nephrons are organized in such a way to facilitate secretion and reabsorption of key plasma constituents – including glucose, sodium, chloride, urea, potassium etc. These small tubular structures are composed of a renal corpuscle, where blood is filtered, and a renal tubule into which the filtrate passes.

1.1 THE NEPHRON

1.1.1 The Renal Corpuscle

The renal corpuscle consists of the glomerulus and Bowman's capsule (Figure 1.1). Bowman's capsule is an epithelial cup that surrounds the glomerulus. During filtration, blood entering through the afferent arteriole is filtered by the glomerulus to produce an ultrafiltrate of renal plasma that flows into Bowman's space and then into the proximal tubule.

The glomerulus (Figure 1.1) consists of several components that work together to form a molecular sieve to restrict the passage of large molecular weight proteins. Between the capillary loops are mesangial cells and extracellular matrix. Mesangial cells have contractile properties believed to play a role in the regulation of glomerular filtration that may modulate blood flow through each capillary (78). These cells also exhibit phagocytic properties and participate in the clearance of macromolecules from the mesangium (57).

The innermost layer consists of fenestrated endothelial cells. They form the initial barrier between the capillary lumen and Bowman's space. Under normal conditions, the cellular elements of blood, including erythrocytes, leukocytes, and platelets, do not gain access to the Bowman's space. The endothelial cells are attached to the glomerular basement membrane (GBM). The GBM possess fixed, negatively charged sites that influence the filtration of macromolecules. Caulfield and

Farquhar demonstrated that when dextrans of different molecular weights were infused into rats, filtration depended on the size of the molecule and that the basement membrane was the main barrier to filtration (19). The GBM is a meshwork of type IV collagen, laminin and fibronectin as well as a number of negatively charged heparin sulfate proteoglycans. Collagen IV is the major constituent and mutations in the isomeric chains, specifically the $\alpha 3$, $\alpha 4$, and $\alpha 5$ cause glomerular disorders, such as Alport Syndrome (43). The outermost layer of the glomerular capillary is covered with epithelial cells, known as podocytes. Podocytes are highly specialized cells equipped with a complex cellular architecture which enables them to contribute to the formation of the final barrier to protein (Figure 1.2). In particular, podocyte differentiation results in cells extending numerous foot processes that establish filtration slits to restrict the passage of large proteins (> 70kD) in the glomerulus. Each foot process is attached to its neighbor along its length by an intercellular adherens-type junction modified for filtration (the slit diaphragm). A specialized cytoskeleton is necessary for maintaining proper morphology of each podocyte. Highly organized arrays of intermediate filaments, actin filaments and microtubule processes work together to provide the scaffolding needed for the formation of the extracellular slit pores through which filtration occurs.

Acting in concert, the endothelial cells of the glomerular capillaries, the GBM and podocytes form the filtration barrier responsible for producing a protein-free ultrafiltrate of renal plasma. Importantly, a nearly protein-free ultrafiltrate passes into the Bowman's capsule from the glomerular capillaries and enters the proximal tubule.

Figure 1.1 The Kidney, Nephron and Glomerulus

Illustration of the human kidney with an enlarged nephron and a glomerulus (From: Somso Modelle, Directed Learning, Elora, ON)

Glomerulus:

1. Proximal tubule
2. Afferent arteriole
3. Efferent arteriole
4. Glomerulus
5. Distal tubule
6. Juxtaglomerular cells
7. Macula densa
8. Mesangial region
9. Bowmans Capsule

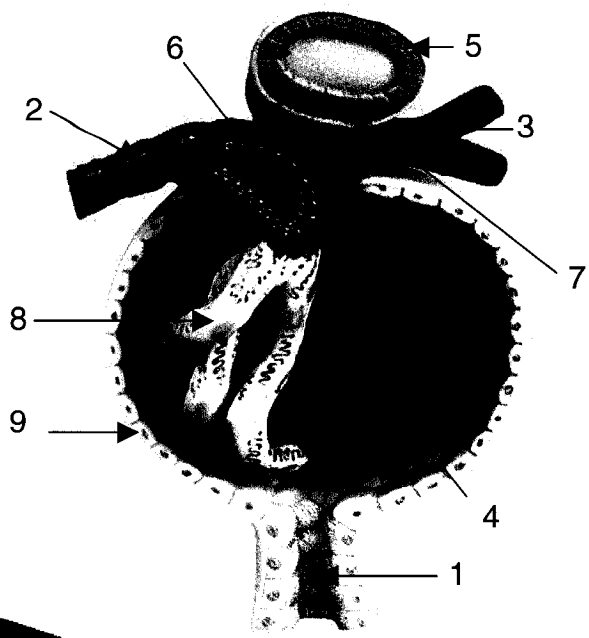

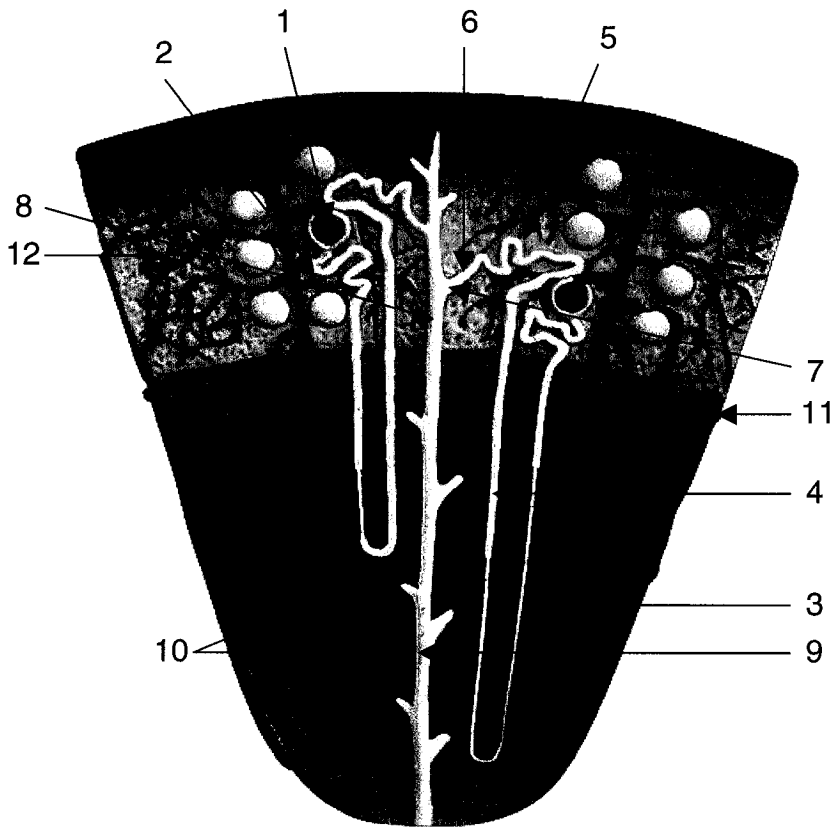

Nephron:

1. Glomerulus
2. Proximal tubule
3. Thin ascending limb of Henle's loop
4. Thick ascending limb
5. Distal convoluted tubule
6. Connecting tubule
7. Initial collecting tubule
8. Cortical collecting duct
9. Medullary collecting duct
10. Vasa recta
11. Arcuate vessels
12. Interlobular vessels

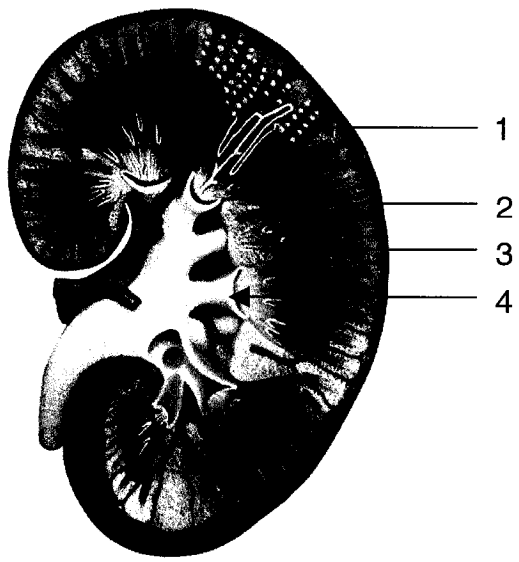

Kidney:

1. Cortex
2. Outer medulla
3. Inner medulla
4. Papilla

Figure 1.2 The Podocyte

Scanning electron microscope image of a podocyte cell embracing the capillary of the glomerulus. The main cell body (P) sends off primary processes (1), which in turn send off secondary processes (2) which interdigitate with similar foot processes of neighboring podocytes (arrow). Magnification ~ 6000X.

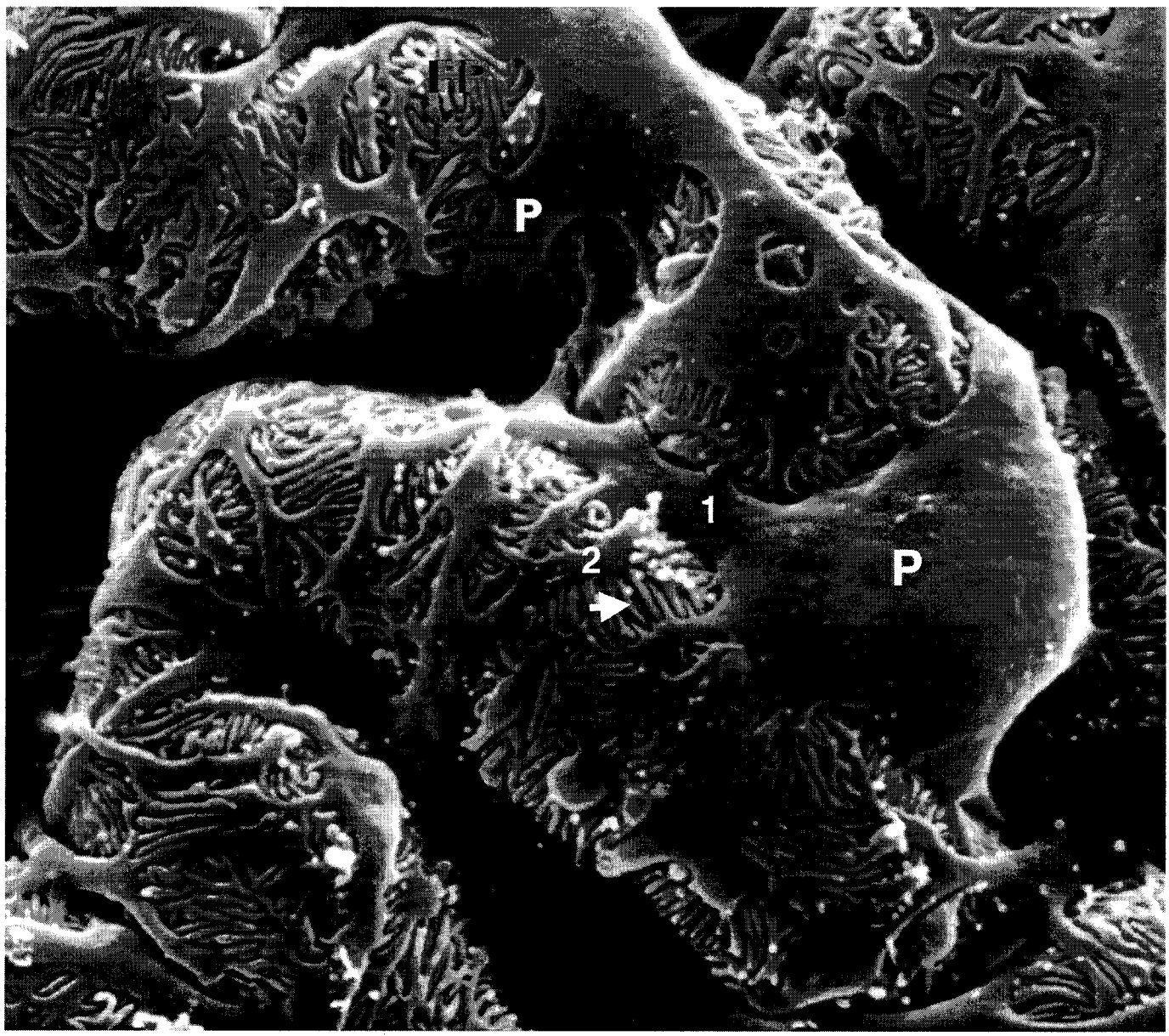
P
1
2
P

1.1.2 Glomerular Filtration Rate

Glomerular function may be assessed on the basis of the kidney's ability to filter the waste products and to retain essential macromolecules such as plasma proteins. In humans, the average glomerular filtration rate (GFR) is 180L/day. Homeostasis of body fluids requires that the kidneys maintain a constant GFR. A high GFR may cause key substances to pass too quickly through the renal tubules resulting in their loss in the urine. A low GFR will cause much of the filtrate to be reabsorbed, without adequately excreting toxic waste products.

There are two main mechanisms that directly regulate GFR. First, adjusting blood flow through the glomerulus; and second, altering the glomerular capillary surface area available for filtration. GFR is elevated as renal blood flow through the glomerular capillaries increases. A coordinated control of diameter between the afferent and efferent arterioles finely regulates the passage of blood flow. The tone of the afferent arterioles can be modulated by a number of factors, such as nitric oxide, prostaglandins and angiotensin II (Ang II). Ang II, a potent vasoconstrictor of the afferent arteriole is regulated by renin release from the granular cells of the juxtaglomerular apparatus (JGA). Under circumstances of reduced renal perfusion brought about by renal disease, reduced blood volume or reduced blood pressure, renin release by the JGA is stimulated where it acts on angiotensinogen to form angiotensin I (Ang I). Angiotensin converting enzyme (ACE) in turn will convert Ang I to Ang II. The vasoconstrictive actions of Ang II are of great significance in the renal vasculature as well at the peripheral vasculature, where its actions have been

linked to elevations in blood pressure (70). Prostaglandins have been shown to have both vasoconstrictive and vasodilatory effects on the renal vasculature (37).

1.1.3 Renal Tubule

The renal tubule can be grossly divided into four segments: the proximal tubule, the loop of Henle, the distal convoluted tubule and the collecting duct. Together, these segments maintain electrolyte homeostasis by promoting reabsorption and secretion of fluid, electrolytes and other key molecules required for homeostasis.

The proximal tubule begins at the pole of the glomerulus. It possesses a system of channels and pumps which direct transport of molecules from the lumen to the basolateral side where they are taken up by the circulation. These channels have been shown to be responsible for the bulk of solute reabsorption. This includes, NaCl, H_2O, glucose, amino acids, protein and bicarbonate. The proximal tubule however, is also the only site of organic acid secretion.

The transition from the proximal tubule to the descending limb of the loop of Henle occurs quite suddenly. The limbs of the loop of Henle play an important role in the countercurrent multiplication process that is responsible for the maintenance of a hypertonic medullary interstitium and for the dilution and concentration of the urine. The loop of Henle can be subdivided into 3 portions: (1) the descending thick limb; (2) the thin loop and (3) the ascending thick limb. The descending thick limb is a straight continuation of the proximal tubule which is permeable to water. This is

followed by the thin ascending limb which is relatively impermeable to water but highly permeable to sodium and urea. The thin loop turns back towards the cortex and is continuous with the ascending thick limb of Henle's loop. The cells of the ascending thick limb are also impermeable to water and urea, but do actively transport sodium, chloride and potassium which creates a dilute luminal fluid, while generating a high osmolality within the renal medullary interstitium. Subsequently, as the tubular fluid flows through the distal convoluted tubule its osmolality progressively decreases since the walls of the limbs are virtually impermeable to water. By the time the fluid reaches the end of the distal convoluted tubule, 95% of the filtered solutes and water have been reabsorbed.

The transition from the distal convoluted tubule to the collecting duct is gradual. There are two cell types that make up the collecting duct: principal and intercalated cells. Intercalated cells are key sites in acid base regulation, whereas the principal cells are the main site of salt and water transport. The principal cells (Figure 1.3) contain epithelial sodium channels (eNaC) localized at the apical side to allow the reabsorption of sodium from the lumen. Intracellular sodium levels remain low (intracellular: 12 mEq/L vs. plasma: 143mEq/L) because the sodium/potassium ATPase actively pumps Na^+ across the basolateral membrane. This causes a lumen-negative potential difference which facilitates the escape of potassium from the principal cells. As a result, intracellular K^+ concentration (intracellular: 140 mEq/L vs. plasma: 5 mEq/L) levels remain high.

Aldosterone promotes Na^+ and water reabsorption and K^+ secretion by the principal cells. Upon binding to its receptor, it enhances the activity and insertion of existing sodium channels into the luminal membrane, while driving the synthesis of new channels and pumps. Several factors control the release of aldosterone from the adrenal cortex, including Ang II, adrenocorticotropic hormone (ACTH) and increased plasma K^+ concentrations. As a consequence increased distal tubular K^+ secretion occurs, returning the plasma K^+ concentration to normal levels.

In addition to aldosterone, Ang II, arginine vasopressin (AVP) and atrial natriuretic peptide (ANP), have important roles in regulating water and electrolyte composition. Ang II affects the kidney by enhancing Na^+, Cl^- , and water reabsorption in the proximal convoluted tubule by stimulating Na^+/H^+ antiporters. Ang II stimulates the release of aldosterone as well as AVP. AVP regulates water reabsorption by increasing the permeability of principal cells by promoting the insertion of aquaporin-2 (AQP2) water channels into the apical membrane. In contrast to the function of AVP, ANP inhibits the reabsorption of Na^+ and water in the collecting duct and suppresses the secretion of AVP and aldosterone. As the tubular fluid flows through the collecting duct it passes through the papillary region and collects within the papillary duct. The final fine tuning of tubular fluid osmolality occurs in this region of the kidney.

The kidney has a remarkable ability to dilute or concentrate urine, according to the organism's changing physiological needs. Impaired renal function has adverse effects on removal of metabolic waste products, blood pressure, fluid balance,

nutrient retention, each of which greatly impact upon an organism's general state of health.

1.2 GLOMERULONEPHRITIS

Disease processes that damage the kidney have a significant impact upon glomerular filtration and renal tubular reabsorption and secretion. These diseases, classified as nephropathies, are brought about by a number of etiologies of both primary and secondary origin. Examples of such diseases include focal (not all glomeruli are affected) and segmental (only a part of each glomerulus is damaged) glomerulosclerosis (FSGS), diabetic nephropathy and glomerulonephritis (GN). GN is a common autoimmune renal disorder, which makes up 10-15% of all cases with end-stage renal disease (ESRD) (49). This inflammatory condition is characterized by haematuria (blood in the urine), proteinuria, hyperkalemia, and reduced GFR occasionally associated with hypertension, and edema (83). The pathology involves glomerular inflammation and cellular proliferation (83) . The term GN defines a group of kidney diseases which include membranous GN, IgA nephropathy, membranoproliferative GN, post-infectious GN, and anti-GBM disease.

1.2.1 Anti-GBM Disease

Anti-GBM disease is a well chacracterized variant of GN. Patients produce antibodies against the α3 chain of type IV collagen found in the GBM (68). Anti-GBM disease has an estimated incidence of one case per 2 million per year in

European Caucasoid populations (49). The disease occurs across all racial groups and all ages, however, its incidence peaks in the third decade of young men with a second peak in the sixth to seventh decades affecting men and woman equally (49). In addition to the elevated serum creatinine levels, haematuria, proteinuria and hypertension, patients have reduced renal blood flow (RBF). Significant reductions in RBF seems to be due to predominant afferent arteriolar vasoconstriction, with subsequent reduction in renal perfusion pressure and GFR. Patients initially demonstrate sodium retention with a low fractional excretion of sodium. With clinical progression of the disease however, sodium wasting with high fractional excretion is observed (48). This may likely be due to the onset of tubular damage initiated by the abnormally high albumin levels within the luminal fluid. Further reductions in GFR alter the rate by which Na^+ and K^+ are transported. Thus, many patients with this renal disorder present with hyperkalemia.

Histology may show glomerular necrosis and inflammation. Inflammation is initiated at the level of the glomerulus by immunologic reactants that trigger the synthesis of secondary mediators (49). Rapid glomerular neutrophil infiltration accompanied by complement activation, leukotriene synthesis and generation of oxygen radicals predominates during the early phase of inflammation (59). The inflammatory process activates podocyte phospholipase A2 and cyclooxygenase isoforms (COX), resulting in the formation of prostaglandins (PG) (Figure 1.4). Elevated PG synthesis can induce many of the major pathophysiologic events that characterize the inflammatory process.

Figure 1.3 Na^+ and K^+ Transport in the Principal Cell

Illustration represents the reabsorption of Na^+ and secretion of K^+ by principal cells in the collecting duct. Na^+ passes through the apical membrane via Na^+ channels and is then actively transported through the basolateral membrane in exchange for K^+ by the Na^+/K^+ ATPase pump. Positively charged K^+ is secreted to the apical side by K^+ leakage channels.

APICAL BASOLATERAL

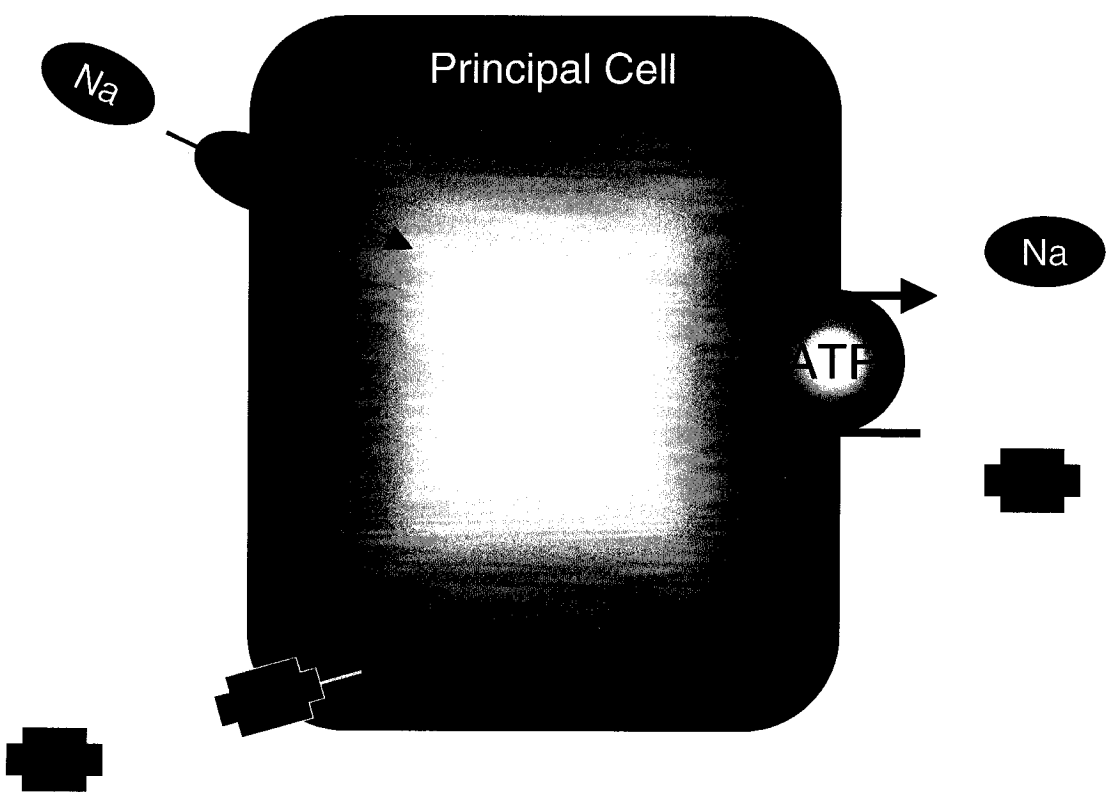

1.2.2 Glomerulonephritis and NSAIDs

Indirect evidence that the arachidonate pathway may play a critical role in glomerulonephritis comes from clinical and experimental observations. Arisz et al. have demonstrated that the urinary protein excretion rate is reduced by treatment with nonsteroidal anti-inflammatory drugs (NSAIDs) such as aspirin and indomethacin, which block prostaglandin synthesis (3). The mechanism by which this anti-proteinuric process occurs is currently unknown. However, NSAID use is precluded in many glomerular diseases due to their renal side effects, which include alterations of sodium homeostasis, hyperkalemia, and reduced RBF/GFR brought about by unopposed renal vasoconstriction, and which can exacerbate renal failure and aggravate preexisting hypertension.

1.3 THE ARACHIDONIC ACID CASCADE

NSAIDs target the COX enzymes, which mediate prostaglandin synthesis from arachidonic acid. Previous studies have demonstrated important physiological roles for one such PG – PGE_2, acting through its four E Prostanoid (EP) receptors ($EP_{1\text{-}4}$) in maintaining vascular tone, fluid and electrolyte balance and blood pressure. However the renal correlates of these observations remain poorly defined within the context of GN. Depending on the site of action and the specific EP receptor(s) involved, the production of PGE_2 might be either contributing to, or preventing the

adverse effects observed in GN. Thus, it is important to define actions of individual receptors under GN conditions.

Synthesis of prostanoids (Figure 1.4) by the COX isoforms is dependent upon the availability of its arachidonic acid (AA) substrate. In response to specific stimuli, elevation in intracellular calcium concentration causes cytosolic phospholipase A_2 ($cPLA_2$) to translocate from the cytosol to the phospholipid membrane of the endoplasmic reticulum in order to release AA from membrane phospholipids. Upon release, COX isoforms catalyze the conversion of AA to prostaglandin G/H_2 (PGG/H_2) to provide substrate for generating five bioactive prostanoids: PGI_2, PGE_2, $PGF_{2\alpha}$, PGD_2, and thromboxane A_2 (TxA_2) (14). These prostanoids are abundantly produced in the kidney, where they act locally through specific transmembrane G protein-coupled receptors designated EP, FP, DP, IP, and TP, respectively (14). Each prostanoid receptor exhibits a unique expression pattern within the kidney.

1.4 THE FUNCTION OF PGE_2 RECEPTORS

PGE_2 is a major product of COX-initiated arachidonic acid metabolism in the kidney and is synthesized at high levels within the glomerulus and along the nephron. Its production is crucial to maintenance of normal kidney function through events including constriction/relaxation of smooth muscle and blood vessels (73). In the kidney it dilates the glomerular microcirculation (62, 73), and regulates salt/water transport in the collecting duct (33). The signaling mechanisms by which PGE_2 mediates its effects are transmitted through the four G-protein coupled EP receptors,

designated EP_1, EP_2, EP_3 and EP_4 (Figure 1.5). The EP_2 and EP_4 receptors promote the activation of adenylate cyclase through a stimulatory G-protein (G_s). Conversely, Gq couples the EP_1 receptor to increases of intracellular Ca^{2+}. Lastly, the EP_3 receptor inhibits adenylate cyclase through a G_i (inhibitory G-protein) protein. The intrarenal distribution and function of EP receptors have only been partially characterized.

1.4.1 The EP_1 Receptor

The EP_1 receptor was originally described as a smooth muscle constrictor found predominantly in the kidney, gastric muscularis mucosae, and adrenal gland (20, 84). Furthermore, EP_1 selective antagonists, such as AH-6809, SC-19220, and SC-53122, have suggested that the EP_1 receptor plays an important role in prostaglandin–mediated pain (15). These antagonists could be useful tools to study the role of the EP_1 receptor; unfortunately, they're not absolutely selective and may thus block other eicosanoid receptors at high concentrations. The generation of a mouse model lacking the EP_1 receptor subtype has provided useful information regarding the role of this receptor. Studies by Stock and colleagues, demonstrated that $EP_1^{-/-}$ mice have reduced pain-sensitivity responses and exhibit hypotension, supporting a role for this receptor in regulating pain perception and maintaining blood pressure (77).

Within the kidney, *in situ* hybridization studies localized EP_1 receptor mRNA primarily in the collecting duct with increasing expression from the cortex to the papilla (15). Activation of the EP_1 receptor increases intracellular calcium levels and inhibits Na^+ reabsorption in the isolated perfused rabbit collecting duct suggesting that renal EP_1 receptors may contribute to diuretic and natriuretic effects of PGE_2 (30). Conversely, $EP_1^{-/-}$ mice fed a low sodium diet experienced extracellular fluid volume (ECFV) loss, which the authors interpret to imply that these animals may have a reduced ability to reabsorb Na^+ (77), however direct evidence to prove this hypothesis is lacking.

The EP_1 receptor may also have a role in glomerular function. Recent studies have detected the EP_1 receptor in podocytes (10) where it might be involved in regulating the permeability barrier during podocyte injury. Expression has also been detected in cultured glomerular mesangial cells (39) were it may play a role as a vasoconstrictor. Finally, Purdy and colleagues demonstrated that PGE_2 stimulated-EP_1 receptor, localized in glomerular blood vessels, can produce transient vasoconstriction (62).

Studies have also implicated the EP_1 receptor in mediating changes during the progression of certain renal disorders. Specifically, an EP_1 antagonist significantly reduced both proteinuria and glomerular lesions in two separate rat models of hypertension and diabetes suggesting that the EP_1 receptor contributes to the progression of renal injury (55, 80).

1.4.2 The EP_2 Receptor

Prior to 1995, the EP_4 receptor was misclassified as the EP_2 receptor (63). The EP_2 receptor is pharmacologically defined as being sensitive to the PGE_2 analogue, butaprost (45). Northern blot analysis revealed EP_2 receptor mRNA expression to be high in the uterus, lung and spleen, with only low levels of expression in the kidney (thought to be mainly vasculature) (45). However, significant expression is found in macrophages (44) and neutrophils (85) that are known to infiltrate the kidney under GN conditions. The cAMP activation associated with this receptor helps mediate the relaxation of smooth muscle induced by PGE_2 (63). Studies by Kennedy et al. using female knockout mice demonstrated reduced litter size suggesting a critical role for the EP_2 receptor in ovulation and fertilization (47). Furthermore, loss of the EP_2 receptor may be involved in salt-sensitive hypertension suggesting an import role in protecting systemic blood pressure, likely through its vasodilator effects on salt excretion (47).

1.4.3 The EP_3 Receptor

The EP_3 receptor generally acts a constrictor of smooth muscle (21). Northern blotting localized its expression to the kidney, uterus, adrenal gland, and stomach (50). This receptor is unique in that it has multiple splice variants encoding proteins with predicted molecular masses ranging from 35 to 40 kDa. The EP_3 receptor is also

known to mediate the pyretic effects of PGE_2 (81). In $EP_3^{-/-}$ mice, neither PGE_2, interleukin (IL-1), or lipopolysaccharide (LPS) could generate a febrile response (81).

In the kidney, *in situ* hybridization localized abundant EP_3 receptor mRNA expression in the thick ascending limb and collecting duct where PGE_2 inhibits salt and water absorption (1, 74). This mechanism is highlighted by studies showing that NSAIDs transiently enhance urine concentration (1). It is likely that PGE_2 – mediated antagonism of vasopressin– stimulated salt reabsorption in the thick ascending limb and water absorption in the collecting duct contributes to such diuretic effects. Based on these studies, one would expect that $EP_3^{-/-}$ mice would exhibit enhanced urine concentration. However, this was not the case. Fleming and colleagues demonstrated that AVP-treated $EP_3^{-/-}$ mice exhibited similar urinary concentrations to that of wt mice (25, 36). These findings suggest that the renal actions normally mediated by the EP_3 may have been taken over by other receptors (such as the EP_1). However, this concept remains untested.

1.4.4 The EP_4 Receptor

Like the EP_2 receptor, ligand bound EP_4 receptors promote cAMP generation (17). The EP_4 receptor may be pharmacologically distinguished from the EP_1 and EP_3 receptors by its insensitivity to sulprostone and from EP_2 receptors by its insensitivity to butaprost (36). The EP_4 receptor is more highly expressed and more widely distributed than the EP_2 receptor. Northern blot analysis revealed EP_4 receptor mRNA expression in the thymus, ileum, lung, spleen, adrenal gland and kidney (18).

Targeted deletion of the EP_4 receptor shows that its expression is crucial for the perinatal closure of the pulmonary ductus arteriosus (60). Interestingly, when bred on to a mixed genetic background, 80% of the $EP_4^{-/-}$ mice died compared to 100 % on a pure background. Preliminary studies from the survivors of the colony support an important role for the EP_4 receptor as a systemic vasodilator (5).

Intrarenal EP_4 receptors are expressed in the collecting duct, the glomerulus, including mesangial cells and podocytes, and vascular tissue (10, 18, 44, 62). Using cultured mesangial cells, PGE_2 stimulation caused relaxation, likely mediated by the EP_4 receptor (39). RT-PCR studies have also localized the EP_4 receptor to podocytes (10) and as such may regulate the filtration barrier. Currently, direct evidence for such a role is lacking. Furthermore, the role of collecting duct EP_4 receptors can only be implied by data showing that PGE_2 stimulates water reabsorption in isolated rabbit collecting ducts in a cAMP-dependent manner (67, 74).

Purdy and colleagues detected the EP_4 receptor, but not the EP_2 receptor, in preglomerular vessels, thereby suggesting a role for the EP_4 receptor in mediating vasodilator effects of PGE_2 in these arterioles (62). Specifically, they demonstrated that the EP_2 agonist, butaprost, had no effect on cAMP, whereas misoprostol, a pan-specific $EP_{2,3,4}$ agonist, significantly increased cAMP (62). Therefore by default, it was suggested that EP_4 receptor may be the primary receptor mediating renal vasodilatation in the afferent arterioles (62). Afferent arteriolar EP_4 receptor expression suggests that it is a key player in regulating RBF and subsequently GFR-major determinants of renal function.

Lastly, a role for the EP_4 receptor in regulating blood pressure has been suggested. Studies have demonstrated that PGE_2 induces renin release in the juxtaglomerular apparatus (JGA) and that EP_4 receptor expression has been detected in microdissected JGA (40), supporting the possibility that renal EP_4 receptor activation contributes to the enhanced renin release.

Figure 1.4 Prostaglandin Synthesis

Arachidonate is metabolized by COX_1 or COX_2 to PGG_2 and then PGH_2. PGH_2 is enzymatically converted, by PGD synthase, PGE synthase, PGF synthase, PGI synthase, and thromboxane synthase, to prostanoids: PGD_2, PGE_2, PGF_2, PGI_2, or TxA_2, respectively. Each prostanoid interacts with distinct G protein-coupled receptors. PGD_2 activates the DP receptor, PGF_2 activates the FP receptor, PGI_2 activates the IP receptor and TxA_2 activates the TP receptor. PGE_2 interacts with four EP receptor subtypes, designated EP_{1-4}, each of which also couples to distinct signalling pathways.

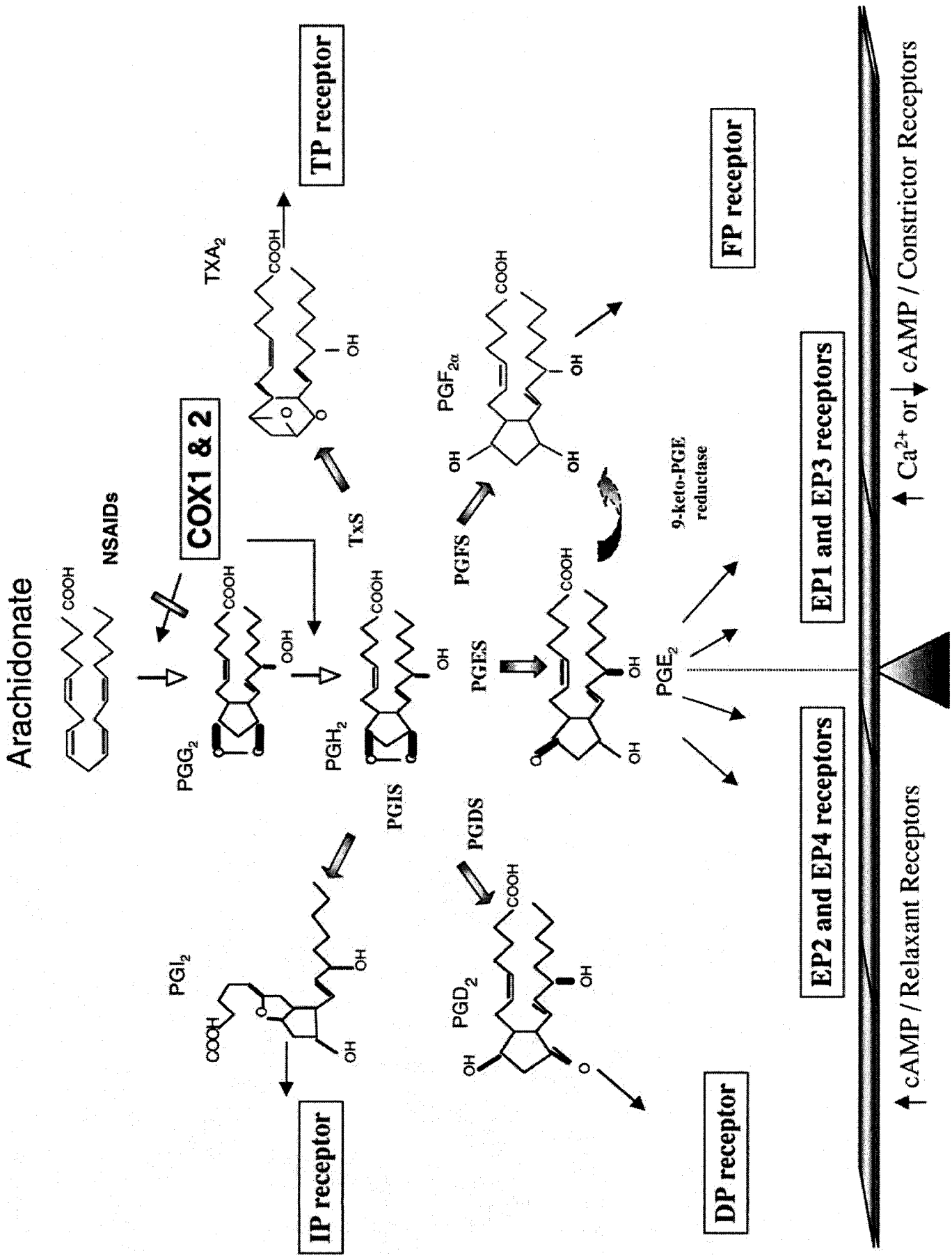

(Brever and Brever 2001)

Figure 1.5 PGE_2 Couples to Multiple Signalling Pathways

PGE_2 interacts through 4 EP receptors. EP_2 and EP_4 receptors can couple to a G_s protein in order to activate AC thereby increasing cytosolic cAMP levels. The EP_1 receptor signals through a Gq protein to elicit phosphatidyl inositol turnover and intracellular Ca^{2+} elevations. The EP_3 receptor inhibits cAMP production by activating a G_i protein which blocks the activity of AC.

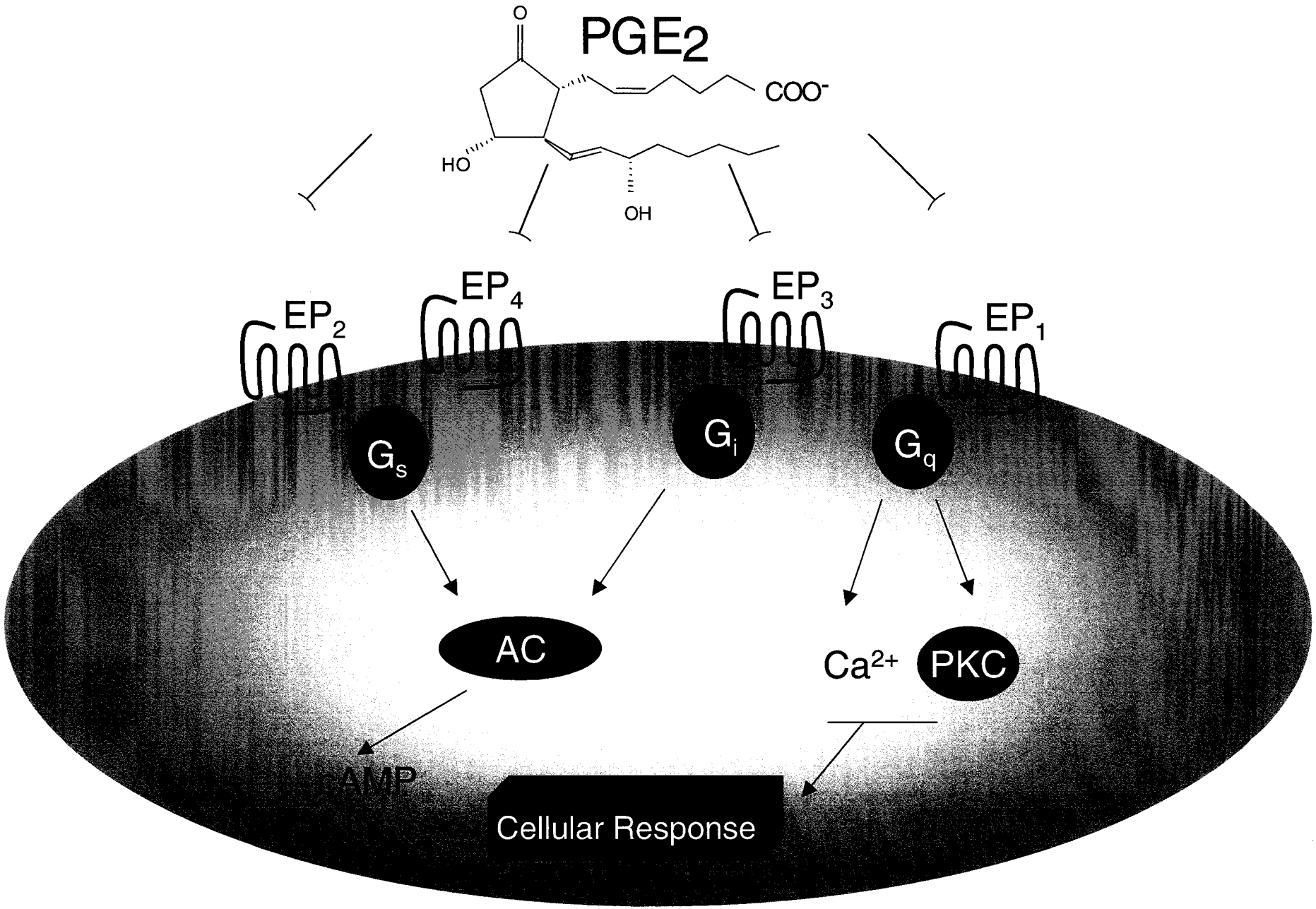
PGE2
O
COO-
HO
OH
EP2
EP4
EP3
EP1
Gs
Gi
Gq
AC
Ca2+
PKC
cAMP
Cellular Response

2 RATIONALE

Non-steroidal anti-inflammatory drugs (NSAIDs) are widely prescribed for their anti-pyretic, anti-inflammatory, and analgesic effects. A large proportion of the population acquires them over-the-counter to gain relief from non-specific aches and pains. Their use is considered safe, well tolerated and their most common side effects involve gastrointestinal tract toxicity, such as gastric erosions, ulcerations, and perforations. The therapeutic effects of NSAIDs stem from their ability to inhibit the activity of the prostaglandin forming enzymes COX-1 and -2, the enzymes that mediate prostaglandin synthesis from arachidonic acid.

Initially, the use of NSAIDs in the treatment of renal disorders seemed promising. Arisz et al. demonstrated that patients with nephrotic syndrome, on long-term indomethacin (non selective COX inhibitor) showed decreased urinary protein excretion (3). As NSAID use became increasingly common however, nephrotoxicity emerged as a potentially devastating contraindicator. NSAID-nephrotoxicities include: acute renal failure, hemodynamic changes in the kidney, tubulointerstitial nephritis, glomerular lesions, hypertension, reduced sodium and water excretion, and hyperkalemia.

Since the diverse renal actions of prostaglandins are frequently opposing (eg., vasodilatory vs. vasoconstrictive; proinflammatory vs. anti-inflammatory, diuretic vs. antidiuretic, etc.) the NSAID-induced renal side effects may emerge upon inactivity of one or more of the EP receptor subtypes.

Renal insufficiency due to enhanced vasoconstriction and sodium transport inhibition can be considered as unwanted renal side effects of NSAIDs. In glomerulonephritis, sodium excretion is altered and RBF decreases, two major events mediated by PGE_2/EP_1 signaling. Therefore we sought to investigate the role of the EP_1 receptor in a mouse model of this glomerular disease. Knowledge of the site of action and specific EP receptor(s) involved during GN is therefore of critical importance for anticipating pharmacological manipulations that would provide novel therapies for proteinuric diseases such as glomerulonephritis.

3 HYPOTHESIS

It is hypothesized that PGE_2 acting through the EP_1 receptor is involved in the progression of glomerulonephritis.

4 OBJECTIVES

1) To successfully induce GN in mice using an anti-GBM antibody.

2) To determine whether the expression of EP receptor subtypes change under GN conditions.

3) To assess the role of the EP_1 receptor under GN conditions.

5 MATERIALS AND METHODS

5.1 INDUCTION OF GN: EXPERIMENTAL DESIGN

GN was induced using sheep anti-rat GBM nephrotoxic serum (a generous gift from Drs. K. Munger and K. Badr, Emory University). The antibody was raised according to the technique of Sraer et al., with minor modifications. In short, renal cortex from 2 Sprague Dawley rats was minced, passed through a 106 mesh screen and suspended in 10 ml of phosphate-buffered saline (PBS). The suspension was triturated through a 25 gauge needle several times and then centrifuged at 3000 rpm for 90sec. The pellet was resuspended in PBS, retriturated, and centrifuged. This cycle was repeated 5 times to obtain the final glomerular preparation. GBM was purified from isolated glomeruli by sonicating with a Vibra Cell sonifier (Soncis & Materials Inc., Danbury CT) (5 pulses of 60sec). GBM fragments were washed by centrifugation (3000 rpm for 10 min) 5 times with PBS. The final pellet was dissolved in 0.5% SDS + 0.25M NaOH. Protein concentration was determined using the Bradford method (Bio-Rad Corp., Philadelphia, PA) and read at 595nm using spectrophotometer (Fluostar Galaxy BMG Lab., Durham, NC). This procedure was repeated until a total of 5 mg of GBM protein was isolated and pooled. Anti-GBM antibodies were raised in sheep. Approximately 200 μg of GBM in PBS mixed with an equal volume of complete Freund's adjuvant was injected once every two weeks for a total of 12 weeks into one sheep. The final preparation contained approximately 1 mg/ml of protein. To assess the specificity of the antibody, kidneys were processed

for immunofluorescence staining. Paraformaldehyde (PFA) - fixed mouse tissue sections were deparaffinized with xylene and rehydrated with graded ethanols. The sections were then rinsed in PBS and incubated for 24hr at 4°C with the anti-GBM antibody (1:500) (Bethyl Lab. Inc, Montgomery, TX). After washing with PBS, the sections were incubated with FITC-conj anti-rabbit IgG (Jackson ImmunoResearch Laboratories Inc., West Grove, PA) for 1 hr at room temperature. Sections were then washed, mounted with fluorescence mounting media (Vector Laboratories, Inc. Burlingame, CA) and coverslipped. Immunofluorescence was visualized using a Zeiss Axioskop 2 fluorescence microscope (Zeiss Axioskop 2 MOT, Zeiss Germany), and digital images were captured with a Zeiss AxioCam.

Induction of glomerulonephritis was carried out according to the protocol of Bird et al. (2000). Briefly, adult mice were immunized by a subcutaneous injection of 0.25 mg Sheep IgG (Sigma Co., St. Louis, MO) in 100 µl of PBS emulsified with an equal volume of complete Freund's adjuvant (Sigma). On day 0 of nephritis, four days post IgG immunization, 100 µl of normal sheep serum (Sigma) or sheep anti-rat GBM nephrotoxic serum was administered through the tail vein to wild-type (wt) and $EP_1^{-/-}$ mice (n=12). Serum was diluted in PBS so that each mouse received a total volume of 150 µl. Both nephrotoxic serum and sheep serum were heat inactivated by heating to 56°C for 45 minutes and kept frozen (-80°C) until needed.

On days 0, 1, 3, 5, and 7, spot urine samples were collected and analyzed. On day 7, mice were anesthetized with halothane and sacrificed, and blood was collected in heparinized syringes by cardiac puncture. One kidney was used to dissect the

cortex, outer medulla, inner medulla and papilla and subsequently frozen in liquid N_2, and stored at -80°C. The second kidney was used for isolation of glomeruli. In some studies, kidneys were cut in half in a cross section, and fixed in 4% paraformaldehyde for histology.

5.2 GLOMERULAR ISOLATION

Glomeruli were isolated by a protocol originally described by Takemoto et al. Briefly, adult mice were perfused through the heart with 4.5 μm diameter magnetic Dynabeads (Dynal, Brown Deer, WI). Kidneys were minced into small pieces, digested by collagenase, filtered using a 100 μm cell strainer (VWR, Mississauga, ON), and collected using a magnet. Almost all glomeruli isolated were lacking Bowman's capsule with a low degree of contaminating tissue (i.e. nephron segments) (Figure 5.1).

5.3 REAL TIME RT-PCR

Total RNA was isolated from whole kidney, glomeruli, cortex, inner medulla, outer medulla and papilla using an RNeasy kit (Qiagen Inc., Valencia, CA). Briefly, a small amount of tissue (<0.3g) in 350 μl of lysis buffer was homogenized for 3 minutes and an equal volume of 70% ethanol was added to the lysate. This mixture was passed through a Qiagen RNA column by centrifuging at 13,000 rpm for 15 sec. The eluant was discarded and the column was treated with RNase-free DNase I and later washed 3 times with buffers supplied with the kit. The RNA was eluted into an

eppendorf tube using RNase free water and centrifuging at 13,000 rpm for 2 min. The concentration and purity of RNA was determined by measuring the absorbance at 260/280 nm in a spectrophotometer (Thermo Spectronic, Rochester, NY).

The probes and primers used in the TaqMan® (Applied Biosystems, Foster City, CA) analysis are listed in Table 5.1. Real time TaqMan RT-PCR was performed using the ABI PRISM 7000 Sequence Detection System (Applied Biosystems). GAPDH was amplified along with the target gene as an endogenous control with VIC-labeled probe to normalize expression between different samples. The probes and primers for target gene and GAPDH were diluted in the TaqMan® One-Step RT-PCR Master Mix (Applied Biosystems) and 25 µl of the reaction mix was added to each reaction tube. Reactions were performed with an initial reverse transcription step at 48.0°C for 30 min followed by denaturation at 95°C for 10 min. PCR cycles were carried out at 95°C for 15 sec and 60°C for 1 min for 45 cycles. Output data generated by the instrument on-board software Sequence Detector Version 1.6.3 (Applied Biosystems) were transferred to a Microsoft Excel template (spread sheet) for analysis. Briefly, a relative standard curve method (log [ ] vs. threshold cycle, C_T) is used to assess the amount of a particular transcript in a group of samples. A template dilution series of a cDNA standard is included for each gene on a plate. Quantities interpolated from the resulting standard curve are used to calculate relative mRNA levels in each unknown sample. The relative mRNA expression of each studied gene is then normalized to the endogenous control, GAPDH.

Table 5.1 Real Time RT-PCR Primers and Probes

A Description of the Primers and Probes Employed for Real Time RT-PCR Experiments

Target	Probe	Forward Primer	Reverse Primer
EP_1	6FAM-TGGGCCTAACCAAGAGTGCCTG TAMRA	5'-AGTGCCAAGGGTGGTC CAA-3'	5'-CCGGGAACTACGCA GTGAAC-3'
EP_2	6FAM-TTGCCTACATGGATGAAACCTC TTCCCTAAA TAMRA	5'-TGCTCCTTGCCTTTCAC AATC-3'	5'-GAGCTCGGAGGTCC CACTTT- 3'
EP_3	6FAM-TCAATCAGATGTCGGTTGAGCA ATGCAA TAMRA	5-' GCCGCTATTGATAATG ATGTTGAA-3'	5' – CCTTCTCCTTTCCCA TCTGTGT-3'
EP_4	6FAM-CATCTGCTCCATTCCGCTCGTG GT TAMRA	5'-ATGGTCATCTTACTCAT CGCCAC-3'	5'-CTTTCACCACGTTTG GCTGAT-3'

Figure 5.1 Glomerular Isolation

Photograph of isolated glomeruli by Dynabead technique. Final isolation is of high purity, lacking the presence of tubular segments. Magnification ~200x.

5.4 URINE AND SERUM ANALYSIS

Serum samples were analyzed for cholesterol, triglycerides, albumin, creatinine and urea using a Beckman LX-20 instrument (Ottawa Hospital Core Service). Serum concentrations of aldosterone were measured by aldosterone EIA (Cayman, Ann Arbor, MI). Briefly, serum was incubated with an aldosterone-acetylcholinesterase (AChE) conjugate and aldosterone-specific rabbit antiserum for 18 hrs at 4˚C to allow efficient binding to the precoated mouse monoclonal anti-rabbit IgG. This was followed by 5 washes with a buffer supplied with the kit. The plate was developed in the dark on an orbital shaker for ~ 2 hrs using the reagent provided with the kit. The plate was read at a wavelength of 405 nm using a spectrofluorometer (Fluostar Galaxy BMG Lab., Durham, NC).

Urinary albumin levels were measured using the Albuwell M competitive ELISA (Exocell Inc., Philadelphia, PA). Briefly, diluted urine samples were incubated with 100 µl of rabbit anti murine albumin antibody for 30 minutes. The plate was washed thoroughly 10 times with the wash buffer provided. The plate was incubated with anti-rabbit HRP conjugate for an additional 30 min and then washed 10 times. 100µl of color developer was added to the plate and incubated for < 10 min. Color stopper was added to the plate and read at 450 nm. Values were determined using a semi-logarithmic plot of standard dilutions with the log [murine serum albumin] vs. absorbance.

Urinary Na^+ and K^+ concentrations were analyzed by flame photometry (Instrumentation Laboratory model IL 943, Milan, Italy), and urine osmolality was determined by freezing point depression (Advanced Instruments Inc. model 3MO plus, Norwood, MA).

5.5 DIETARY SODIUM EXPERIMENTS

Adult mice were housed in metabolic cages (Nalge Nunc International) (Figure 5.2) and had free access to food and water. Mice were first fed a control diet containing 0.4% NaCl. This was followed by a 7 day period in which the animals were fed a low salt (LS) (0.02% NaCl) or a high salt (HS) (4.0% NaCl) diet (Harlan-Teklad Laboratory, Madison, WI). Some groups of the LS treated mice were water deprived (WD) on days 8 and 9 prior to sacrifice. In each experiment, urine spot samples, urine volume output, water intake, body weight, and blood pressure were taken daily. Urinary Na^+ and K^+ concentrations were analyzed by flame photometry (Instrumentation Laboratory model IL 943), and urine osmolality was determined by freezing point depression (Advanced Instruments Inc. model 3MO plus).

5.6 BP STUDIES

Systolic blood pressure (BP) was measured daily by tail-cuff plethysmography (BP-2000; Visitech Systems, Apex, NC). The system measures BP by determining the cuff pressure at which blood flow to the tail is eliminated. Briefly, mice are placed on a preheated platform of 39°C to allow efficient dilatation of blood

vessels in the tail. Their tails are passed through a cuff and immobilized by adhesive tape between a light source above and a photoresistor below the tail. Evaluated photoelectrically, blood flow in the tails produces oscillating waveforms that are digitally sampled 200 times per second per channel. The waveforms, displayed in real time on a monitor, are computer analyzed before and during a programmable routine of cuff inflation and deflation. Mice were trained for an initial period of 5 consecutive days, and measurements were subsequently collected for an additional 5 days. Values were compared among wt (n=12), and $EP_1^{-/-}$ mice (n=12).

5.7 HISTOPATHOLOGY

Kidneys were fixed in 4% paraformaldehyde, embedded in paraffin, sectioned at 7 μm, and stained with hematoxylin-eosin (H&E) or periodic acid-Schiff (PAS) reagent to assess differences between WT and $EP_1^{-/-}$ groups.

5.8 STATISTICAL ANALYSIS

The values are presented as means ± SEM. Statistical comparisons between 2 groups were performed using an unpaired student *t*-test. Comparisons between 3 or more groups were carried out using an ANOVA, followed by a Newman - Keuls post test. $p<0.05$ was considered statistically significant.

Figure 5.2 Metabolic Mouse Cages

Metabolic mouse cages allow separation of urine and feces. Urine is collected in a graduated tube. In addition, the specially designed feeding and drinking water bottle assemblies allow for the quantification of consumed food and water during the experiment.

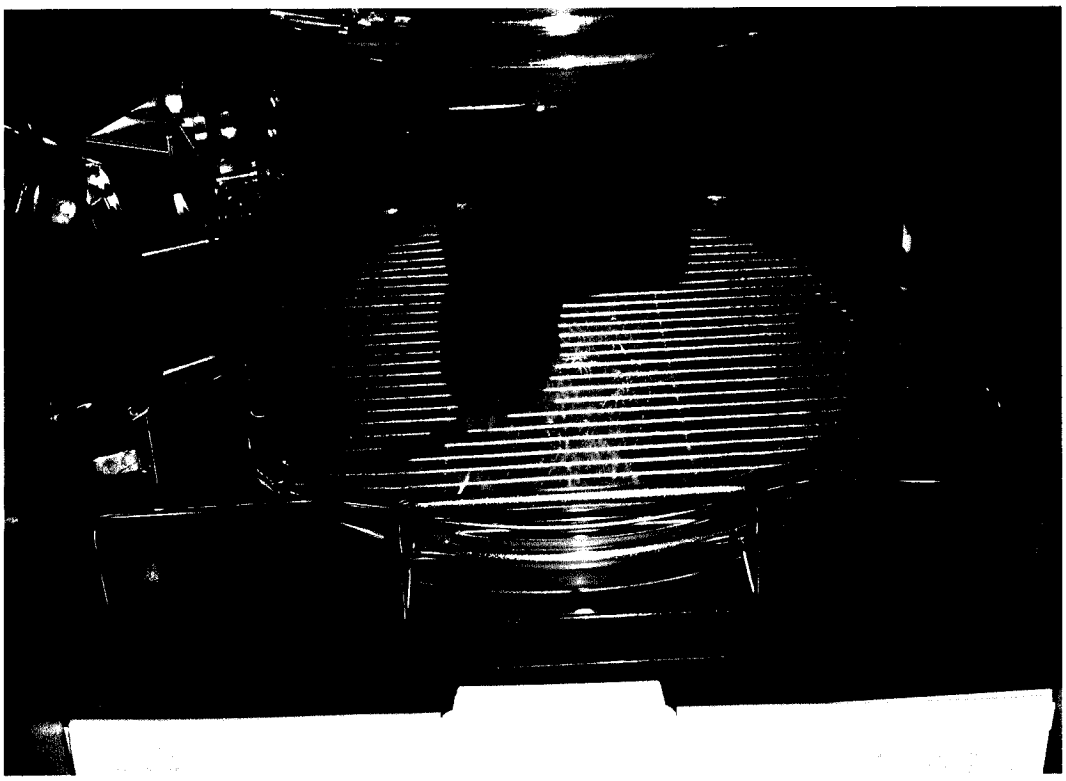

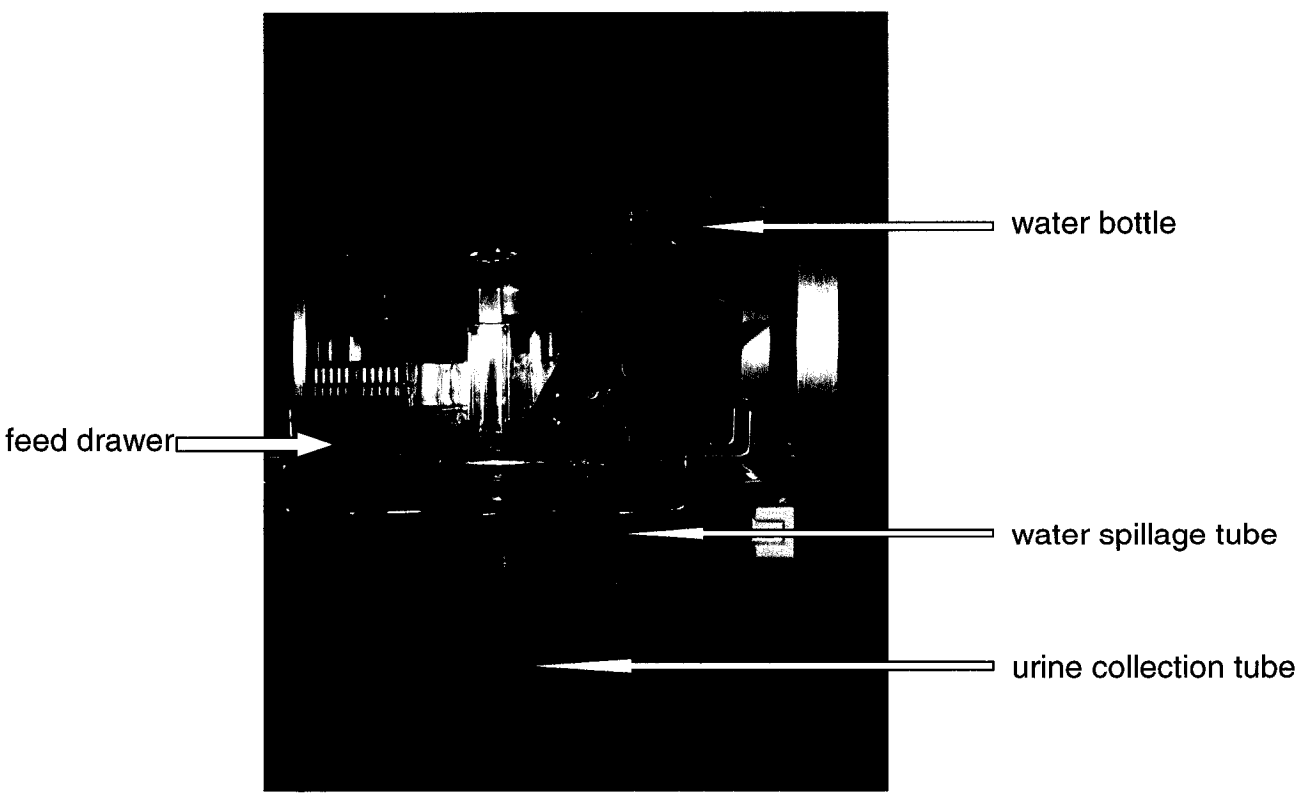
water bottle
feed drawer
water spillage tube
urine collection tube

6 RESULTS

6.1 GN $EP_1^{-/-}$ MICE EXHIBIT INCREASED SEVERITY IN RENAL IMPAIRMENT

6.1.1 Successful Induction of GN in Mice.

A mouse model of GN was induced using an anti-rat-GBM antibody. This model of nephrotoxic nephritis has previously been employed in mice (11). The specificity of the antibody for GBM is indicated by immunofluorescence (Figure 6.1) showing anti-GBM binding at the basement membranes of glomeruli and tubules of wt mice.

In order to determine the suitability of this model, mice were sacrificed on day 7 after receiving the anti-GBM antibody and the following parameters were measured: serum cholesterol, triglycerides, albumin, creatinine, and urea (Figures 6.3, 6.4), along with urine albumin (Figure 6.2). In addition, glomerular pathology was assessed histologically. Consistent with a nephritic phenotype, GN mice displayed albuminuria (GN wt: 1003 ± 33 µg/ml, n=11 vs. wt: 33 ± 11 µg/ml, n=11; $^{*}p<0.05$) indicating an increase in glomerular permeability. Serum cholesterol (GN wt: 4.4 ± 0.6 mmol/L, n=16 vs. wt: 1.4 ± 0.1 mmol/L, n=16; $^{*}p<0.05$), triglycerides (GN wt: 2.4 ± 0.3 mmol/L, n=17 vs. wt: 0.8 ± 0.1 mmol/L, n=17; $^{*}p<0.05$), urea (GN wt: 25.6 ± 10.8 mmol/L, n=11 vs. wt: 6.1 ± 0.3 mmol/L, n=11; $^{*}p<0.05$) and creatinine (GN wt: 33.8 ± 8.0 µmol/L, n=11 vs. wt: 15.6 ± 1.9 µmol/L, n=11; $^{*}p<0.05$) levels were significantly higher compared to those of vehicle-treated

animals. Serum albumin levels were reduced in GN wt mice to below 10 g/L, $p<0.0005$. Elevated serum levels of both creatinine and urea indicate a decrease in renal function. Histologically, PAS and H&E staining revealed an increased mesangial matrix and dilated tubules containing proteinaceous material in GN mice (Figure 6.5). These results demonstrate that the use of the anti-GBM antibody was successful in inducing a model of GN similar to that seen in humans.

Figure 6.1 Anti-GBM Antibody Immunofluorescence

Immunofluorescence microscopy of paraffin embedded wt kidney tissue. **A.** Secondary antibody alone - FITC conjugated anti-rabbit IgG (dilution, 1:2000). **B.** Basement membrane of the capillary loops detected with anti-GBM antibody (dilution, 1:500) and FITC conjugated anti-rabbit IgG (dilution, 1:2000).

A

B

Figure 6.2 Urinary Albumin Levels for WT and GN WT Mice.

On day 7, GN wt mice displayed significant albuminuria compared to wt littermates ($^{*}p < 0.05$). The data presented are the means ± S.E.M in μg/ml.

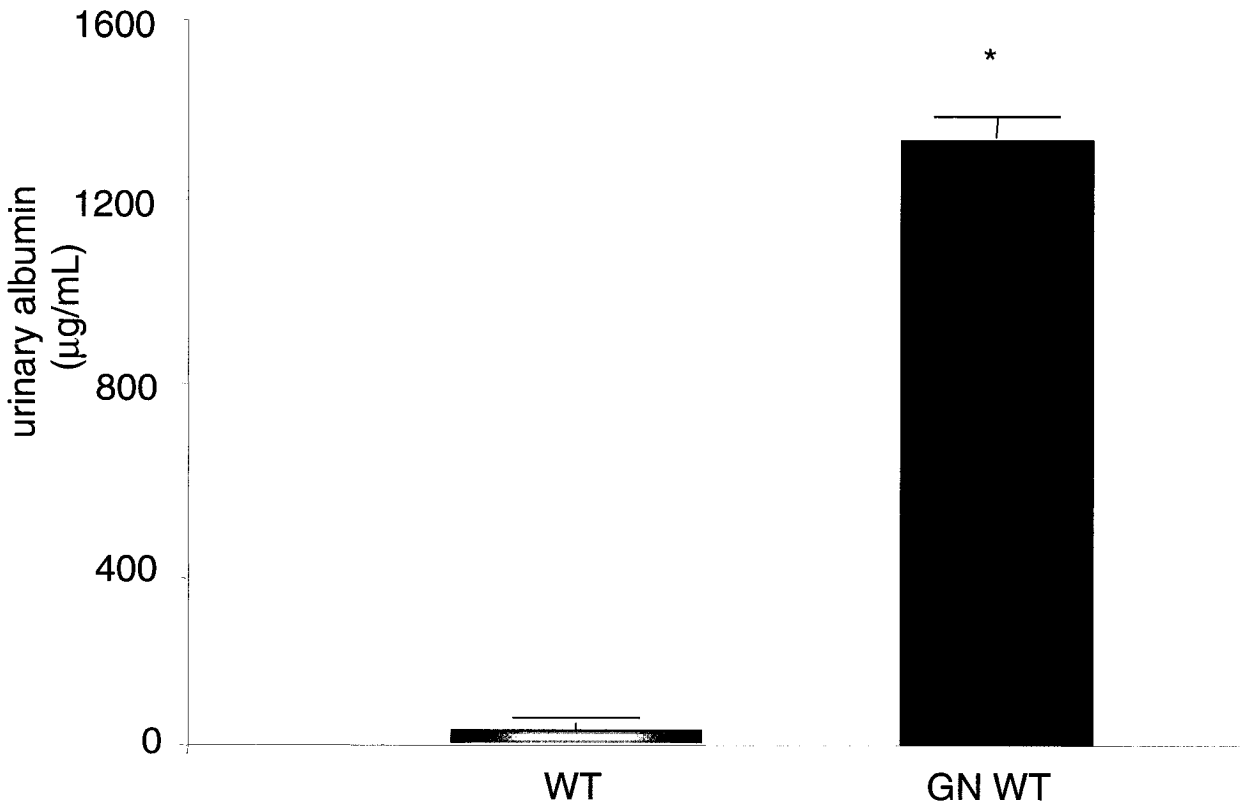
1600
1200
800
400
0
urinary albumin (µg/mL)
*
WT
GN WT

Figure 6.3 Serum Analysis of WT and GN WT Mice.

Day 7 following anti-GBM injections, serum obtained by cardiac puncture was analyzed for cholesterol and triglycerides using a Beckman LX-20 instrument. GN wt mice displayed elevated **A.** serum cholesterol (*$p<0.05$) and **B.** serum triglycerides (*$p< 0.05$) levels compared to pre immune serum treated animals. Values presented are the means ± S.E.M in mmol/L.

A

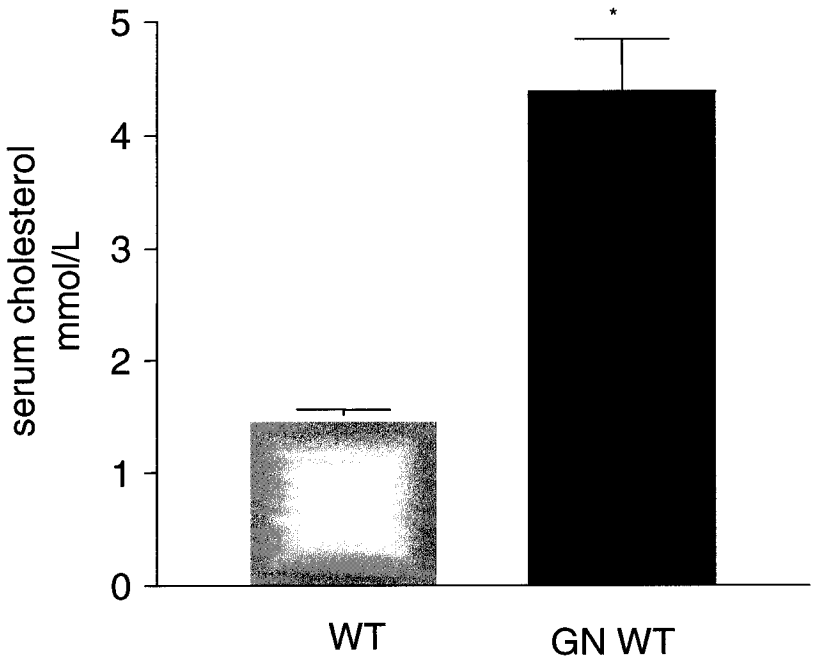
serum cholesterol
mmol/L
5
4
3
2
1
0
*
WT
GN WT

B

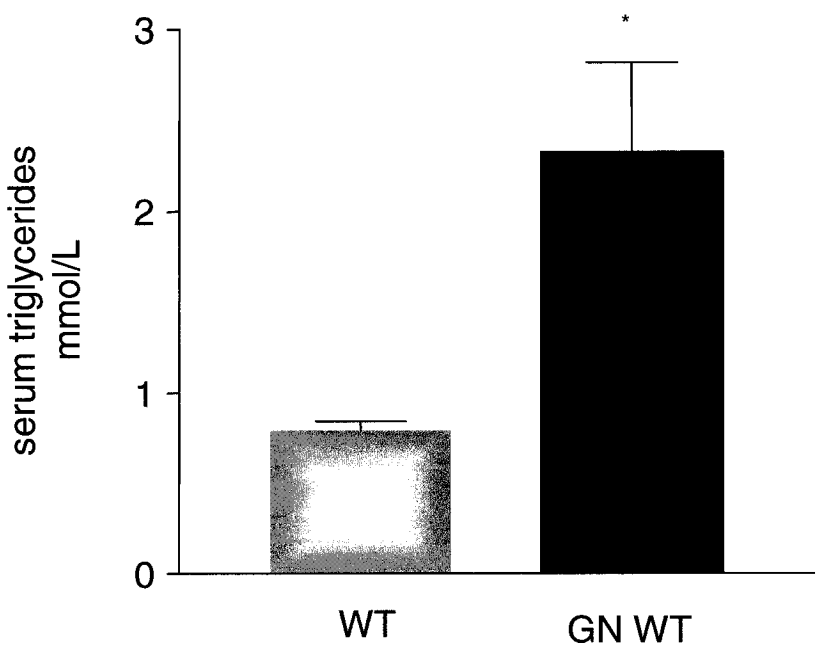
serum triglycerides
mmol/L
3
2
1
0
*
WT
GN WT

Figure 6.4. Serum Urea and Creatinine Levels in WT and GN WT Mice.

Day 7 following anti-GBM injections, serum obtained by cardiac puncture was analyzed for urea and creatinine levels using a Beckman LX-20 instrument. GN wt mice displayed elevated serum urea (mmol/L) (*$p<0.05$) and serum creatinine (μmol/L) (*$p< 0.05$) levels compared to pre immune serum treated animals. Values presented are the means ± S.E.M.

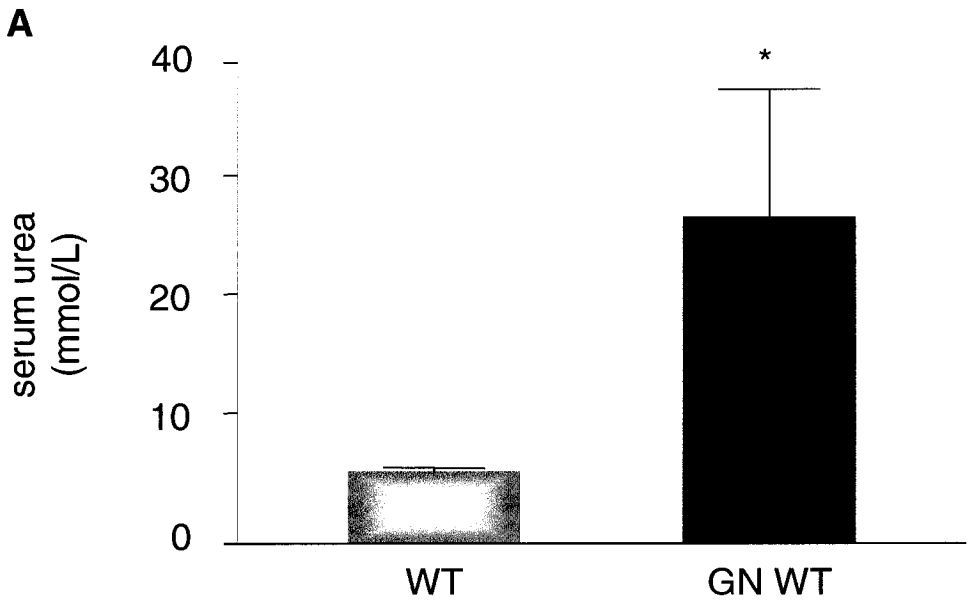
A
40
30
20
10
0
serum urea
(mmol/L)
*
WT
GN WT

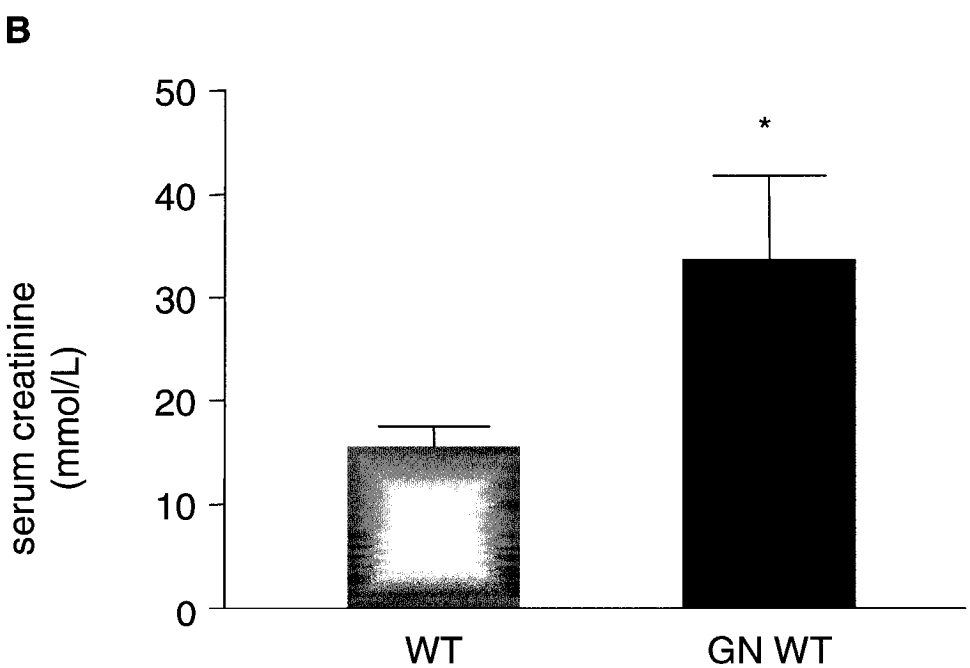
B
50
40
30
20
10
0
serum creatinine
(mmol/L)
*
WT
GN WT

Figure 6.5 H&E and PAS Staining of Kidneys from WT and GN WT Mice.

Photomicrograph of the cortical region from 7μm sections of paraffin embedded mouse kidneys stained with H&E and PAS. Staining revealed increased mesangial matrix and dilated tubules containing proteinaceous material (indicated by arrows) in GN wt mice which is absent in pre immune serum treated animals (n=12).

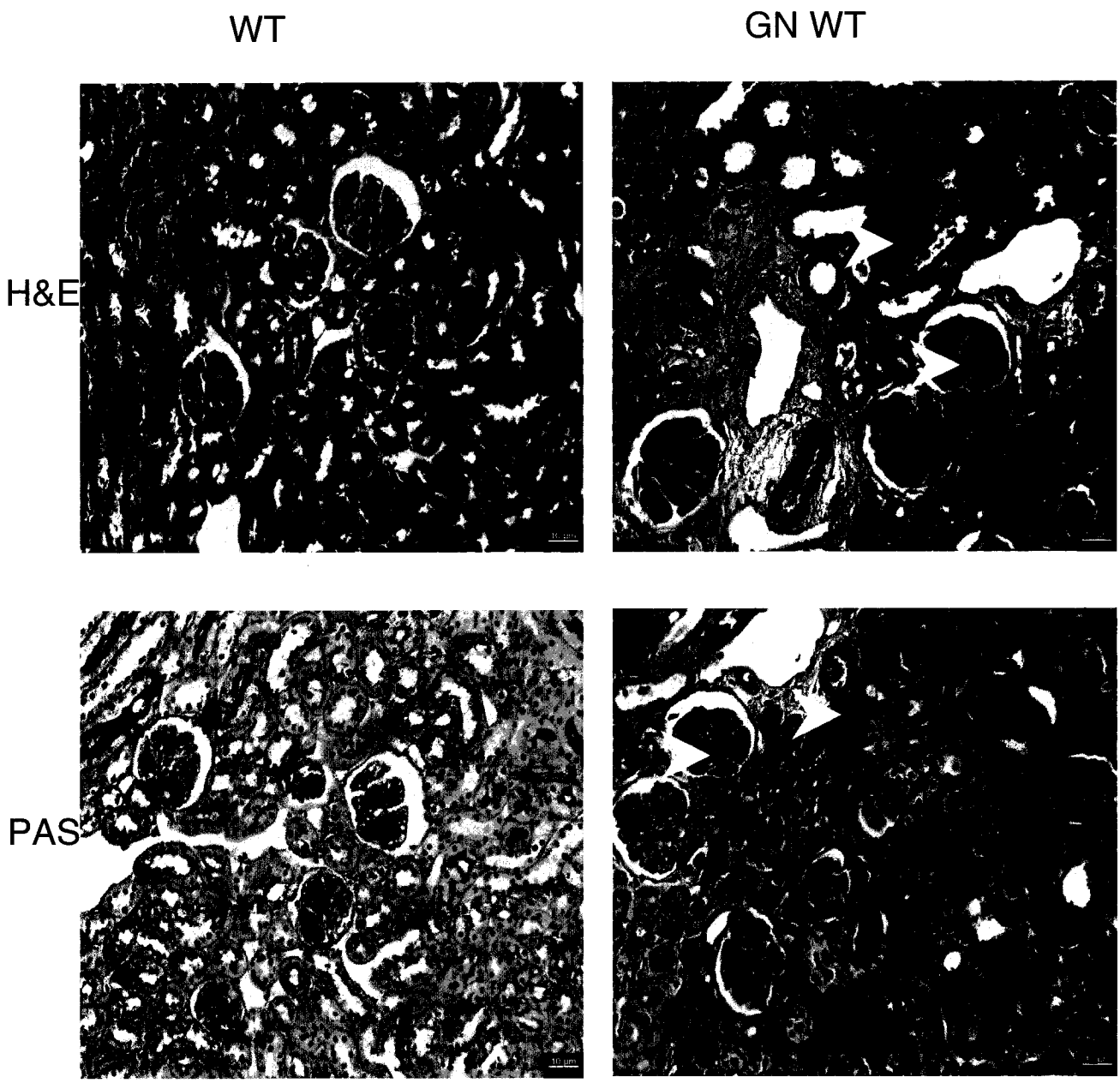
WT
GN WT
H&E
PAS

6.1.2 The Role of the EP_1 Receptor During the Progression of GN

In order to assess the role of the EP_1 receptor subtype in the progression of GN, the mouse model of GN was induced in mice with gene-targeted deletion of the EP_1 receptor. The EP_1 receptor is expressed primarily in the vasculature, podocytes and the collecting duct, with increasing levels from the cortex to the papillae (30). If the EP_1 receptor has a role in regulating the permeability barrier, salt reabsorption and /or vasoconstriction of renal vasculature, then its absence in gene-targeted mice may alter the progression of glomerular damage, alter tubular maintenance of sodium homeostasis and /or perturb renal vascular resistance.

Blood pressure measurements were taken daily following anti-GBM injections. GN $EP_1^{-/-}$ mice showed a slight decline in systolic blood pressure compared to GN wt mice (GN $EP_1^{-/-}$: 89 ± 2 mmHg, n=5 vs. GN wt: 100 ± 1 mmHg n=5; $p<0.05$) (Figure 6.6). However, control $EP_1^{-/-}$ mice also exhibited a similar decline, rendering ambiguous any interpretation of the effects of GN and the role of the EP_1 subtype.

In order to assess renal function and glomerular permeability, mice were sacrificed on day 7 following anti-GBM injections. Urinalysis revealed no significant differences in albuminuria between $EP_1^{-/-}$ GN mice compared to wt GN animals (GN wt: 1495 ± 243 µg/ml, n=10 vs. GN $EP_1^{-/-}$: 1364 ± 228 µg/ml, n=8) (Figure 6.7). There were no histological differences between GN wt and GN $EP_1^{-/-}$; both showed increased mesangial matrix, and dilated tubules containing proteinaceous material

(Figure 6.8). In contrast however, hyperkalemia was significantly more profound in GN $EP_1^{-/-}$ mice than GN wt animals (GN $EP_1^{-/-}$: 8.9 ± 0.6 mmol/L, n=12 vs. GN wt: 7.4 ± 0.3 mmol/L, n=17; $^*p<0.05$) and control littermates (wt: 6.1 ± 0.2 mmol/L n=12; $EP_1^{-/-}$: 6.0 ± 2.7 mmol/L n=12, *p<0.05) (Figure 6.9). Aldosterone is a major regulator of serum potassium (61). Serum aldosterone levels (Figure 6.10), measured 7 days following anti-GBM injections, were suppressed equally in both GN wt (GN wt: 366 ± 129 pg/ml, n=5 vs. wt: 729.1 ± 75.78 pg/ml, n=5; $^*p<0.05$) and GN $EP_1^{-/-}$ (GN $EP_1^{-/-}$: 381 ± 49 pg/ml, n=5 vs. $EP_1^{-/-}$: 719 ± 159 pg/ml, n=5; $^*p<0.05$). The reduction in serum aldosterone is likely not accounting for the enhanced hyperkalemia observed in the GN $EP_1^{-/-}$ mice. However, the observed elevations in serum potassium could be explained by reductions in GFR (12). Accordingly, serum creatinine levels (GN $EP_1^{-/-}$: 37.8 ± 4.7 µmol/L, n=12 vs. GN wt: 30.6 ± 3.7 µmol/L, n=12; $^*p<0.05$) and urea levels (GN $EP_1^{-/-}$: 30.9 ± 4.1 mmol/L, n=12 vs. GN wt: 15.5 ± 2.3 mmol/L, n= 12; $^*p<0.05$) were significantly greater in GN $EP_1^{-/-}$ mice compared to GN wt mice and control littermates (creatinine: wt: 14 ± 1 µmol/L; $EP_1^{-/-}$: 14 ± 1 µmol/L, n=12, *p<0.05; urea: wt: 6.8 ± 0.3 mmol/L ; $EP_1^{-/-}$: 7.7 ± 0.4, mmol/L, n=12, *p<0.05) (Figure 6.11), together indicating renal impairment due to a decline in GFR. Taken together these results suggest that the EP_1 receptor is not involved in the appearance of proteinuria in GN. Nevertheless nephritic $EP_1^{-/-}$ mice display greater renal dysfunction that GN wt mice.

Figure 6.6 Systolic Blood Pressure of GN WT and GN $EP_1^{-/-}$ Mice.

Systolic blood pressure was measured by tail-cuff plethysmography. Blood pressure measurements were taken daily both prior to and for the 7 days following anti-GBM injections. GN $EP_1^{-/-}$ mice showed a slight drop in systolic blood pressure levels compared to GN wt littermates over the 7 day period. ($p<0.05$) Values presented are the means ± S.E.M in mmHg.

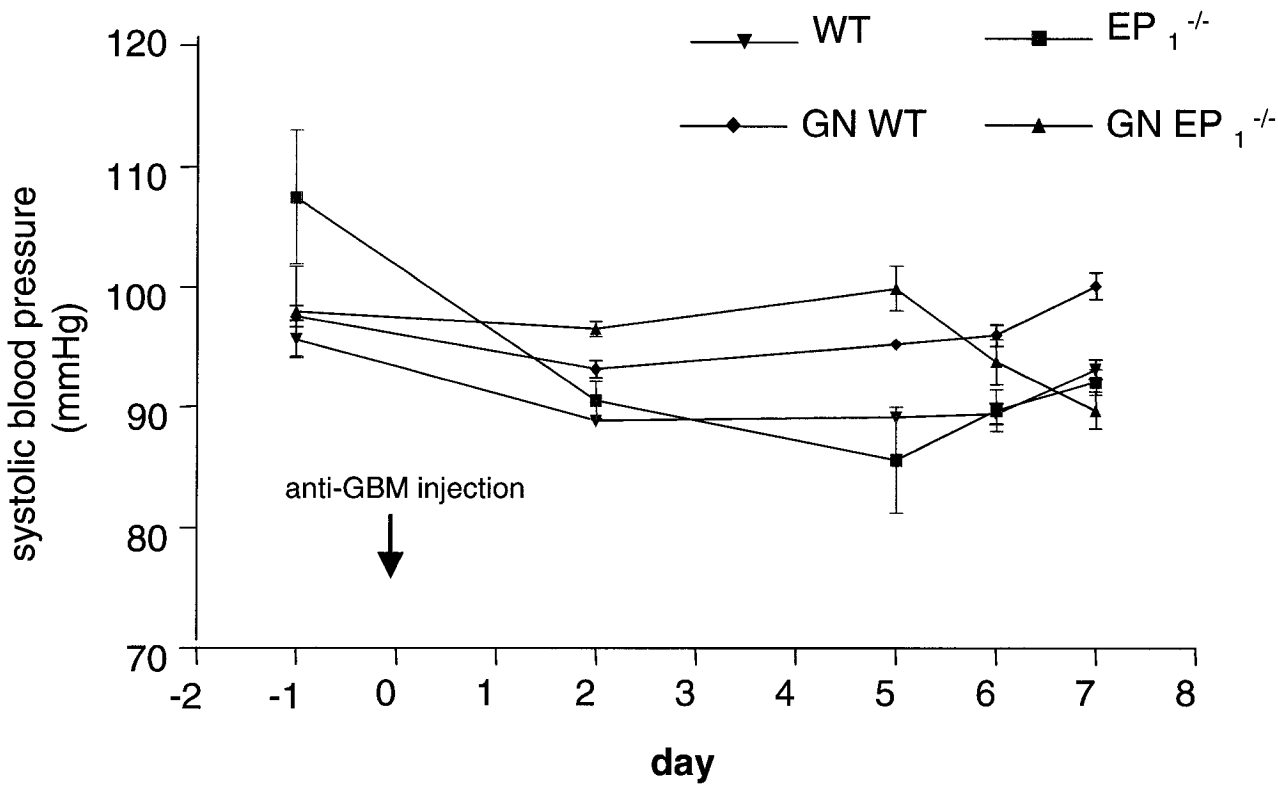
WT
EP 1 -/-
GN WT
GN EP 1 -/-
systolic blood pressure (mmHg)
120
110
100
90
80
70
anti-GBM injection
-2
-1
0
1
2
3
4
5
6
7
8
day

Figure 6.7 Urinary Albumin Levels of Control and GN Groups

Seven days after administration of the anti-GBM antibody, GN groups showed significant urinary albumin compared to pre immune serum treated animals. There were no differences between GN $EP_1^{-/-}$ and GN wt mice. Values presented are the means ± S.E.M in µg/ml.

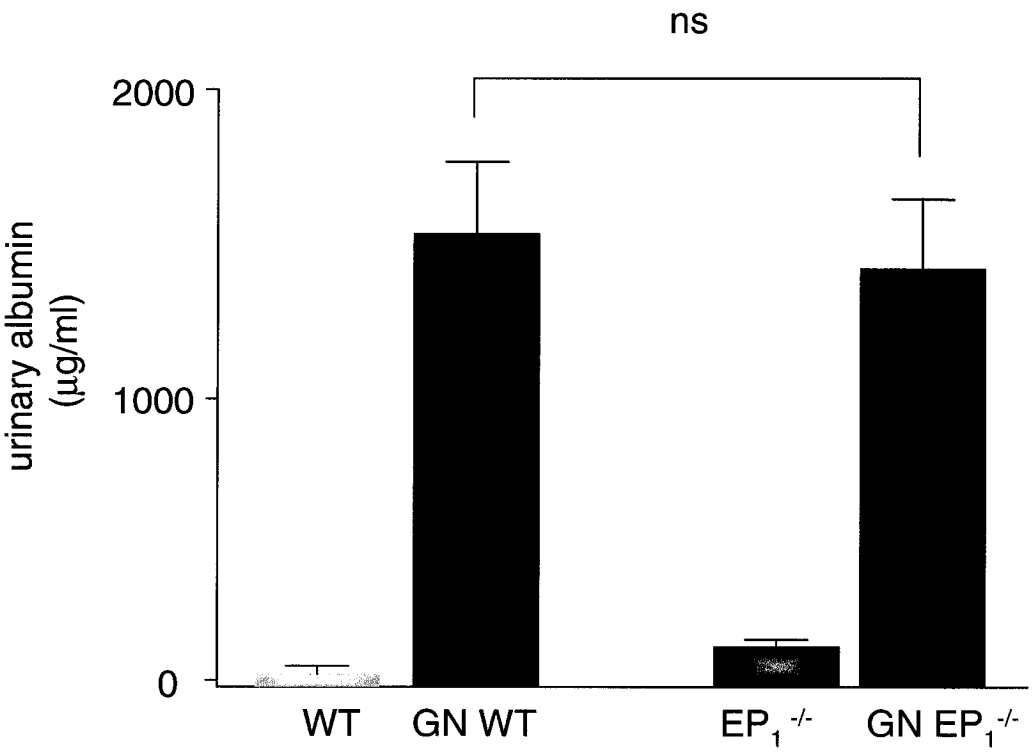
ns
2000
1000
0
urinary albumin
(µg/ml)
WT
GN WT
EP1 -/-
GN EP1 -/-

Figure 6.8 Kidney H&E Staining of WT and $EP_1^{-/-}$ Mice.

Photomicrographs of 7μm sections of paraffin embedded mouse kidneys stained with H&E. Staining revealed increased mesangial matrix and dilated tubules containing pertinacious material (indicated by arrows) in GN mice which was absent in pre-immune serum-treated animals (n=10).

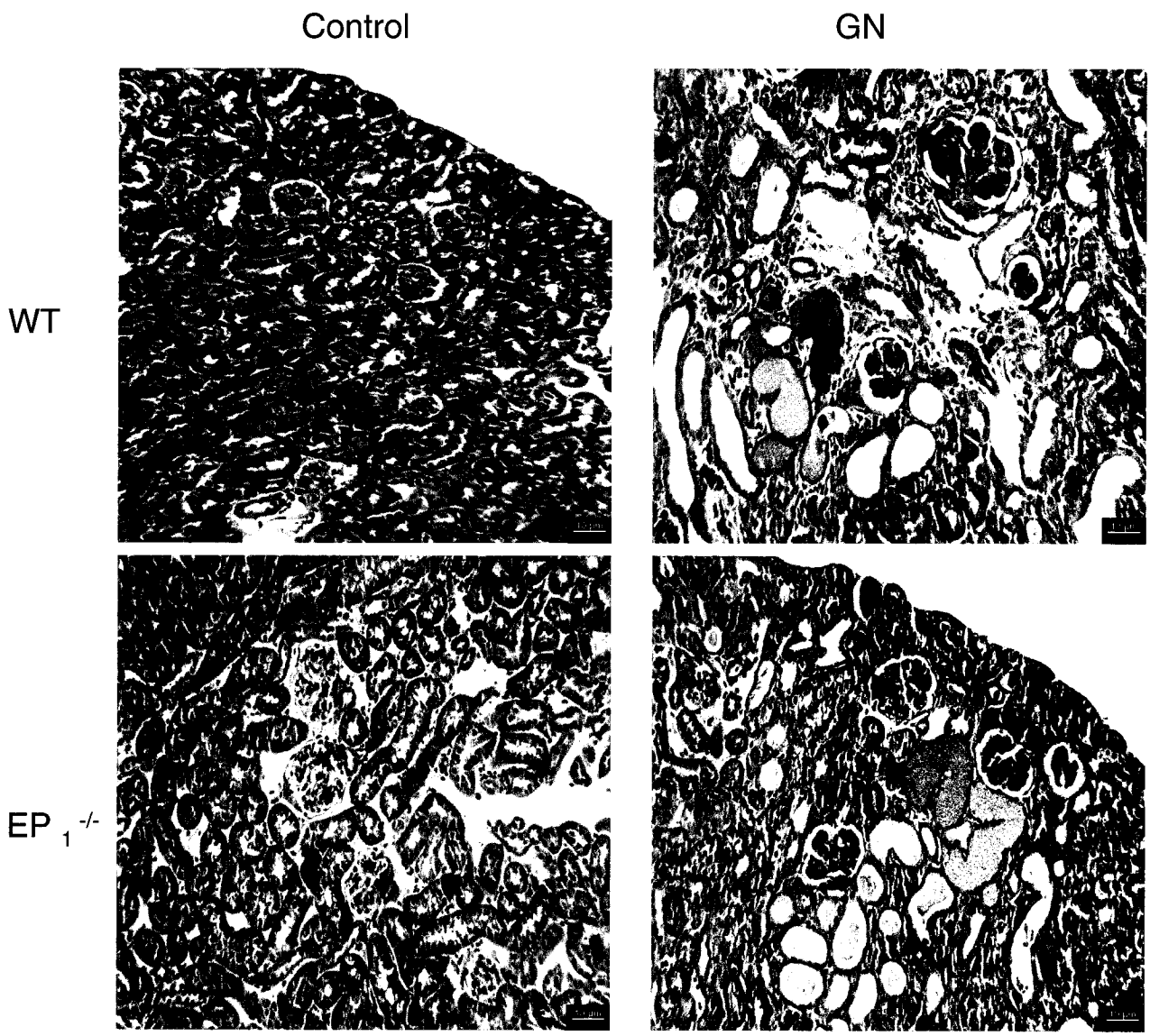
Control
GN
WT
EP 1 -/-

Figure 6.9 Serum Potassium Levels in GN WT and GN $EP_1^{-/-}$ Mice.

Day 7 following anti-GBM injections, serum obtained by cardiac puncture was analyzed for potassium levels using a Beckman LX-20 instrument. GN $EP_1^{-/-}$ revealed significantly elevated serum potassium compared to GN wt mice and control littermates (*$p<0.05$). Values presented are the means ± S.E.M in mmol/L.

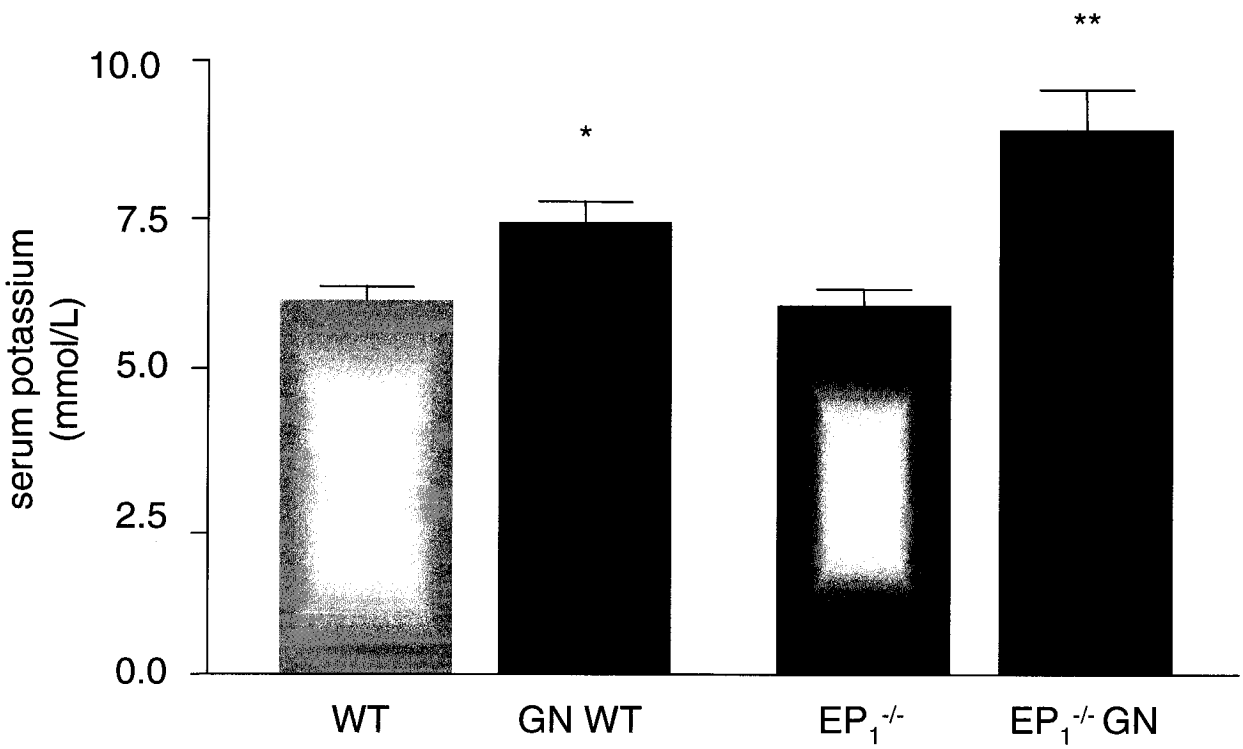
10.0
7.5
5.0
2.5
0.0
serum potassium (mmol/L)
*
**
WT
GN WT
EP1-/-
EP1-/- GN

Figure 6.10 Serum Aldosterone Levels in GN WT and GN $EP_1^{-/-}$Mice.

Day 7 following anti-GBM injections, serum obtained by cardiac puncture was purified from organic contaminants and assayed for aldosterone using the Cayman Aldosterone EIA kit. GN wt and GN $EP_1^{-/-}$ mice revealed equally reduced serum aldosterone levels compared to control groups (*$p<0.05$). Values presented are the means ± S.E.M in pg/ml.

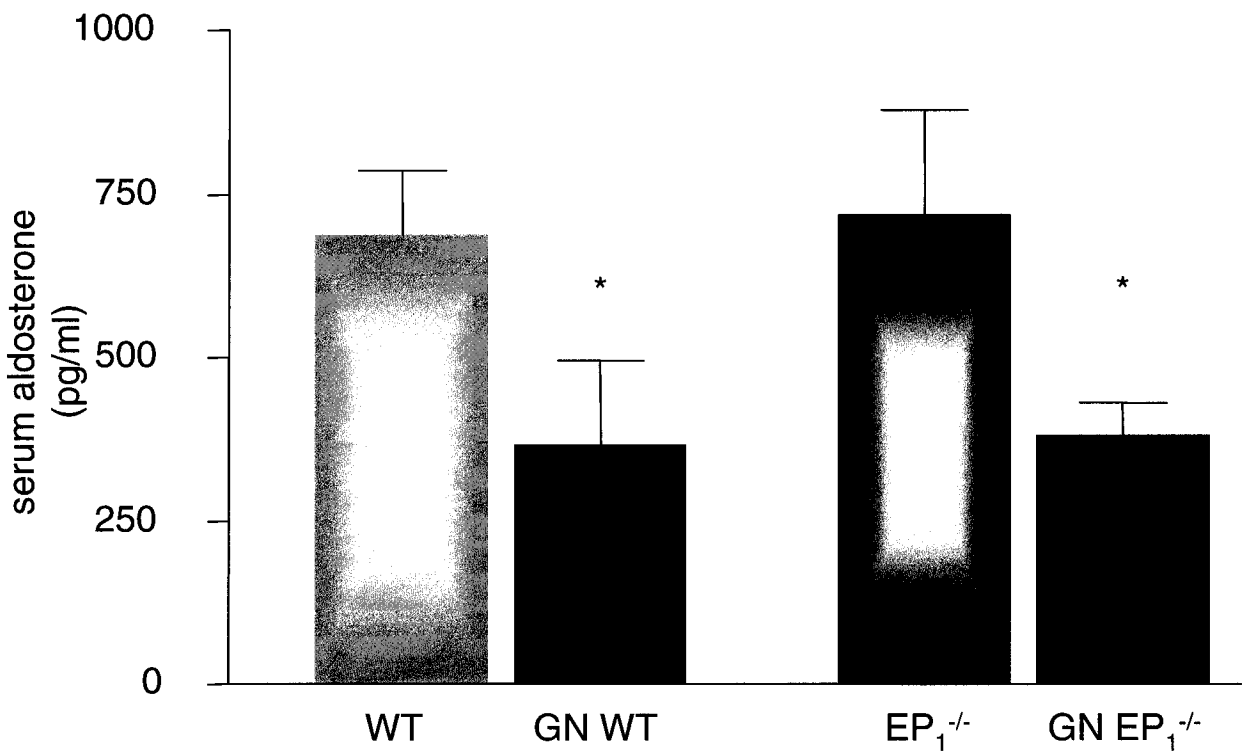
1000
750
500
250
0
serum aldosterone (pg/ml)
*
*
WT
GN WT
EP1-/-
GN EP1-/-

Figure 6.11 Enhanced Elevations in Serum Urea and Creatinine Levels in $EP_1^{-/-}$ GN Mice.

Day 7 following anti-GBM injections, serum obtained by cardiac puncture was analyzed for urea and creatinine levels using a Beckman LX-20 instrument. **A.** GN $EP_1^{-/-}$ mice displayed significantly higher serum urea levels (mmol/L) compared to GN wt mice and control littermates (*$p<0.05$). Furthermore, **B.** serum creatinine (μmol/L) was significantly higher in GN $EP_1^{-/-}$ compared to GN wt (*$p<0.05$). Values presented are the means ± S.E.M.

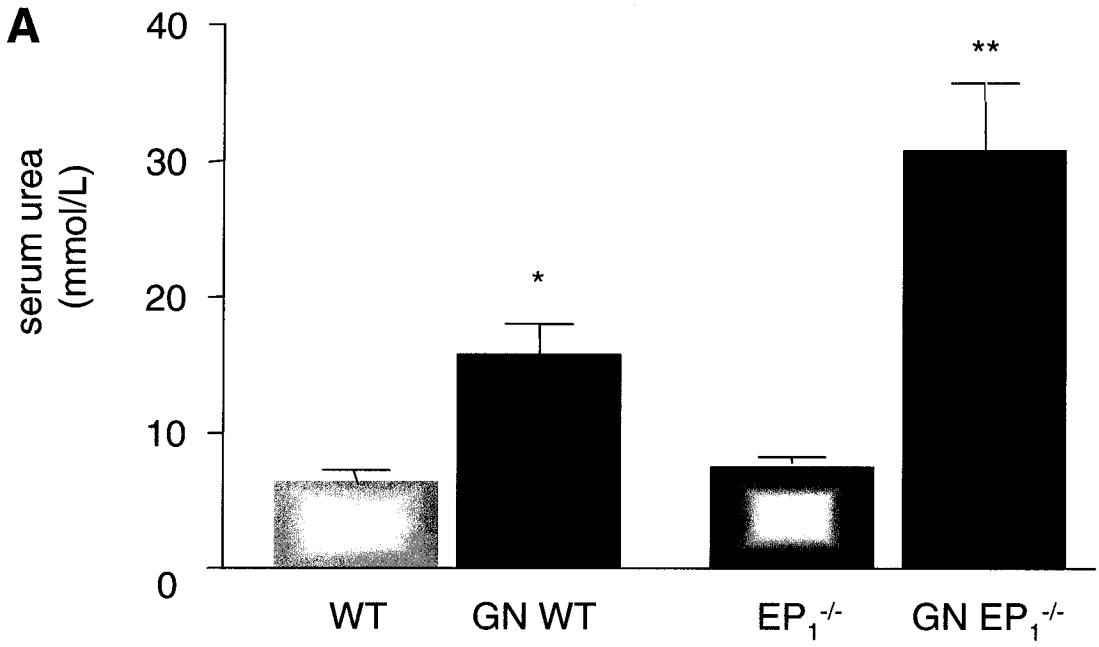
A
serum urea (mmol/L)
40
30
20
10
0
*
**
WT
GN WT
EP1-/-
GN EP1-/-

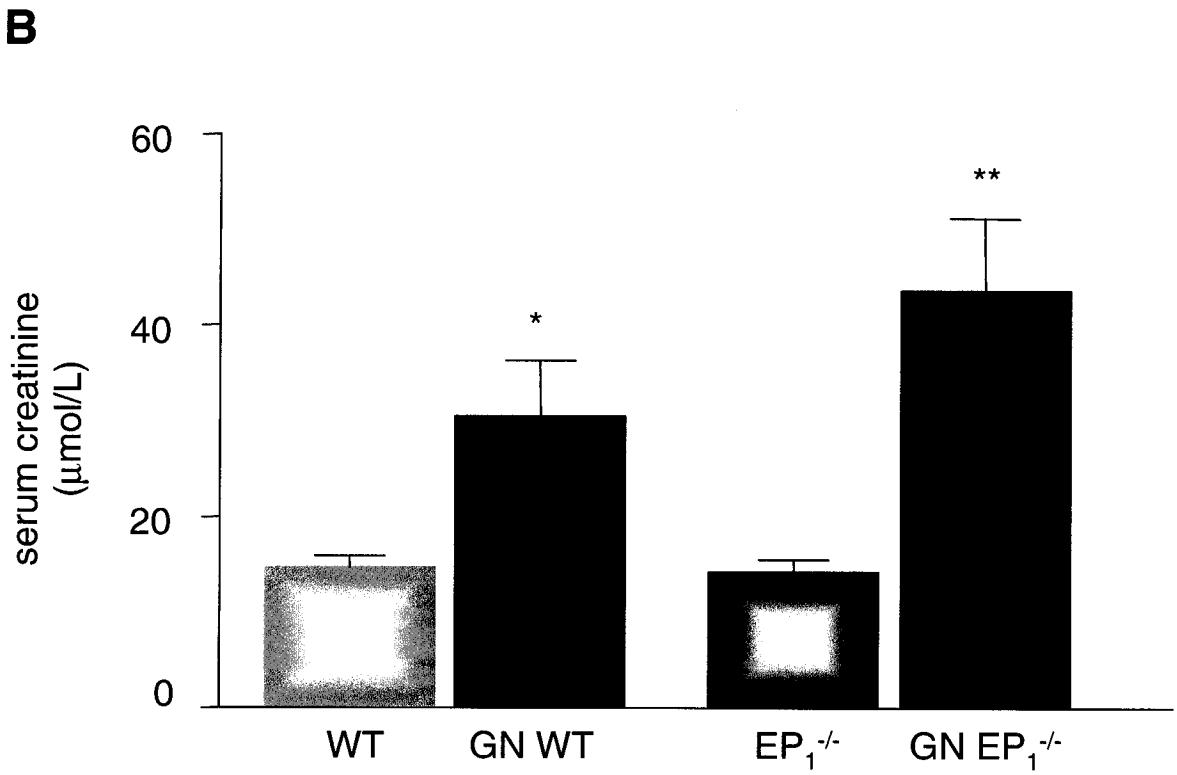
B
serum creatinine (µmol/L)
60
40
20
0
*
**
WT
GN WT
EP1-/-
GN EP1-/-

6.1.3 GN $EP_1^{-/-}$ Mice Display Impaired Ability to Maintain ECFV

Urine concentration is significantly altered under GN conditions. At day 7 following anti-GBM injections, GN $EP_1^{-/-}$ mice displayed significantly lower urine osmolality levels compared to GN wt mice (GN $EP_1^{-/-}$: 340 ± 38, n=5 vs. GN wt: 701 ± 55 mmol/L, n=5; $^*p<0.05$) and control littermates (wt: 2255 ± 59, n=5; $EP_1^{-/-}$: 1701 ± 57 mmol/L, n=5) (Figure 6.12). Furthermore, GN $EP_1^{-/-}$ mice had significantly elevated serum sodium concentrations compared to GN wt mice (GN $EP_1^{-/-}$: 150 ± 1.0 vs. GN wt: 147.0 ± 1 mmol/L, n=10, $^*p<0.05$) and control littermates (wt: 144 ± 1, n=9; $EP_1^{-/-}$: 144 ± 1 mmol/L, n=10) (Figure 6.13). Under conditions requiring greater sodium reabsorption, the activity of collecting duct epithelial sodium channels (ENaC) increases. Guan and colleagues demonstrated that PGE_2 activation of the EP_1 receptor *inhibits* sodium reabsorption (30). In contrast, Stock et al., showed that when mice lacking the EP_1 receptor were placed on sodium deficient diet, they observed additional drop in blood pressure, suggesting that the EP_1 receptor *promotes* sodium reabsorption in order to maintain ECFV (77). Our data show that under GN conditions, $EP_1^{-/-}$ mice have elevated sodium levels in their urine compared to their GN wt mice (GN $EP_1^{-/-}$: 145 ± 48 mmol/L, n=11 vs. GN wt: 46 ± 5 mmol/L, n=11; $^*p<0.05$) and control groups (wt: 109 ± 12 mmol/L, n=11 ; $EP_1^{-/-}$: 81 ± 18, mmol/L, n=11, *p<0.05) (Figure 6.13). Decreased sodium reabsorption, and consequently elevated serum potassium, suggests that GN $EP_1^{-/-}$ mice are unable to maintain their ECFV, thus contributing to the decline in their GFR. Consistent with this notion, GN $EP_1^{-/-}$ mice exhibited greater weight loss than did GN wt (GN $EP_1^{-/-}$: -11.0± 1.2 %, n=17 vs. GN wt: -1.8 ± 1.0 %, n=17; $^*p<0.05$) and control mice (wt: 0.4 ± 0.5 %

n=11; $EP_1^{-/-}$: 4.4 ± 1.6 %, n=11, *p<0.05) (Figure 6.14). These results provide further evidence for increased severity of renal impairment in GN $EP_1^{-/-}$ mice and imply a role for this receptor subtype in tempering the progression of GN.

Figure 6.12 Urine Osmolality Levels in GN WT and GN $EP_1^{-/-}$ GN Mice.

Day 7 following anti-GBM injections, urine osmolality was determined by freezing point depression. GN wt and GN $EP_1^{-/-}$ mice displayed significantly lower urine osmolality levels compared to control groups (*$p<0.05$). Furthermore, GN $EP_1^{-/-}$ mice demonstrated significantly lower osmolality levels than GN wt mice (*$p<0.05$). Values presented are the means ± S.E.M in mmol/L.

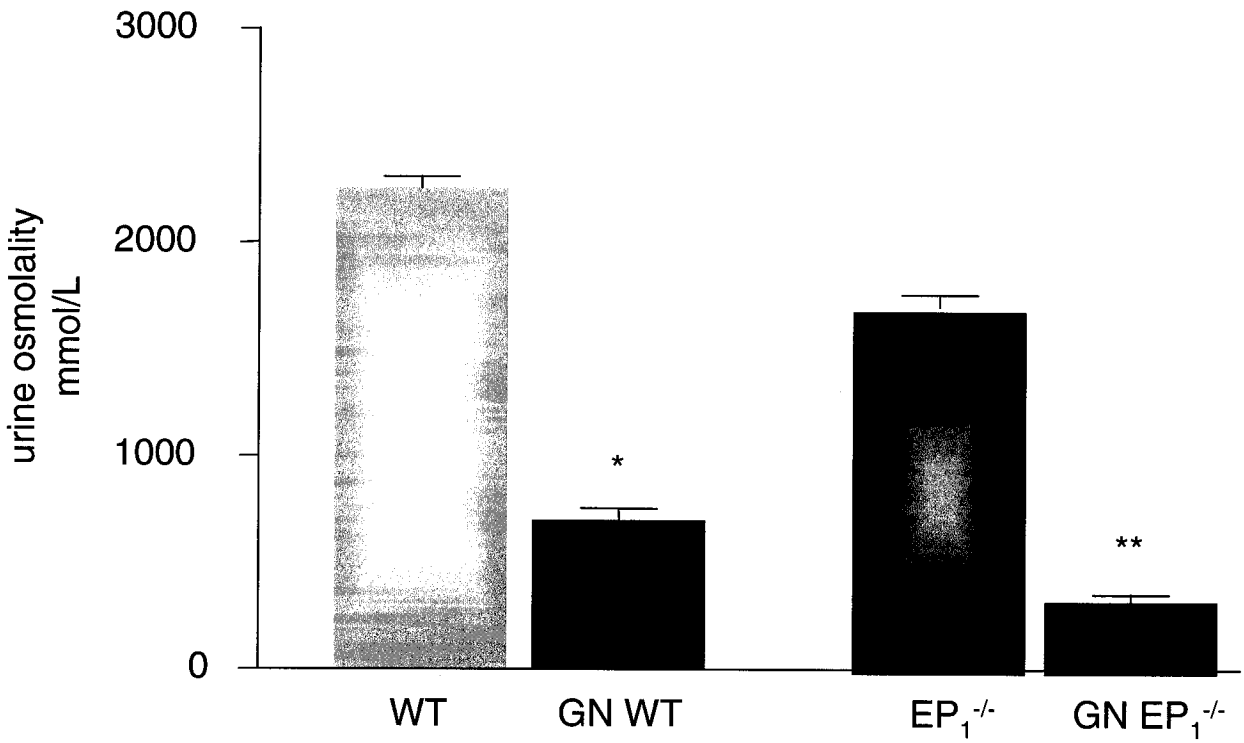
3000
2000
1000
0
urine osmolality
mmol/L
*
**
WT
GN WT
EP1-/-
GN EP1-/-

Figure 6.13 Serum and Urinary Na^+ Concentration in GN WT and GN $EP_1^{-/-}$ Mice.

Day 7 following anti-GBM injections, **A.** spot urine samples were analyzed for Na^+ content by flame photometry. GN $EP_1^{-/-}$ mice displayed significantly higher urinary Na^+ levels than GN wt mice and control groups (*$p<0.05$). **B.** Day 7 following anti-GBM injections, serum obtained by cardiac puncture was analyzed for potassium using a Beckman LX-20 instrument. GN $EP_1^{-/-}$ mice displayed significantly higher serum Na^+ concentration than GN wt and control mice (*$p<0.05$). Values presented are the means ± S.E.M in mmol/L.

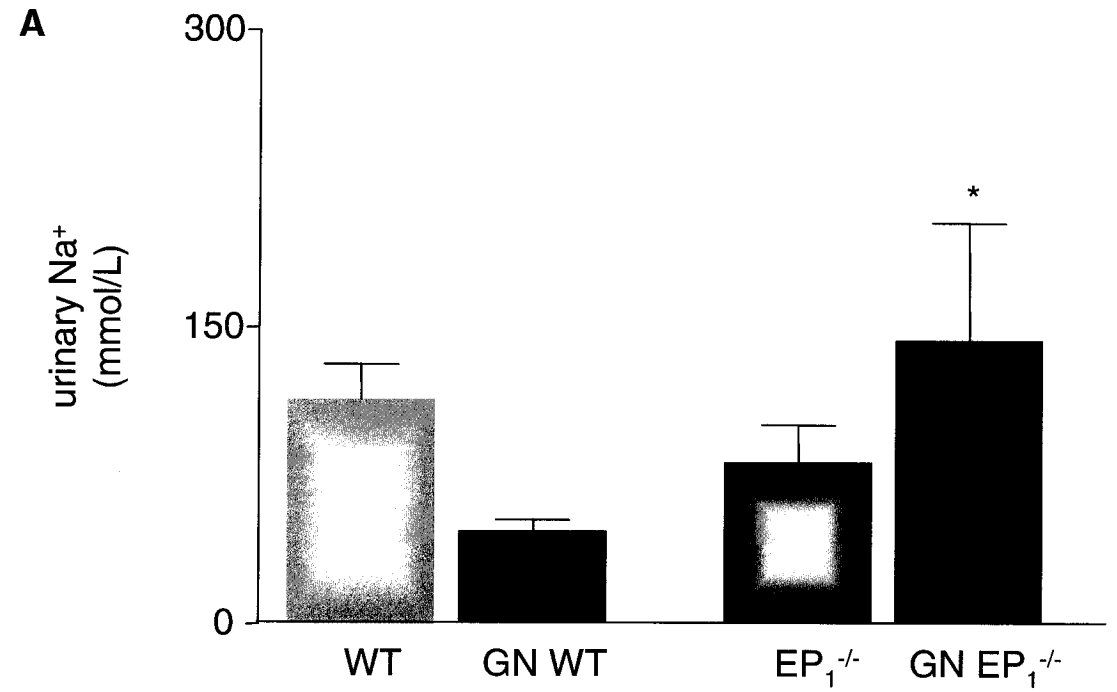
A
300
150
0
urinary Na+
(mmol/L)
*
WT
GN WT
EP1-/-
GN EP1-/-

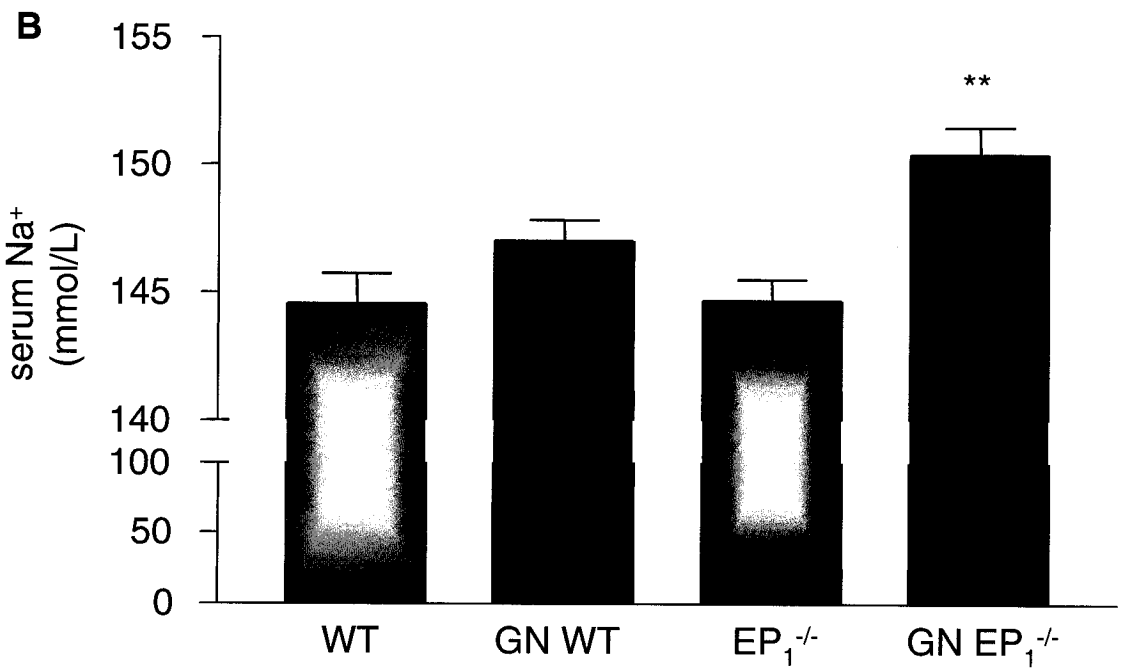
B
155
150
145
140
100
50
0
serum Na+
(mmol/L)
**
WT
GN WT
EP1-/-
GN EP1-/-

Figure 6.14 Percent Change in Body Weight for GN WT and GN $EP_1^{-/-}$ Mice.

Body weights were measured daily following anti-GBM injections. Values are expressed as the percent change in body weight between day 0 and the maximal body weight loss. This day was usually day 5. Results revealed that GN $EP_1^{-/-}$ mice displayed significantly greater body weight loss compared to GN wt mice and control groups (*$p<0.05$). Values presented are the means ± S.E.M. in percent change.

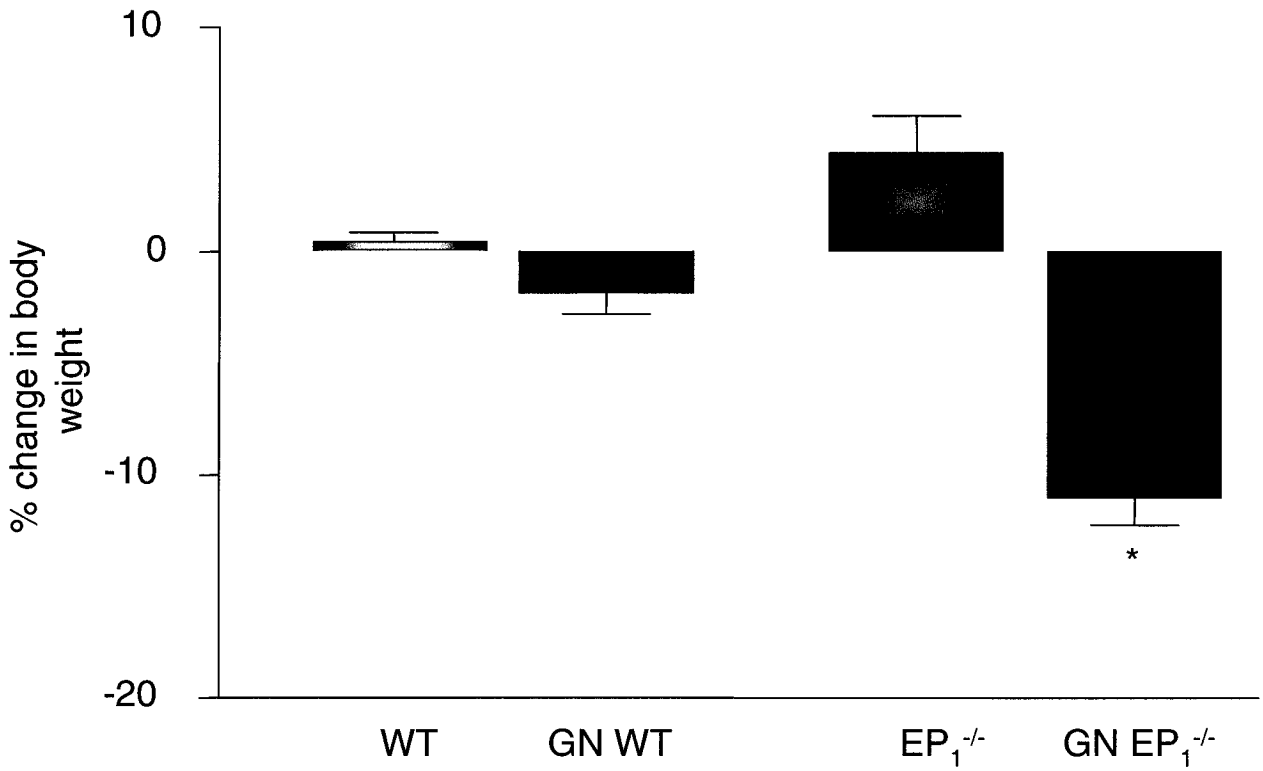
10
0
-10
-20
% change in body weight
*
WT
GN WT
EP1-/-
GN EP1-/-

6.1.4 EP $_1^{-/-}$ Mice Exhibit Normal Na^+ Excretion in Response to Changes in Dietary Na^+

To determine if $EP_1^{-/-}$ mice have a defect in their ability to maintain sodium balance, wt and $EP_1^{-/-}$ mice were fed control, low sodium (LS) and high sodium (HS) diets. Initially mice were fed a normal diet containing 0.4% sodium content. This was followed by a period of 7 days during which the mice were restricted to a LS diet containing <0.02% sodium. In some experiments LS fed mice were water deprived (WD) for up to 48 hrs after day 7. Throughout the period of study, mice were monitored in metabolic cages for urine output, urine osmolality, blood pressure, and urine sodium levels.

Urine output (LS wt: 0.04 ± 0.01ml/g, n=12 vs. LS $EP_1^{-/-}$: 0.05 ± 0.01 ml/g, n=12), water intake (LS wt: 0.38 ± 0.02, ml/g, n=12 vs. LS $EP_1^{-/-}$: 0.38 ± 0.02 ml/g, n=12), and blood pressure (LS wt: 104 ± 1 mmHg, n=9 vs. LS $EP_1^{-/-}$: 101 ± 1 mmHg, n=9) did not differ between LS wt and LS $EP_1^{-/-}$ mice (Figure 6.15). Serum aldosterone levels were equally elevated in both LS groups, as expected (LS wt: 376 ± 50 pg/ml, n=5 vs. LS $EP_1^{-/-}$: 396 ± 142 pg/ml, n=5) compared to control mice (wt: 136 ± 90 pg/ml, n=5 vs. $EP_1^{-/-}$: 139 ± 19 pg/ml, n=5). Urine sodium content (LS $EP_1^{-/-}$: 9.3 ± 2.3 mmol/L, n=16 vs. LS wt: 4.6 ± 1.3 mmol/L, n=16; $^*p<0.05$) was slightly higher in the LS $EP_1^{-/-}$ group (Figure 6.15). However, urine osmolality in LS $EP_1^{-/-}$ mice ($EP_1^{-/-}$: 2241 ± 90 mmol/L, n=10 vs. LS $EP_1^{-/-}$: 2098 ± 103 mmol/L n=10, $^*p<0.05$) did not increase as in LS wt mice (wt: 2375 ± 62 mmol/L, n=10 vs. LS wt: 2914 ± 99 mmol/L, n=10, $^*p<0.05$) (Figure 6.16).

When mice were water deprived for 24hrs, urine osmolalities rose dramatically (LS wt: 2914 ± 99 n=10 vs. WD wt: 3825 ± 107, n=10, mmol/L $^{*}p<0.05$). However, urine osmolalities in WD $EP_1^{-/-}$ did not reach levels achieved by WD wt mice (WD wt: 3825 ± 107 n=10 vs. WD $EP_1^{-/-}$: 3047 ± 161 n=10, mmol/L $^{*}p<0.05$). Body weights decreased equally among WD wt and WD $EP_1^{-/-}$ mice (WD wt: -9.5 ± 0.5 %, n=10 vs. WD $EP_1^{-/-}$: -8.0 ± 0.5 %, n=10) (Figure 6.16).

Mice were then placed on a HS diet containing 4% NaCl for 7 days. Mice were monitored in metabolic cages for urine output, urine osmolality, blood pressure, and urine sodium levels. Throughout the 7 day study on the HS diet, wt and $EP_1^{-/-}$ mice showed similar changes in water intake (HS wt: 0.27 ± 0.02 ml/g, n=6 vs. HS $EP_1^{-/-}$:0.29 ± 0.03 ml/g, n=6) and urine output levels (HS wt: 0.08 ± 0.02 ml/g, n=8 vs. HS $EP_1^{-/-}$:0.07 ± 0.02, ml/g, n=8) (Figure 6.17). Urine osmolality decreased in both groups on a HS diet, however no significant differences were observed between them (HS wt: 1847 ± 115 mmol/L, n=6 vs. HS $EP_1^{-/-}$: 1822 ± 84 mmol/L, n=6) (Figure 6.17). Furthermore, urine sodium content increased equally as expected, among HS wt and HS $EP_1^{-/-}$ mice (HS wt: 317 ± 27 mmol/L, n=10 vs. HS $EP_1^{-/-}$: 291 ± 28 mmol/L, n=10) (Figure 6.17). Equal but small elevations in blood pressure were seen suggesting that both groups are able to adapt equally to changes in sodium diet (HS wt: 101 ± 1 mmHg, n=10 vs. HS $EP_1^{-/-}$: 99 ± 1 mmHg, n=10) (Figure 6.17). Lastly, serum aldosterone levels were reduced equally between the two groups compared to control groups (wt: 165 ± 81 pg/ml, n=6 vs. HS wt: 90 ± 15 pg/ml, n=6;

$EP_1^{-/-}$: 166 ± 17, n=5 vs. HS $EP_1^{-/-}$: 54 ± 11 pg/ml, n=6; *$p<0.05$) as expected (Figure 6.17).

Figure 6.15 WT and $EP_1^{-/-}$ Mice - Phenotypic Characteristics on a Low Sodium Diet.

LS fed $EP_1^{-/-}$ mice displayed significantly higher urine Na^+ concentrations compared to LS wt mice (*$p<0.05$). However there was no significant differences observed in blood pressure (mmHg), urine output (ml/g), and water intake (ml/g) between LS $EP_1^{-/-}$ and LS wt mice. Serum aldosterone levels were equally elevated in both groups compared to control fed mice (*$p<0.05$). Values presented are the means ± S.E.M.

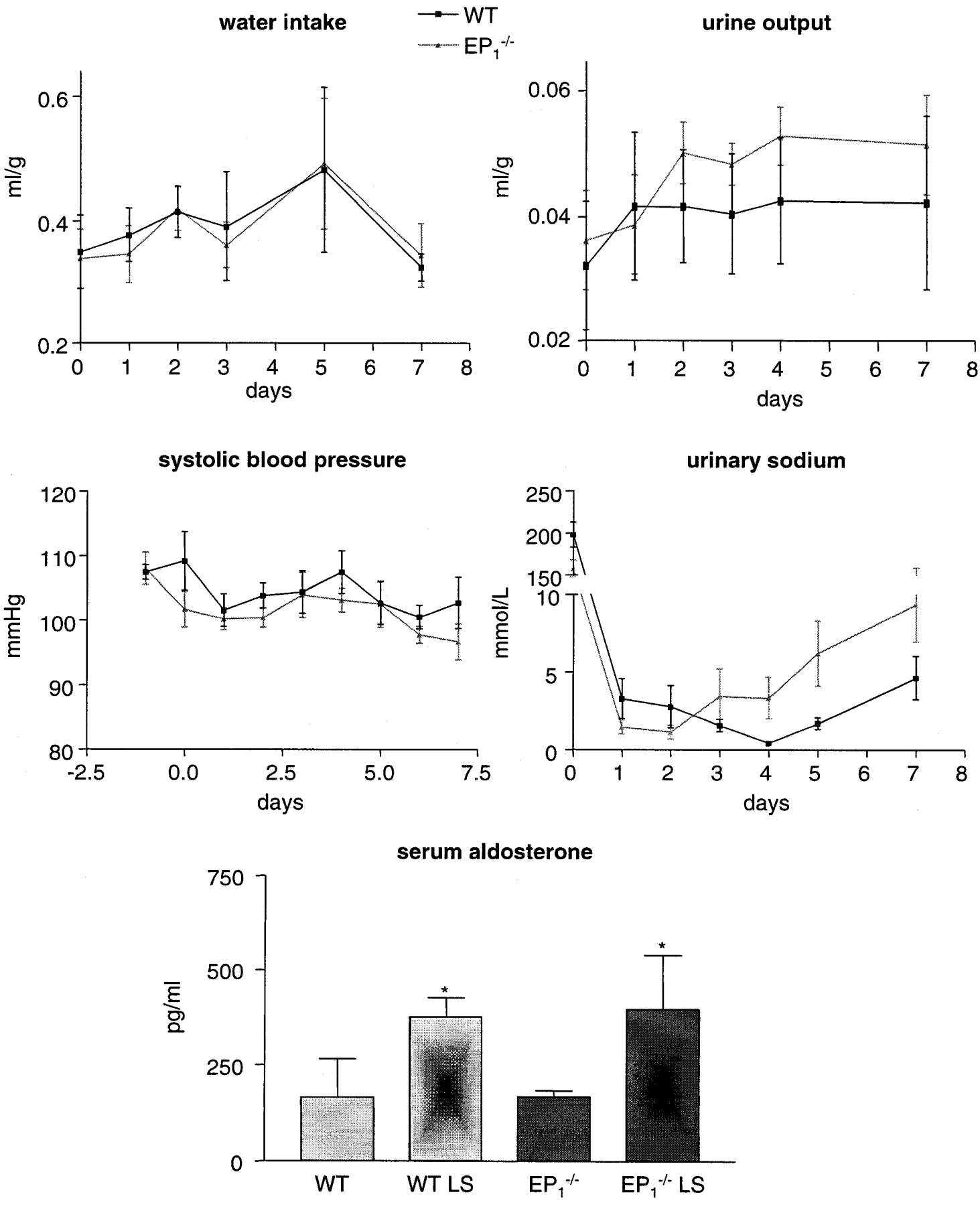
water intake
WT
EP1-/-
ml/g
0.6
0.4
0.2
0 1 2 3 4 5 6 7 8
days
urine output
ml/g
0.06
0.04
0.02
0 1 2 3 4 5 6 7 8
days
systolic blood pressure
mmHg
120
110
100
90
80
-2.5 0.0 2.5 5.0 7.5
days
urinary sodium
mmol/L
250
200
150
10
5
0
0 1 2 3 4 5 6 7 8
days
serum aldosterone
pg/ml
750
500
250
0
*
*
WT
WT LS
EP1-/-
EP1-/- LS

Figure 6.16 Phenotypic Characteristics of Na^+ and Water Deprived WT and $EP_1^{-/-}$ Mice.

LS wt and WD wt mice displayed **A.** significantly higher urine osmolality (mmol/L) compared to wt mice (*$p<0.05$). Furthermore, WD $EP_1^{-/-}$ mice displayed significantly higher urine osmolality (mmol/L) compared $EP_1^{-/-}$ and LS $EP_1^{-/-}$ mice (*$p<0.05$). **B.** Changes in body weight were equally reduced in WD mice compared to control mice (*$p<0.05$). Values presented are the means ± S.E.M.

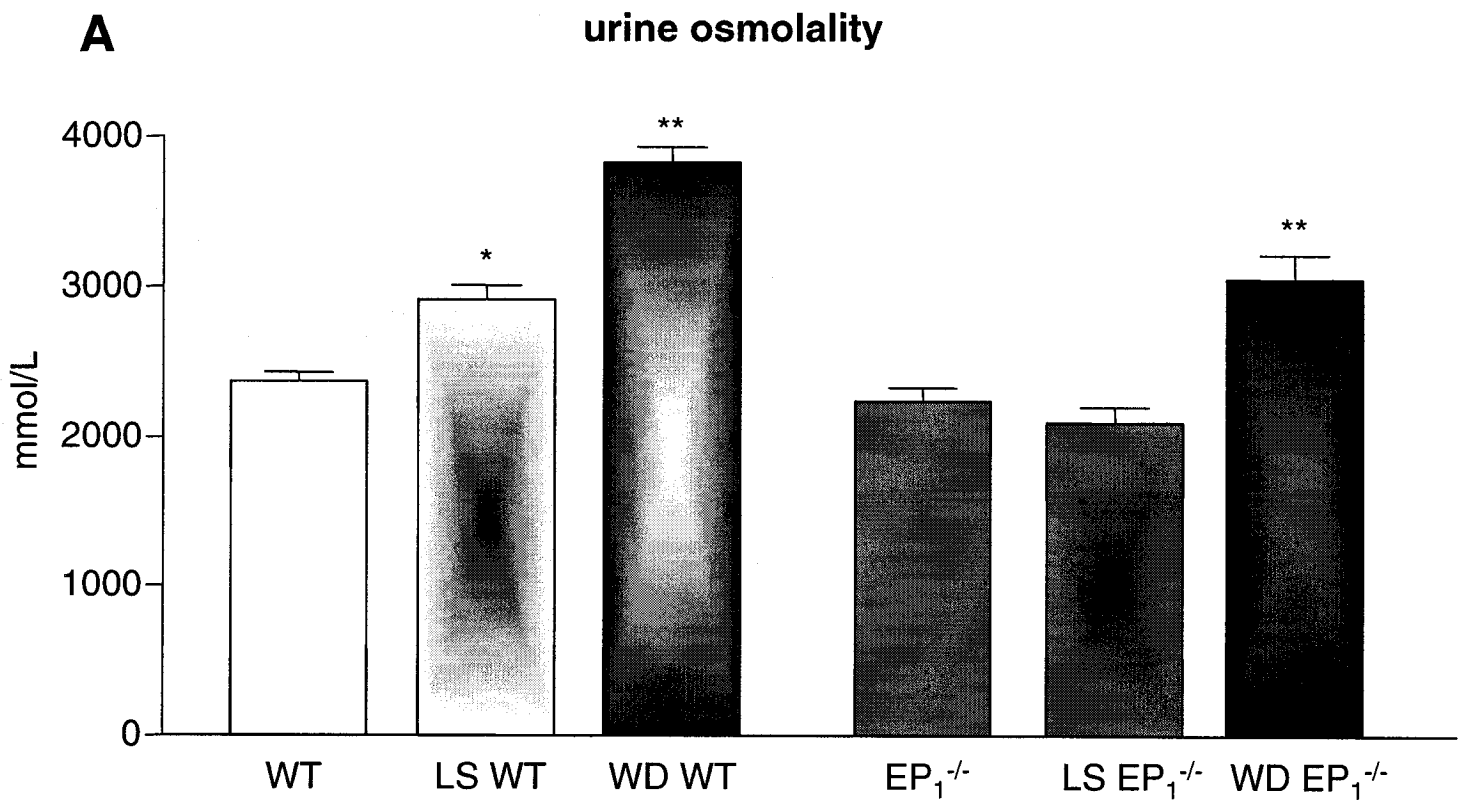
A
urine osmolality
4000
3000
2000
1000
0
mmol/L
**
*
**
WT
LS WT
WD WT
EP1-/-
LS EP1-/-
WD EP1-/-

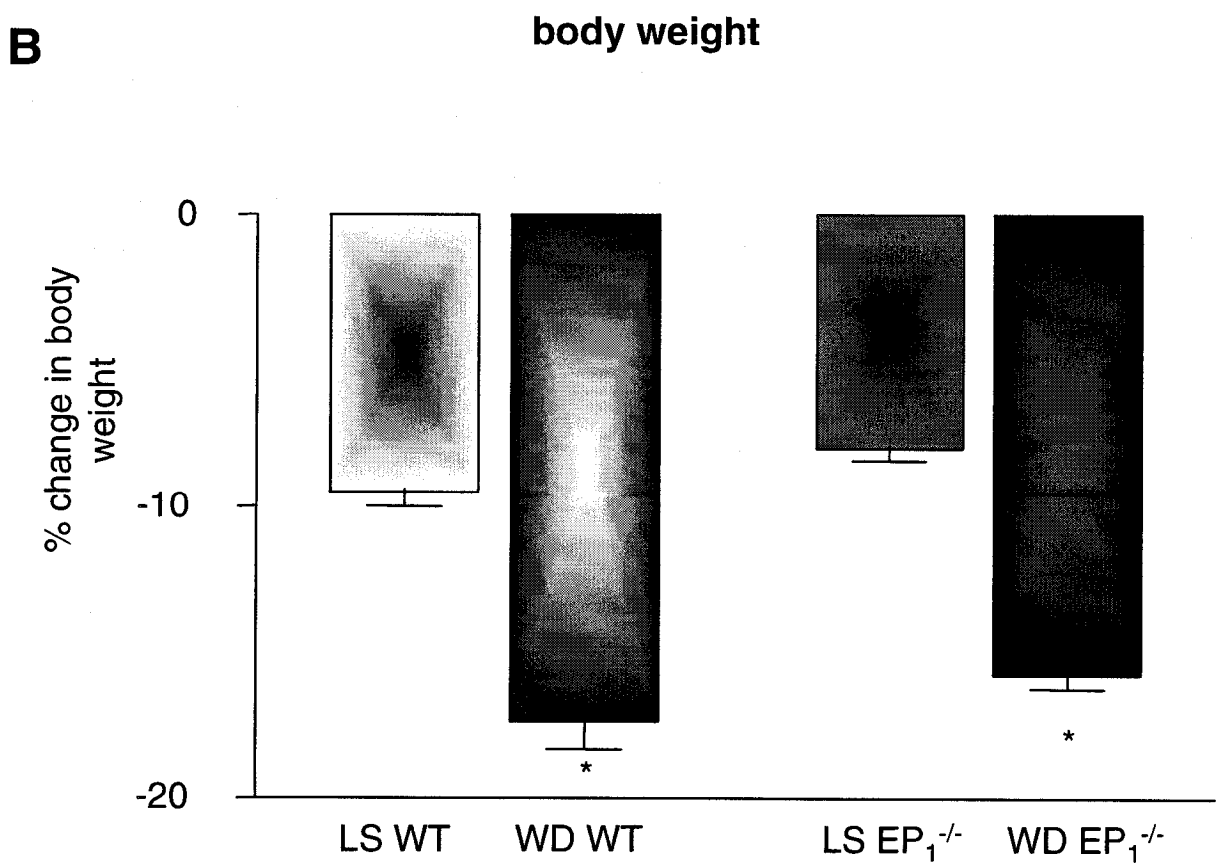
B
body weight
0
-10
-20
% change in body weight
*
*
LS WT
WD WT
LS EP1-/-
WD EP1-/-

Figure 6.17 WT and $EP_1^{-/-}$ Mice - Phenotypic Characteristics on a High Sodium Diet.

HS $EP_1^{-/-}$ mice displayed no significant differences in urine output (ml/g), water intake (ml/g), urine osmolality (mmol/L), urine Na^+ concentration (mmol/L) and blood pressure (mmHg) compared to HS wt mice. HS wt and HS $EP_1^{-/-}$ mice displayed equally reduced serum aldosterone (pg/ml) compared to control groups (*$p<0.05$). Values presented are the means ± S.E.M.

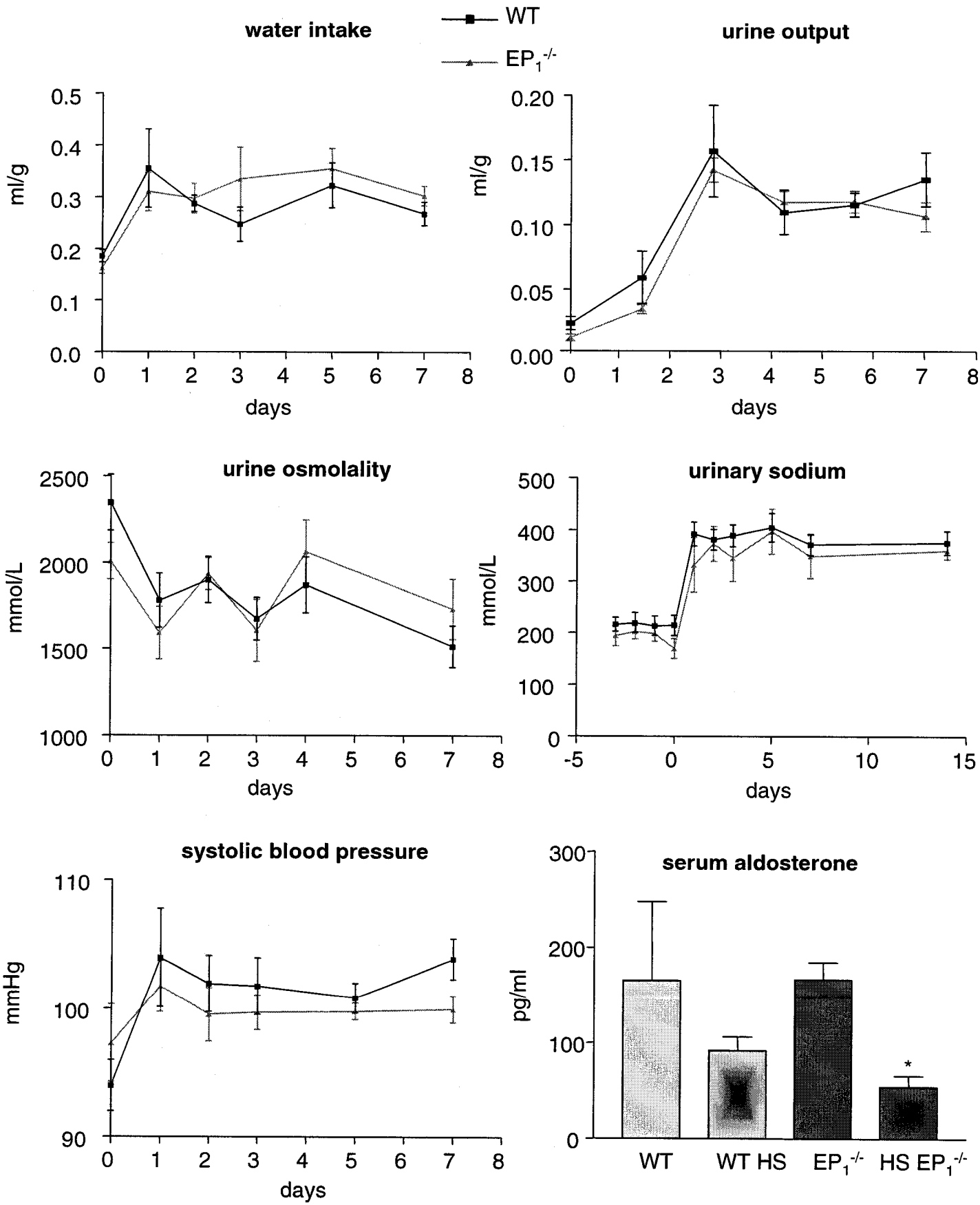
WT
EP1-/-
water intake
ml/g
0.5
0.4
0.3
0.2
0.1
0.0
0 1 2 3 4 5 6 7 8
days
urine output
ml/g
0.20
0.15
0.10
0.05
0.00
0 1 2 3 4 5 6 7 8
days
urine osmolality
mmol/L
2500
2000
1500
1000
0 1 2 3 4 5 6 7 8
days
urinary sodium
mmol/L
500
400
300
200
100
0
-5 0 5 10 15
days
systolic blood pressure
mmHg
110
100
90
0 1 2 3 4 5 6 7 8
days
serum aldosterone
pg/ml
300
200
100
0
*
WT
WT HS
EP1-/-
HS EP1-/-

6.2 GN INDUCES DIFFERENTIAL REGULATION OF EP_4 RECEPTOR EXPRESSION IN WT AND $EP_1^{-/-}$ MICE.

6.2.1 Elevated EP_4 Receptor Expression in GN wt and GN $EP_1^{-/-}$ Mice

Changes in EP receptor expression levels may underlie some of the effects seen in GN in response to PGE_2 production such as glomerular damage, proteinuria and reduced GFR. In order to determine whether altered expression of EP receptor subtypes accompanies the onset of GN, total kidney EP receptor mRNA expression levels in both control and nephritic mice were quantified by real-time RT-PCR using EP-specific TaqMan probes. Results indicate that when normalized to GAPDH mRNA, EP_1 EP_2 and EP_3 receptor mRNA expression levels were not significantly different between control and GN mice groups (GN wt: EP_1, 1.5 ± 0.3 fold above control; EP_2, 1.7 ± 0.3 fold above control, EP_3, 0.7 ± 0.1 fold of control n=12; GN $EP_1^{-/-}$: EP_2, 1.6 ± 0.2 fold above control; EP_3 0.6 ± 0.1 fold of control, n=12). In contrast, EP_4 mRNA levels were significantly elevated in the kidney of GN wt mice (EP_4, 4.1 ± 0.4 fold above control, n=12; $*p<0.05$) compared to control (Figure 6.18). Furthermore, kidney EP_4 receptor mRNA expression levels in GN $EP_1^{-/-}$ mice were significantly higher compared to GN wt mice (GN $EP_1^{-/-}$: 8.6±0.2 fold above control, vs. GN wt: 4.1 ±0.4 fold above control, n= 9; $*p<0.05$) (Figure 6.18). These results suggest a potential role for the renal induction of the EP_4 receptor in mice under nephritic conditions.

Figure 6.18 Total Kidney EP Receptor mRNA Expression Levels in WT and $EP_1^{-/-}$ Mice Under GN Conditions.

Total kidney mRNA was isolated from adult mice seven days after receiving the anti-GBM antibody. When normalized to GAPDH GN wt and GN $EP_1^{-/-}$ mice exhibited significant elevations in kidney mRNA EP_4 receptor expression levels compared to control groups. Furthermore, GN $EP_1^{-/-}$ mice displayed significantly higher EP_4 receptor mRNA expression than GN wt mice (*$p<0.05$). However, EP_1, EP_2 and EP_3 receptor mRNA expression was no different among GN groups. Values presented are the means ± S.E.M.

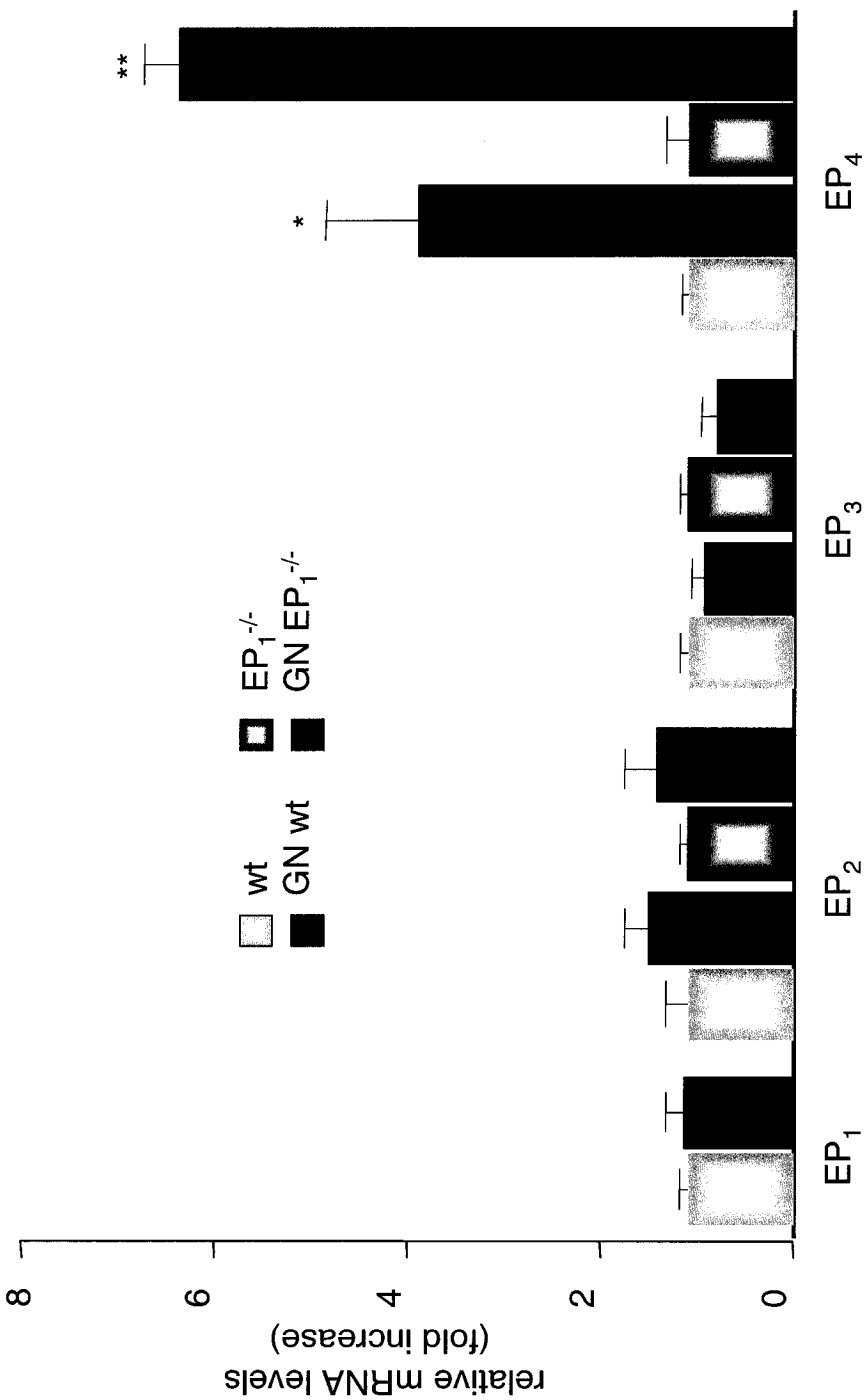
relative mRNA levels
(fold increase)
0
2
4
6
8
wt
GN wt
EP1-/-
GN EP1-/-
EP1
EP2
EP3
EP4
*
**

6.2.2 Localization of Elevated EP_4 Receptor Expression Under GN Conditions in Wt and $EP_1^{-/-}$ Mice

In order to localize EP_4 receptor elevations, different kidney regions, including cortex, outer medulla, inner medulla and papilla, were dissected from kidneys of control and GN mice. EP_4 receptor mRNA expression levels in both control and GN groups were quantified by real-time RT-PCR. Results indicate that there were no significant elevations in EP_4 receptor mRNA expression in outer medullary regions (GN wt: 0.9 ± 0.1 fold of control, n=5; GN $EP_1^{-/-}$: 1.2 ± 0.1 fold above control, n=5) and isolated glomeruli (GN wt: 0.5 ± 0.1 fold of control, n=5; GN $EP_1^{-/-}$: 0.6 ± 0.1 fold of control, n=5) of both groups (Figure 6.19). In contrast, increases in EP_4 receptor expression were found in both GN groups in the inner medullary region (GN wt: 1.6 ± 0.1 fold above control, n=5 *p<0.05; GN $EP_1^{-/-}$:1.9 ± 0.2 fold above control, n=5; *p<0.05) (Figure 6.19). Furthermore, significant elevations in EP_4 receptor mRNA expression were found in the papillary region of the kidney in GN wt mice but not in GN $EP_1^{-/-}$ mice (GN wt: 2.2 ± 0.4 fold above control, n=5 vs. GN $EP_1^{-/-}$: 0.5± 0.1 fold of control, n=5; *p<0.05) (Figure 6.19). Furthermore, EP_4 receptor mRNA expression levels were significantly elevated in cortical regions of GN $EP_1^{-/-}$ mice compared to GN wt mice (GN $EP_1^{-/-}$: 2.7 ± 0.5 fold above control, n=5 vs. GN wt: 1.5 ± 0.2 fold above control, n=5; *p<0.05) (Figure 6.19). Elevated EP_4 receptor mRNA expression in the inner medulla, papillary and cortical regions of both GN groups suggests that these sites may be involved in mediating some of the effects seen in GN.

Figure 6.19 Spatial EP_4 Receptor mRNA Expression Levels in Control and GN Mouse Kidneys.

Day 7 following anti-GBM injection **A.** GN $EP_1^{-/-}$ mice displayed increased cortical EP_4 receptor mRNA levels (*$p<0.05$). **B.** In contrast, EP_4 receptor mRNA levels were significantly elevated in the papillary region of GN wt mice compared to GN $EP_1^{-/-}$ mice (*$p<0.05$). **C.** Furthermore, significant EP_4 receptor expression elevations were observed in the inner medullary regions of GN mice compared to control groups (*$p<0.05$) However, there were no significant changes of EP_4 receptor expression in the outer medullary regions **D.** and glomeruli **E.** of both groups. Values presented are the means ± S.E.M.

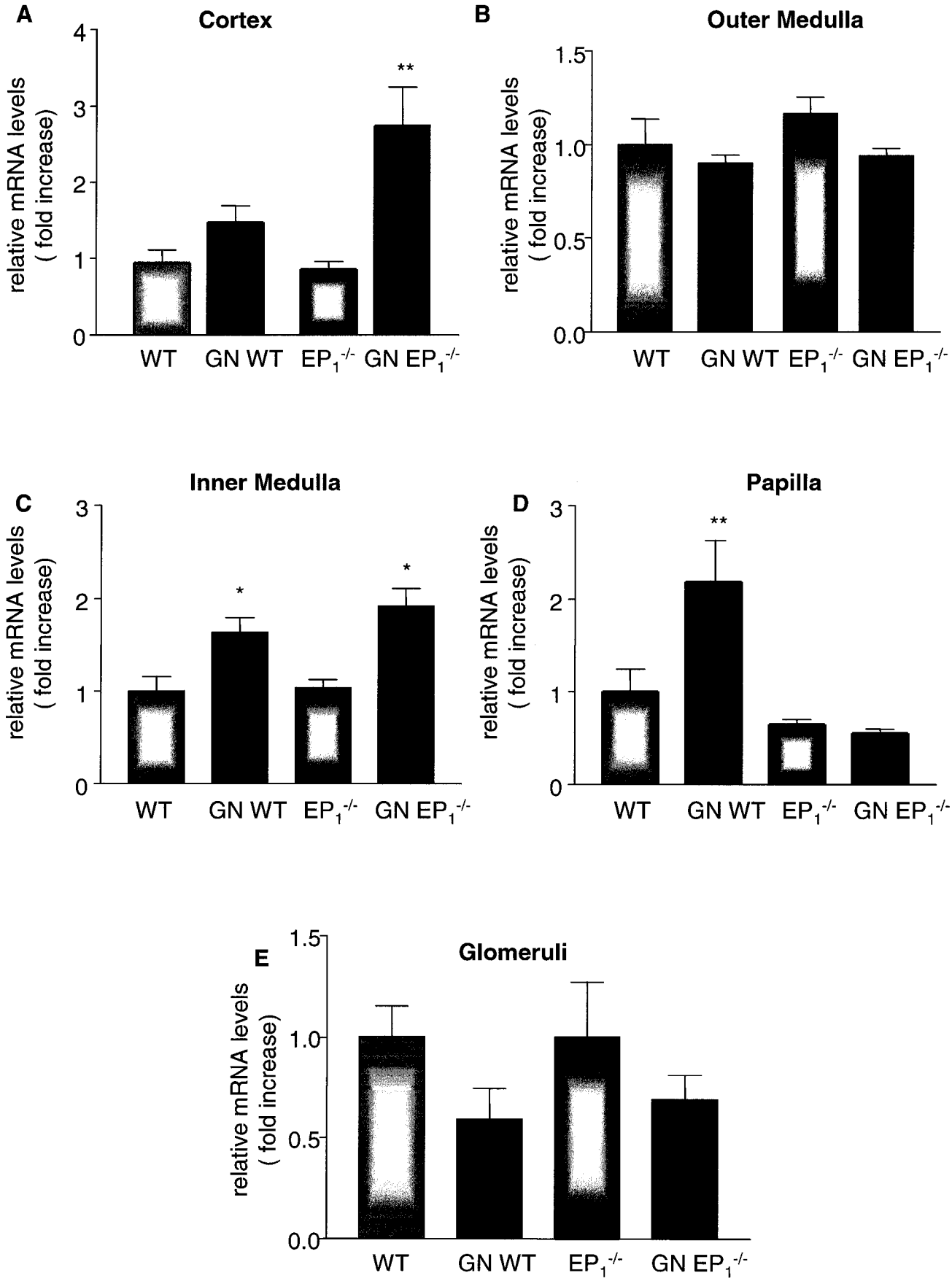
A
Cortex
relative mRNA levels
(fold increase)
4
3
2
1
0
**
WT
GN WT
EP1-/-
GN EP1-/-
B
Outer Medulla
relative mRNA levels
(fold increase)
1.5
1.0
0.5
0.0
WT
GN WT
EP1-/-
GN EP1-/-
C
Inner Medulla
relative mRNA levels
(fold increase)
3
2
1
0
*
*
WT
GN WT
EP1-/-
GN EP1-/-
D
Papilla
relative mRNA levels
(fold increase)
3
2
1
0
**
WT
GN WT
EP1-/-
GN EP1-/-
E
Glomeruli
relative mRNA levels
(fold increase)
1.5
1.0
0.5
0.0
WT
GN WT
EP1-/-
GN EP1-/-

7 DISCUSSION

7.1 INDUCTION OF GN IN WT MICE

Over the past forty years, several species, including sheep (8, 75), rat (8), and mouse (4), have been used to develop models of glomerulonephritis induced by the injection of antibodies raised against the glomerular basement membrane. Original studies by Steblay (1962) demonstrated that sheep immunized with isolated human GBM developed crescentic glomerulonephritis (75). The induction of experimental anti-GBM glomerulonephritis in mice has proved to be an excellent model of the human disease. Avisthi *et al.* first showed that mice immunized with bovine GBM in Freund's complete adjuvant developed circulating and deposited anti-GBM antibodies on the GBM, accompanied by crescentic GN (crescent-shaped abnormalities) (7, 75).

The model currently used in our laboratory has been previously characterized by other investigators (11, 65) correlating several key disease parameters with those of the human disease, including proteinuria, mesangial cell matrix accumulation, and elevated prostaglandin synthesis (46, 76). The induction of GN in preimmunized c57Bl6 mice was achieved by a single injection of anti-GBM antibody (kindly provided by Drs. Munger and Badr, Emory University). The onset of nephritis led to albuminuria (Figure 6.2) accompanied by elevated serum cholesterol, triglycerides, creatinine, urea (Figures 6.3, 6.4), and a decrease in serum albumin. Elevated urinary albumin, combined with decreased serum albumin, are indications of a defective

glomerular permeability barrier – a classic hallmark of renal glomerular disorders. Furthermore, elevated serum cholesterol and triglycerides reflect impairment of enzymes controlling their biosynthesis (72, 82).

The measurement of GFR is commonly used to assess renal function. GFR is an indication of the renal clearance of a given substance from plasma and is calculated according to the following formula:

$$GFR = [Urinary\ Cr] * [Vol.\ urine] / [Plasma\ Cr]$$

When an adequate volume of urine is obtained, creatinine (Cr) clearance is routinely used to measure GFR in clinical practice. However, under nephritic conditions where urine output is minimal, calculating GFR using the above formula is not possible. We therefore used serum levels of creatinine and urea as indirect indices of GFR. Elevated levels of both markers suggest a decreased GFR. Indeed, the study of kidney function began with the measurement of urea. In 1827, Richard Bright observed that urea accumulated in the blood of patients with decreased urine concentration, proteinuria and diseased kidneys. Serum [urea] is a semi-quantitative estimate of GFR (64). With a molecular weight of 60 Da, urea is freely filtered through the glomerulus; however it can also be readily reabsorbed along the nephron back into the circulation, resulting in underestimation of the true GFR. Creatinine, a small (113 Da) metabolic product of creatine and phosphocreatine, is also freely

filtered by the glomerulus. Small amounts of creatinine are secreted by the nephron resulting in an overestimation of GFR. Although an ideal endogenous marker for accurately measuring GFR has yet to be discovered, the large elevations in serum urea and creatinine (as observed in our mouse model of GN), are adequate semi-quantitative indicators of a reduced GFR.

Histological changes were also observed in GN animals. The presence of increased mesangial matrix and dilated tubules containing proteinaceous material were found upon examination of kidneys from GN mice (Figure 6.5). As in the human disease, the presence of protein accumulation in tubular sites in GN mice suggests severe disruption of the permeability barrier.

In summary, our *in vivo* murine model of GN was successfully induced in mice. Because of its simplicity, reproducibility, and phenotypic similarity to the human disease, we believe this model to be a valuable tool enabling *in vivo* analysis of this disease, including an investigation of the role of PGE_2 acting through the EP receptor subtypes.

Table 7.1 GN-Induced Phenotypic Characteristic in WT Mice.

Qualitative summary of the relevant findings in our anti-GBM model in WT mice.

GN-Induced Phenotypic Characteristics in WT Mice

	GN wt
body weight	↓
serum creatinine	↑
serum urea	↑
serum K^+	↑
serum Na^+	↑
urine osmolality	↓
albuminuria	Yes

7.2 PROGRESSION OF GLOMERULONEPHRITIS IN $EP_1^{-/-}$ MICE

During the pathogenesis of glomerulonephritis, the biosynthesis of PGE_2 has important implications for renal function including the regulation of glomerular permselectivity, fluid/electrolyte balance, RBF and GFR (53, 54). The significance of this eicosanoid in the nephritic kidney is illustrated by the occurrence of both beneficial and undesirable renal effects associated with the use of NSAIDs, which block prostaglandin synthesis. For example, NSAIDs (such as aspirin, ibuprofen etc.) are known to reduce glomerulopathy-associated proteinuria, however their use is precluded due to their propensity to severely reduce RBF/GFR and alter Na^+ reabsorption along the nephron. Since PGE_2 levels rise in GN, it is reasonable to suggest that one or more EP receptor subtypes might underlie some of the effects seen in the disease. Therefore, identifying which EP receptor subtype(s) contribute either *for* or *against* preservation of renal function will allow the development and implementation of more powerful and specific therapeutic strategies.

In order to begin to assess the role of the EP receptor subtypes in the progression of GN, anti-GBM GN was induced in mice with gene-targeted deletion of the EP_1 receptor (obtained from Dr. Matthew Breyer, Vanderbilt University).

7.2.1 The Role of the EP_1 Receptor in the Glomerulus under GN Conditions

The EP_1 receptor is expressed in mouse podocytes, as detected by RT-PCR (10). The podocytes are equipped with an elaborate intracellular contractile apparatus and are thought to respond to vasoactive hormones thereby altering the permeability of the glomerulus. Due to its vasoconstrictive actions, the EP_1 receptor may mediate potential effects of PGE_2 upon the size selectivity of the permeability barrier. Coupled with the fact that NSAIDs have well-known anti-proteinuric effects in glomerulonephritis, we tested the hypothesis that GN mice lacking the EP_1 receptor would demonstrate increased glomerular permeability damage. However, we observed that urinary albumin levels-were elevated similarly in both GN $EP_1^{-/-}$ and GN wt mice (Figure 6.7) while histological analysis revealed equal glomerular damage (mesangial matrix accumulation) within both groups (Figure 6.8). We therefore conclude that glomerular expression levels of the EP_1 receptor are not sufficient to mediate any PGE_2 -induced permeability changes and glomerular damage in GN (10, 15).

In contrast to our findings, other studies have suggested that the PGE_2/EP_1 signaling pathway contributes to the pathogenesis of some renal disorders (55, 80). Makino and colleagues showed that an EP_1 antagonist prevented renal injury, including proteinuria, in streptozotocin (STZ)-induced diabetic rats (55). Furthermore, Suganami et al., demonstrated significantly reduced glomerular injury, including improvements in serum creatinine and proteinuria, in spontaneously hypertensive rats (SHR) treated with an EP_1 antagonist (80). The discrepancies

between these studies and ours may be due to incompatible disease-specific etiologies and/or species differences. It is interesting to note that both the diabetic and SHR models are characterized by glomerular hyperfiltration, while anti-GBM GN displays no such elevation in glomerular capillary pressures.

7.2.2 GN $EP_1^{-/-}$ Mice Displayed Reduced Blood Pressure

The expression of the EP_1 receptor in the peripheral vasculature suggests that it plays an important role in regulating blood pressure. Changes in blood pressure initiated by vasoconstrictive or vasodilatory effects can directly influence GFR. In the kidney, PGE_2 is known to exert both vasodilatory (24, 62) and vasoconstrictive actions (62). Furthermore, by inhibiting the synthesis of PGE_2, NSAIDs exacerbate hypertension in some individuals (13). The ability of PGE_2 to induce opposing effects on renal blood flow suggests the involvement of multiple EP receptors coupled to specific signaling pathways (62). Using a pharmacological approach with isolated rat preglomerular (afferent arteriole) vascular smooth muscle cells (VSMC), Purdy and Arendshorst showed that EP_4 receptors likely mediate the vasodilatory effects of PGE_2. Since EP_1 receptor expression was absent in preglomerular VSMC (62), it is likely that the EP_1 receptor is expressed preferentially in other renal vascular segments, including the efferent arterioles. Studies of $EP_1^{-/-}$ mice demonstrating reduced resting blood pressure (77) are consistent with the known vasoconstrictive actions of the EP_1 receptor.

7.2.3 GN $EP_1^{-/-}$ Mice Display an Impaired Ability to Maintain ECFV

As discussed earlier, NSAIDs, which block prostaglandin synthesis, can reduce proteinuria associated with a number of renal disorders. However, use of these drugs is restricted due to their undesirable renal side effects – including those contributing to the regulation of body fluid and electrolyte balance. Consistent with the notion of NSAID-induced blockade of PGE_2 biosynthesis contributing to these unwanted renal side effects, our data show that GN $EP_1^{-/-}$ mice display greater decreases in body weight compared to GN wt mice (Figure 6.14). The dramatic loss of body weight in GN $EP_1^{-/-}$ mice could be due to impairment of Na^+ / water reabsorption along the collecting tubule resulting in significant fluid loss. Maintenance of ECFV depends in part upon net renal Na^+ reabsorption and excretion. Since Na^+ is the major electrolyte in the body, its presence in the luminal fluid as well as the renal interstitium controls the transport of water. For example, excessive urinary loss of Na^+ results in a significant diuretic effect. Our results demonstrate that GN $EP_1^{-/-}$ mice displayed lower urine osmolalities (Figure 6.12) accompanied by elevated urinary and serum Na^+ concentrations (Figure 6.13). This hypovolemic hypernatremia in GN $EP_1^{-/-}$ mice was surprising given that the putative role of this receptor subtype in relation to Na^+ balance is thought to be natriuretic.

In vitro studies by Stokes and Kokko, were the first to demonstrate that PGE_2 decreases Na^+ reabsorption using isolated-perfused rabbit collecting duct (79). These studies were later corroborated by Hebert et al., who showed that Na^+ reabsorption by isolated-perfused rabbit collecting ducts is inhibited by PGE_2 (34). Furthermore, this

inhibitory action of PGE_2 on Na^+ transport is mediated by a calcium-coupled mechanism consistent with an EP_1-mediated signal transduction pathway (34). Lastly, Guan and colleagues showed that an EP_1 receptor antagonist abrogated PGE_2-stimulated increases in intracellular calcium in isolated rabbit collecting ducts thereby suggesting that the EP_1 receptor functions to inhibit Na^+ transport, and further supporting the notion of a natriuretic role for this receptor subtype (30).

In contrast to such *in vitro* studies, limited *in vivo* studies suggest an anti-natriuretic role for the EP_1 receptor (77). $EP_1^{-/-}$ mice fed a low Na^+ diet displayed reduced blood pressure and elevated plasma renin activity – consistent with a reduced extracellular fluid volume (77), implying an impaired ability to reabsorb Na^+ and hence water. In agreement with the hypovolemic hypernatremia observed in our GN $EP_1^{-/-}$ mice, Stock et al., suggest that the EP_1 receptor functions to promote Na^+ reabsorption (77). However such conclusions must be tempered by the possibility that under GN conditions, the putative natriuretic influence of the EP_1 receptor subtype may be superseded by other downstream mechanisms designed to promote water/sodium retention in the face of deteriorating tubular function. Irrespective of the precise relation of the EP_1 receptor to sodium homeostasis, nephritis in mice lacking this receptor subtype presented a serious challenge to these animals' capacity to maintain ECFV and urine concentrating ability.

7.2.4 $EP_1^{-/-}$ Mice Exhibit Normal Na^+ Excretion in Response to Changes In Dietary Na^+.

Our observation that GN $EP_1^{-/-}$ mice were unable to maintain adequate ECFV prompted us to directly investigate whether these mice could adapt to changes in dietary Na^+. Activation of the EP_1 receptor increases intracellular calcium levels and inhibits Na^+ reabsorption by *in vitro* microperfused rabbit collecting duct (30, 34), suggesting that renal EP_1 receptor activation might contribute to the natriuretic effects of PGE_2. On the basis of these findings, one would expect healthy, non-nephritic $EP_1^{-/-}$ mice to exhibit inappropriately enhanced urinary concentration. However, our data revealed that $EP_1^{-/-}$ mice maintained blood pressure and exhibited similar urinary Na^+ excretion as wt mice on a Na^+ restricted diet (Figure 6.15). In fact, the only clear difference was that $EP_1^{-/-}$ mice displayed a lower urine osmolality that remained unchanged in response to a Na^+-restricted diet (Figure 6.16). Furthermore, when mice were water deprived for 24hrs to assess if they could maximally concentrate their urine, urine osmolality did not rise to the same extent as their wt littermates (Figure 6.16). Taken together, these findings suggest a subtly impaired concentrating mechanism in otherwise healthy $EP_1^{-/-}$ mice. When allowed free access to drinking water, $EP_1^{-/-}$ mice may compensate to allow normal renal water excretion. Since the EP_3 receptor can also promote natriuresis and diuresis, this subtype might take over the function of the EP_1 receptor, thereby obscuring the phenotype. Evidence for this derives from studies showing that PGE_2 directly inhibits sodium transport in microperfused thick ascending limb and salt/water transport in collecting duct (29, 34, 35). These effects can be blocked by the G_i inhibitor, pertussis toxin – consistent with an EP_3-mediated signaling pathway (29). Taken together, the accumulated data

support a role for the EP_3 receptor as a natriuretic and diuretic effector - similar to that of the EP_1 receptor. It is interesting to note however, that mice lacking the EP_3 receptor exhibit normal urinary concentrating/diluting responses – suggesting that the EP_1 receptor assumes the natriuretic/diuretic role in the face of EP_3 receptor ablation.

Cyclooxygenase expression changes in different regions of the kidney with dietary salt intake (16, 32, 86). Studies by Yang et al., demonstrated using rats placed on varying Na^+ diets, that cortical COX-2 production is upregulated during volume depletion (i.e. low salt intake), whereas medullary COX-2 production increases in volume expansion (i.e. high salt in take), thus promoting the excretion of Na^+ and water (86).

Because COX-2 increases in the medullary collecting duct region under high salt conditions and that EP_1 receptor expression increases from cortex to the papilla, we assessed Na^+-fluid volume homeostasis in $EP_1^{-/-}$ mice fed a high salt diet. Our results showed that with high dietary sodium content, $EP_1^{-/-}$ mice increased urinary Na^+ levels, decreased urinary osmolality and maintained blood pressure similar to wt mice (Figure 6.17). As previously suggested it is likely that the renal actions of PGE_2 normally mediated by the EP_1 receptor have been co-opted by the EP_3 receptor in $EP_1^{-/-}$ mice in order to sustain natriuretic and diuretic actions demanded by a high salt diet.

On the basis of these results we conclude that healthy, non-nephritic mice lacking the EP_1 receptor are able to adequately maintain normal Na^+ homeostasis, but

display a subtle urinary concentrating defect. This concentrating defect may however, predispose $EP_1^{-/-}$ mice to a more severe renal phenotype with the induction of nephritis – rendering them extremely dehydrated and hypernatremic, not unlike the renal side effects encountered with NSAID usage in the context of GN.

7.2.5 GN Mice Display Enhanced EP_4 Receptor Expression in a Tissue-Specific Manner: Outer Medullary and Papillary Regions

Since the $EP_1^{-/-}$ mice displayed a physiologically relevant defect in urine concentrating ability, we investigated what might account for this difference. Our attention focused on the EP_4 receptor since a major role for this subtype in regulating renal water transport has been suggested (35, 67). PGE_2 stimulates water reabsorption in isolated rabbit collecting ducts (35, 67). These stimulatory effects of PGE_2 on water transport were not mimicked by butaprost, an EP_2 agonist, and could therefore be attributed to activation of the EP_4 receptor (67).

On the basis of the preceding functional considerations, we expected that GN mice would display elevated EP_4 receptor expression to stimulate water reabsorption and thereby compensate for the observed natriuresis and diuresis. The inner medullary and papillary regions of the kidney consist of cAMP-responsive nephron segments (i.e., collecting duct). It is well established that cAMP acts as the second messenger in response to EP_4 coupled G_s stimulated adenylyl cyclase activation (10, 18, 63). Interestingly, the EP_4-cAMP signaling pathway is shared with arginine-vasopressin (AVP) in the activation and insertion of AQP2 water channels to promote

water reabsorption along the collecting duct (23, 51, 67). Our data show that EP_4 receptor expression is significantly elevated in the inner medullary region of the kidney of GN wt and GN $EP_1^{-/-}$ mice (Figure 6.19). These findings imply that GN mice are likely responding to promote water reabsorption through EP_4- cAMP signaling pathway in order to correct for their concentrating defect brought about by nephritis-induced tubular necrosis and reduced GFR.

Interestingly, we also observed significant differences in papillary EP_4 receptor expression between GN wt and GN $EP_1^{-/-}$ mice. The papillary region of the collecting duct, where the highest expression of EP_1 receptors is found, regulates the final fine tuning of urine osmolality. Like the medullary collecting duct, the papillary collecting duct is composed predominately of cAMP-responsive principal cells (41). One would expect that part of the mechanism for maintaining ECFV in GN would be to employ a cAMP-activating EP_4 response along this segment to promote water reabsorption. This seemed to be the case in GN wt mice but not in GN $EP_1^{-/-}$ mice (Figure 6.19). This lack of papillary EP_4 receptor induction in GN $EP_1^{-/-}$ mice could account for their additional drop in urine osmolality.

How would the absence of EP_1 receptor expression negate a nephritis-induced papillary EP_4 receptor elevation? The expression of the EP_4 receptor may depend on EP_1 receptor stimulation. This interconnected relationship has been observed in other signaling pathways (31). Hamelink et al., demonstrated that the signaling activity of a neuropeptide found during brain development requires the coincident activation of two different second-messenger pathways, calcium influx and elevated cAMP.

Hypothetically speaking, in mice lacking the EP_1 receptor, PGE_2 would be unable to drive expression of the EP_4 gene, either directly or indirectly, thereby reducing the ability of PGE_2 to promote urine concentrating activities in the papilla. However, at this time there is no evidence to support this claim and further studies will be needed to uncover the precise mechanism (see Future Studies section).

7.2.6 Severe Hyperkalemia in GN $EP_1^{-/-}$ Mice

Acute renal insufficiency brought about by GN is often associated with reduced GFR and hyperkalemia. Rare cases of hyperkalemia associated with NSAIDs have been reported for human patients with GN (24, 27). Our GN $EP_1^{-/-}$ mice displayed severe hyperkalemia compared to GN wt mice (Figure 6.9). Maintenance of extracellular potassium balance is vital. High intracellular and low extracellular potassium concentrations are required to maintain normal cell excitability and muscle contraction, including that of the heart. In fact, hyperkalemia in human patients requires immediate intervention to prevent life-threatening heart arrhythmias. Several physiological systems are known to regulate K^+ homeostasis, including the renin-angiotensin system as well as serum [K^+] (28). Additionally, seminal studies by August and colleagues first demonstrated that K^+ excretion increases while Na^+ excretion decreases after subjects were given aldosterone injections (6). Aldosterone is secreted from the adrenal cortex in response to either angiotensin II or adrenocorticotropic hormone (ACTH) stimulation, acting upon the late distal nephron to stimulate Na^+ reabsorption at the expense of luminal K^+ secretion.

ACTH is stored in the anterior pituitary and its release is triggered in response to inflammatory stress. Studies assessing the effects of bacterial endotoxin in mice lacking the EP_1 receptor revealed that $EP_1^{-/-}$ mice had an impaired ACTH response (56). One hour after receiving LPS injections, $EP_1^{-/-}$ mice demonstrated significantly reduced plasma ACTH levels. We hypothesized that GN $EP_1^{-/-}$ mice may have an impaired ACTH response yielding low aldosterone levels, since previous studies identified the presence of endotoxin in anti-GBM serum (42). Although we did not test the anti-GBM antiserum used in the current studies for LPS content, our data nevertheless shows that serum aldosterone levels were suppressed to similar levels in GN wt and GN $EP_1^{-/-}$ animals (Figure 6.10). Thus, although reduced serum aldosterone levels likely contribute to elevated serum K^+ observed in both GN groups, they cannot account for the severe hyperkalemia observed in GN $EP_1^{-/-}$ mice.

Hyperkalemia has been associated with changes in vascular tone that control RBF and consequently GFR. Angiotensin II is a potent vasoconstrictor that is involved in mediating GFR (2). However recent studies have also implicated the vasoconstrictive and vasodilatory actions of prostaglandins in RBF and GFR regulation (38, 62). Using *in vivo* renal blood flow studies, PGE_2-treated rats displayed immediate vasoconstriction followed by a prolonged dilatory phase (62). Treatment with various $EP_{1\text{-}4}$ agonists suggested that the EP_1 receptor is the primary receptor mediating transient renal vasoconstriction, whereas the EP_4 receptor elicits vasodilatation in the renal vasculature (62). Interestingly, nephritic patients treated with NSAIDs, exhibited significant declines in GFR accompanied by hyperkalemia (52). Such observations are consistent with our data showing that GN $EP_1^{-/-}$ mice

displayed enhanced creatinine and urea levels as compared to GN wt mice (Figure 6.11), implying a greater drop in GFR and thus a more severe state of renal dysfunction. These effects on GFR suggest a role for the EP_1 receptor in adequately maintaining RBF under GN conditions.

7.2.7 GN Mice Display Enhanced EP_4 Receptor Expression in a Tissue-Specific Manner: Cortical Region

The preglomerular afferent and postglomerular efferent resistance vessels can respond to vasoconstrictive and vasodilatory hormones to modulate RBF and GFR. However, the available evidence indicates that the afferent arteriole has the greatest role in the control of the intrarenal hemodynamics (9, 22). The severe reduction in GFR observed in GN $EP_1^{-/-}$ mice prompted us to assess whether these mice maximize their intrarenal vasodilatory capacity through elevated EP_4 receptor expression in order to sustain GFR. Our results indicate that GN $EP_1^{-/-}$ mice had significant elevations in cortical EP_4 receptor expression compared to GN wt mice (Figure 6.19). Although we do not yet have direct evidence, by process of elimination (since EP_4 receptor expression does not change in the glomeruli of GN mice (Figure 6.19)), the afferent arteriole is the likely location of elevated EP_4 receptor expression. Studies by Ruan el al., showed that PGE_2 produces an increase in cAMP levels from isolated rat VSMC, suggesting a dominance of vasodilator EP receptors coupled to G_s proteins (66). Furthermore, studies of second messenger signal transduction indicate the presence of EP_4 and absence of EP_2 receptors in the afferent arteriole of rats (62), making the EP_4 receptor the primary vasodilatory receptor. The elevated expression of EP_4 receptors

in the cortex of GN $EP_1^{-/-}$ mice suggests that it is a key player in regulating RBF and consequently GFR in nephritic conditions. Our results also support the notion that the NSAID-induced reduction of RBF, frequently exhibited by patients with compromised renal function (e.g. glomerulonephritis) may be due to reduced stimulation of EP_1 receptors.

With a high probability that the EP_4 receptor transduces the protective vasodilator signal in the afferent arteriole, it is tempting to speculate that mice lacking the EP_1 receptor require enhanced vasodilatation to help maintain RBF and by extension - GFR.

Previous studies have shown that PGE_2 exerts a dilator effect on the afferent arteriole but not on the efferent arteriole of rabbit glomeruli (9, 22). Furthermore, Purdy et al., demonstrated that while the EP_1 receptor is also present in the afferent arteriole, it plays a weaker role compared with that of the prolonged vasodilatation mediated by EP_4 (62). These observations imply that the EP_1 receptor may have a more dominant role in other segments of the renal vasculature. One likely location would be at the efferent arteriole where it might act as a vasoconstrictor, buffering the drop in GFR during the progression of GN.

GFR is markedly reduced with the onset of glomerulonephritis (26, 58). The kidney counters this condition by increasing vasodilatation at the afferent arteriole, allowing RBF to increase. Simultaneously, vasoconstriction is triggered at the efferent arteriole in order to enhance filtration through the glomerulus in an attempt to

sustain GFR. Our data suggest that GN causes reductions in GFR that are more profound in GN $EP_1^{-/-}$ mice (Figure 6.13). Such differences may be reflective of an inability to constrict efferent arterioles and consequently counter the drop in GFR. We believe that mice lacking the EP_1 receptor may respond to this exacerbated GFR by promoting vasodilatation at the afferent arteriole, likely through the EP_4 receptor. If so, this would explain the elevated cortical EP_4 receptor expression observed in GN $EP_1^{-/-}$ mice and not GN wt mice (Figure 6.19).

7.3 FUTURE STUDIES

Our present study has assessed changes in mRNA expression, however the activity and function of the EP_4 receptor within the context of GN remains to be addressed. Three main approaches could be employed: 1) EP_4 protein expression/localization; 2) pharmacological blockade of this receptor subtype; and 3) the use of gene-targeted $EP_4^{-/-}$ mice.

EP_4 mRNA levels may not reflect the protein expression of this gene. At this time, the available EP_4 antibodies are inadequate in their specificity and are unable to detect the protein in kidney lysates - either by western, or through immunohistochemical approaches. Future work will require the development of more powerful and specific antibodies against this GPCR.

Similarly, the available EP_4 receptor antagonists exhibit limited specificity as well as questionable bio-efficacy – rendering them inappropriate for testing the role of this receptor subtype *in vivo*. Once again, future studies will require the synthesis of better agonists and antagonists.

Currently, the most powerful approach to assess the role of the EP_4 receptor in the progression of GN is through the use of gene-targeted knockout mice. However, the majority of $EP_4^{-/-}$ mice die shortly after birth from patent *ductus arteriosus* (71), making it impossible to address the function of such a gene in the adult mouse. To avoid such developmental defects our lab is currently generating podocyte-specific

deletion of the EP_4 receptor using the Cre/loxP system. Concurrent with the development of this line, our lab will also employ Myxovirus resistance-1-Cre recombinase mice (Mx1-Cre) (commercially available from Jackson Labs). Widespread Cre activity can be induced in a temporal manner upon injection of these mice with γ-interferon. Such an approach will facilitate the deletion of the EP_4 receptor in the glomeruli, vasculature as well as collecting duct (69).

As a continuation of my project, this future endeavor should address several questions that remain unanswered: 1) During the onset of glomerulonephritis, is the EP_4 receptor required to dilate the afferent arteriole and thus sustain GFR? 2) Does PGE_2, acting via the EP_4 receptor, promote urinary concentrating processes in the late collecting duct in order to counter the loss of tubular function as GN progresses?

Taken together, our data strengthen the argument that an understanding of the role of PGE_2 and its receptors in the nephritic kidney is an important area of research. Since NSAIDs (such as aspirin, ibuprofen etc.) reduce glomerulopathy-associated proteinuria – they would appear to be potentially useful therapeutics. However – as discussed repeatedly, their use is precluded by unwanted effects on RBF/GFR and Na^+ reabsorption. Therefore, identifying which EP receptor subtype(s) contribute either *for* or *against* preservation of renal function will allow for the development and implementation of more powerful and specific therapeutic strategies.

Table 7.2 GN Phenotypic Characteristics in WT and $EP_1^{-/-}$ Mice

Qualitative summary comparing the relevant findings in our anti-GBM model in both wt and $EP_1^{-/-}$ mice.

GN Phenotypic Characteristics in WT and EP $_1^{-/-}$ Mice

	GN wt	GN EP $_1^{-/-}$
body weight	↓	↓↓↓
serum creatinine	↑	↑↑↑
serum urea	↑	↑↑↑
serum K^+	↑	↑↑↑
serum Na^+	↑	↑↑
urine osmolality	↓	↓↓↓
albuminuria	Yes	Yes

Figure 6.20 Physiological Events Involved in the Induction of GN in $EP_1^{-/-}$ Mice

GN $EP_1^{-/-}$ mice displayed elevated EP_4 receptor expression in the afferent arteriole possibly to enhance vasodilatation in order to sustain GFR. GN $EP_1^{-/-}$ mice displayed significantly reduced urine osmolality perhaps due to their inability to elevate EP_4 receptor expression in the papillary region. Water reabsorption may be mediated by AQP2 channels through EP_4 signaling.

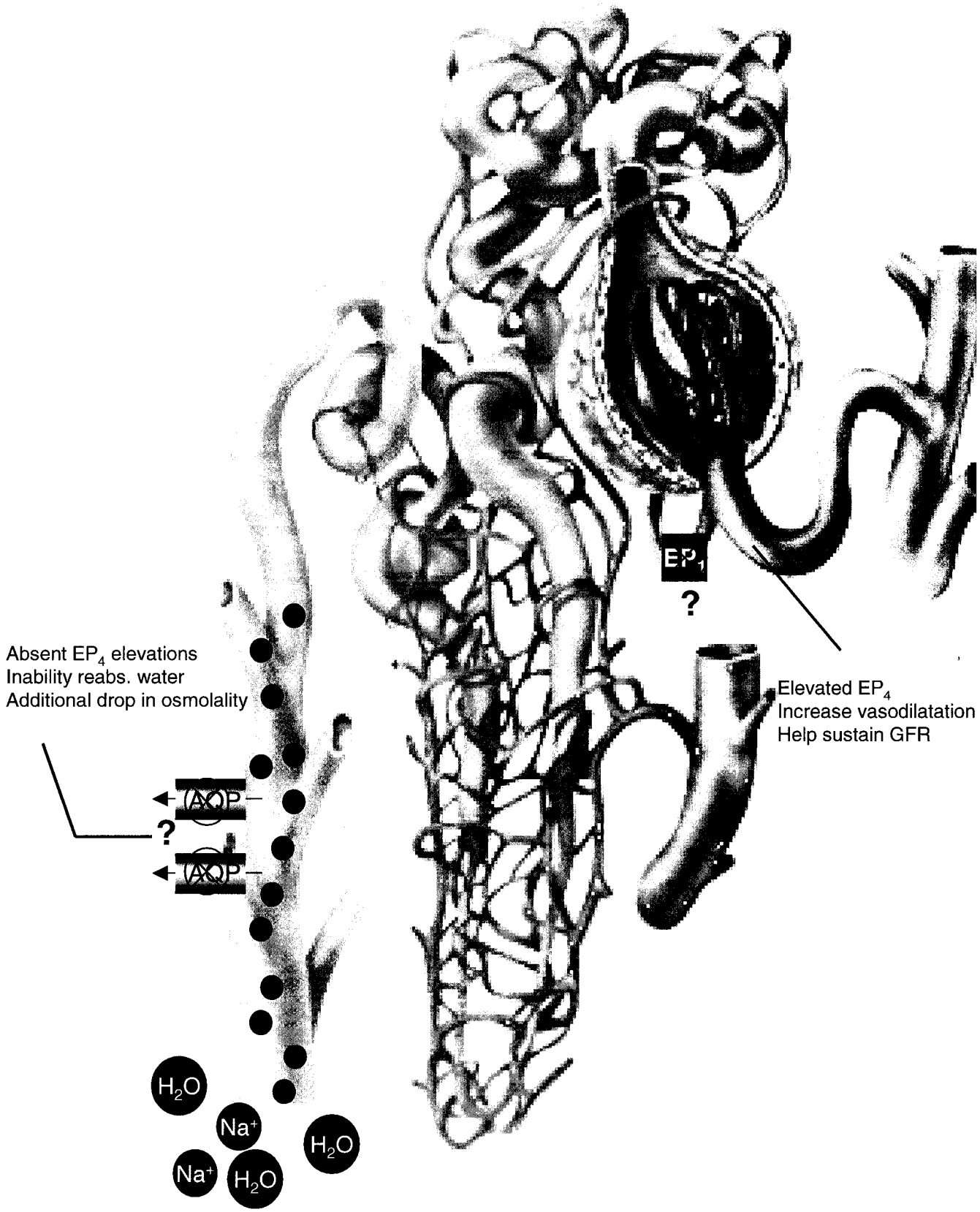
Absent EP_4 elevations
Inability reabs. water
Additional drop in osmolality
AQP
?
AQP
H_2O
Na^+
H_2O
Na^+
H_2O
EP_1
?
Elevated EP_4
Increase vasodilatation
Help sustain GFR

8 REFERENCES

1. **Anderson RJ, Berl T, McDonald KD, and Schrier RW.** Evidence for an in vivo antagonism between vasopressin and prostaglandin in the mammalian kidney. *J Clin Invest* 56: 420-426, 1975.

2. **Arendshorst WJ, Brannstrom K, and Ruan X.** Actions of angiotensin II on the renal microvasculature. *J Am Soc Nephrol* 10 Suppl 11: S149-161, 1999.

3. **Arisz L, Andres GA, and Brentjens JR.** The morphological basis of the glomerular permeability to proteins. *Ric Clin Lab* 7: 312-327, 1977.

4. **Assmann KJ, Tangelder MM, Lange WP, Schrijver G, and Koene RA.** Anti-GBM nephritis in the mouse: severe proteinuria in the heterologous phase. *Virchows Arch A Pathol Anat Histopathol* 406: 285-299, 1985.

5. **Audoly LP, Tilley SL, Goulet J, Key M, Nguyen M, Stock JL, McNeish JD, Koller BH, and Coffman TM.** Identification of specific EP receptors

responsible for the hemodynamic effects of PGE2. *Am J Physiol* 277: H924-930, 1999.

6. **August JT, Nelson DH, and Thorn GW.** Response of normal subjects to large amounts of aldosterone. *J Clin Invest* 37: 1549-1555, 1958.

7. **Avasthi PS, Avasthi P, Tokuda S, Anderson RE, and Williams RC, Jr.** Experimental glomerulonephritis in the mouse. I. The model. *Clin Exp Immunol* 9: 667-676, 1971.

8. **Badr KF, Schreiner GF, Wasserman M, and Ichikawa I.** Preservation of the glomerular capillary ultrafiltration coefficient during rat nephrotoxic serum nephritis by a specific leukotriene D4 receptor antagonist. *J Clin Invest* 81: 1702-1709, 1988.

9. **Baylis C, Deen WM, Myers BD, and Brenner BM.** Effects of some vasodilator drugs on transcapillary fluid exchange in renal cortex. *Am J Physiol* 230: 1148-1158, 1976.

10. **Bek M, Nusing R, Kowark P, Henger A, Mundel P, and Pavenstadt H.** Characterization of prostanoid receptors in podocytes. *J Am Soc Nephrol* 10: 2084-2093, 1999.

11. **Bird JE, Giancarli MR, Kurihara T, Kowala MC, Valentine MT, Gitlitz PH, Pandya DG, French MH, and Durham SK.** Increased severity of glomerulonephritis in C-C chemokine receptor 2 knockout mice. *Kidney Int* 57: 129-136, 2000.

12. **Braam B, Mitchell KD, Koomans HA, and Navar LG.** Relevance of the tubuloglomerular feedback mechanism in pathophysiology. *J Am Soc Nephrol* 4: 1257-1274, 1993.

13. **Brater DC.** Effect of indomethacin on salt and water homeostasis. *Clin Pharmacol Ther* 25: 322-330, 1979.

14. **Breyer MD and Breyer RM.** G protein-coupled prostanoid receptors and the kidney. *Annu Rev Physiol* 63: 579-605, 2001.

15. **Breyer MD, Davis L, Jacobson HR, and Breyer RM.** Differential localization of prostaglandin E receptor subtypes in human kidney. *Am J Physiol* 270: F912-918, 1996.

16. **Breyer MD and Harris RC.** Cyclooxygenase 2 and the kidney. *Curr Opin Nephrol Hypertens* 10: 89-98, 2001.

17. **Breyer MD, Jacobson HR, and Breyer RM.** Functional and molecular aspects of renal prostaglandin receptors. *J Am Soc Nephrol* 7: 8-17, 1996.

18. **Breyer RM, Davis LS, Nian C, Redha R, Stillman B, Jacobson HR, and Breyer MD.** Cloning and expression of the rabbit prostaglandin EP4 receptor. *Am J Physiol* 270: F485-493, 1996.

19. **Caulfield JP and Farquhar MG.** The permeability of glomerular capillaries to graded dextrans. Identification of the basement membrane as the primary filtration barrier. *J Cell Biol* 63: 883-903, 1974.

20. **Coleman RA and Kennedy I.** Characterisation of the prostanoid receptors mediating contraction of guinea-pig isolated trachea. *Prostaglandins* 29: 363-375, 1985.

21. **Coleman RA, Smith WL, and Narumiya S.** International Union of Pharmacology classification of prostanoid receptors: properties, distribution, and structure of the receptors and their subtypes. *Pharmacol Rev* 46: 205-229, 1994.

22. **Edwards RM.** Effects of prostaglandins on vasoconstrictor action in isolated renal arterioles. *Am J Physiol* 248: F779-784, 1985.

23. **Edwards RM, Jackson BA, and Dousa TP.** ADH-sensitive cAMP system in papillary collecting duct: effect of osmolality and PGE2. *Am J Physiol* 240: F311-318, 1981.

24. **Fierro-Carrion GA and Ram CV.** Nonsteroidal anti-inflammatory drugs (NSAIDs) and blood pressure. *Am J Cardiol* 80: 775-776, 1997.

25. **Fleming EF, Athirakul K, Oliverio MI, Key M, Goulet J, Koller BH, and Coffman TM.** Urinary concentrating function in mice lacking EP3 receptors for prostaglandin E2. *Am J Physiol* 275: F955-961, 1998.

26. **Friedman S, Strober S, Field EH, Silverman E, and Myers BD.** Glomerular capillary wall function in human lupus nephritis. *Am J Physiol* 246: F580-591, 1984.

27. **Galler M, Folkert VW, and Schlondorff D.** Reversible acute renal insufficiency and hyperkalemia following indomethacin therapy. *Jama* 246: 154-155, 1981.

28. **Giebisch GH.** A trail of research on potassium. *Kidney Int* 62: 1498-1512, 2002.

29. **Good DW and George T.** Regulation of HCO3- absorption by prostaglandin E2 and G proteins in rat medullary thick ascending limb. *Am J Physiol* 270: F711-717, 1996.

30. **Guan Y, Zhang Y, Breyer RM, Fowler B, Davis L, Hebert RL, and Breyer MD.** Prostaglandin E2 inhibits renal collecting duct Na+ absorption by activating the EP1 receptor. *J Clin Invest* 102: 194-201, 1998.

31. **Hamelink C, Lee HW, Chen Y, Grimaldi M, and Eiden LE.** Coincident elevation of cAMP and calcium influx by PACAP-27 synergistically regulates vasoactive intestinal polypeptide gene transcription through a novel PKA-independent signaling pathway. *J Neurosci* 22: 5310-5320, 2002.

32. **Harris RC and Breyer MD.** Physiological regulation of cyclooxygenase-2 in the kidney. *Am J Physiol Renal Physiol* 281: F1-11, 2001.

33. **Hebert RL, Breyer RM, Jacobson HR, and Breyer MD.** Functional and molecular aspects of prostaglandin E receptors in the cortical collecting duct. *Can J Physiol Pharmacol* 73: 172-179, 1995.

34. **Hebert RL, Jacobson HR, and Breyer MD.** Prostaglandin E2 inhibits sodium transport in rabbit cortical collecting duct by increasing intracellular calcium. *J Clin Invest* 87: 1992-1998, 1991.

35. **Hebert RL, Jacobson HR, Fredin D, and Breyer MD.** Evidence that separate PGE2 receptors modulate water and sodium transport in rabbit cortical collecting duct. *Am J Physiol* 265: F643-650, 1993.

36. **Honda A, Sugimoto Y, Namba T, Watabe A, Irie A, Negishi M, Narumiya S, and Ichikawa A.** Cloning and expression of a cDNA for mouse prostaglandin E receptor EP2 subtype. *J Biol Chem* 268: 7759-7762, 1993.

37. **Imig JD.** Eicosanoid regulation of the renal vasculature. *Am J Physiol Renal Physiol* 279: F965-981, 2000.

38. **Imig JD, Breyer MD, and Breyer RM.** Contribution of prostaglandin EP(2) receptors to renal microvascular reactivity in mice. *Am J Physiol Renal Physiol* 283: F415-422, 2002.

39. **Ishibashi R, Tanaka I, Kotani M, Muro S, Goto M, Sugawara A, Mukoyama M, Sugimoto Y, Ichikawa A, Narumiya S, and Nakao K.** Roles of prostaglandin E receptors in mesangial cells under high-glucose conditions. *Kidney Int* 56: 589-600, 1999.

40. **Jensen BL and Kurťz A.** Differential regulation of renal cyclooxygenase mRNA by dietary salt intake. *Kidney Int* 52: 1242-1249, 1997.

41. **Jo I, Harris HW, Amendt-Raduege AM, Majewski RR, and Hammond TG.** Rat kidney papilla contains abundant synaptobrevin protein that participates in the fusion of antidiuretic hormone-regulated water channel-containing endosomes in vitro. *Proc Natl Acad Sci U S A* 92: 1876-1880, 1995.

42. **Karkar AM and Rees AJ.** Influence of endotoxin contamination on anti-GBM antibody induced glomerular injury in rats. *Kidney Int* 52: 1579-1583, 1997.

43. **Kashtan CE.** Alport syndrome and thin glomerular basement membrane disease. *J Am Soc Nephrol* 9: 1736-1750, 1998.

44. **Katsuyama M, Ikegami R, Karahashi H, Amano F, Sugimoto Y, and Ichikawa A.** Characterization of the LPS-stimulated expression of EP2 and EP4 prostaglandin E receptors in mouse macrophage-like cell line, J774.1. *Biochem Biophys Res Commun* 251: 727-731, 1998.

45. **Katsuyama M, Nishigaki N, Sugimoto Y, Morimoto K, Negishi M, Narumiya S, and Ichikawa A.** The mouse prostaglandin E receptor EP2 subtype: cloning, expression, and northern blot analysis. *FEBS Lett* 372: 151-156, 1995.

46. **Kelley VE, Sneve S, and Musinski S.** Increased renal thromboxane production in murine lupus nephritis. *J Clin Invest* 77: 252-259, 1986.

47. **Kennedy CR, Zhang Y, Brandon S, Guan Y, Coffee K, Funk CD, Magnuson MA, Oates JA, Breyer MD, and Breyer RM.** Salt-sensitive hypertension and reduced fertility in mice lacking the prostaglandin EP2 receptor. *Nat Med* 5: 217-220, 1999.

48. **Khan RZ and Badr KF.** Endotoxin and renal function: perspectives to the understanding of septic acute renal failure and toxic shock. *Nephrol Dial Transplant* 14: 814-818, 1999.

49. **Kluth DC and Rees AJ.** Anti-glomerular basement membrane disease. *J Am Soc Nephrol* 10: 2446-2453, 1999.

50. **Kunapuli SP, Fen Mao G, Bastepe M, Liu-Chen LY, Li S, Cheung PP, DeRiel JK, and Ashby B.** Cloning and expression of a prostaglandin E receptor EP3 subtype from human erythroleukaemia cells. *Biochem J* 298 (Pt 2): 263-267, 1994.

51. **Kurokawa K and Massry SG.** Interaction between catecholamines and vasopressin on renal medullary cyclic AMP of rat. *Am J Physiol* 225: 825-829, 1973.

52. **Kutyrina IM, Androsova SO, Warshavskii VA, and Tareyeva IE.** Effects of indomethacin on the renal function and renin-aldosterone system in chronic glomerulonephritis. *Nephron* 32: 244-248, 1982.

53. **Lianos EA.** Biosynthesis and role of arachidonic acid metabolites in glomerulonephritis. *Nephron* 37: 73-77, 1984.

54. **Lianos EA, Andres GA, and Dunn MJ.** Glomerular prostaglandin and thromboxane synthesis in rat nephrotoxic serum nephritis. Effects on renal hemodynamics. *J Clin Invest* 72: 1439-1448, 1983.

55. **Makino H, Tanaka I, Mukoyama M, Sugawara A, Mori K, Muro S, Suganami T, Yahata K, Ishibashi R, Ohuchida S, Maruyama T, Narumiya S, and Nakao K.** Prevention of diabetic nephropathy in rats by prostaglandin E receptor EP1-selective antagonist. *J Am Soc Nephrol* 13: 1757-1765, 2002.

56. **Matsuoka Y, Furuyashiki T, Bito H, Ushikubi F, Tanaka Y, Kobayashi T, Muro S, Satoh N, Kayahara T, Higashi M, Mizoguchi A, Shichi H, Fukuda Y, Nakao K, and Narumiya S.** Impaired adrenocorticotropic hormone response to bacterial endotoxin in mice deficient in prostaglandin E receptor EP1 and EP3 subtypes. *Proc Natl Acad Sci U S A* 100: 4132-4137, 2003.

57. **Michael AF, Keane WF, Raij L, Vernier RL, and Mauer SM.** The glomerular mesangium. *Kidney Int* 17: 141-154, 1980.

58. **Myers BD, Okarma TB, Friedman S, Bridges C, Ross J, Asseff S, and Deen WM.** Mechanisms of proteinuria in human glomerulonephritis. *J Clin Invest* 70: 732-746, 1982.

59. **Nassar GM and Badr KF.** Novel approaches to treatment of glomerulonephritis. *J Nephrol* 11: 177-184, 1998.

60. **Nguyen M, Camenisch T, Snouwaert JN, Hicks E, Coffman TM, Anderson PA, Malouf NN, and Koller BH.** The prostaglandin receptor EP4 triggers remodelling of the cardiovascular system at birth. *Nature* 390: 78-81, 1997.

61. **Palmer LG.** Potassium secretion and the regulation of distal nephron K channels. *Am J Physiol* 277: F821-825, 1999.

62. **Purdy KE and Arendshorst WJ.** EP(1) and EP(4) receptors mediate prostaglandin E(2) actions in the microcirculation of rat kidney. *Am J Physiol Renal Physiol* 279: F755-764, 2000.

63. **Regan JW, Bailey TJ, Pepperl DJ, Pierce KL, Bogardus AM, Donello JE, Fairbairn CE, Kedzie KM, Woodward DF, and Gil DW.** Cloning of a novel human prostaglandin receptor with characteristics of the pharmacologically defined EP2 subtype. *Mol Pharmacol* 46: 213-220, 1994.

64. **Rickers H, Brochner-Mortensen J, and Rodbro P.** The diagnostic value of plasma urea for assessment of renal function. *Scand J Urol Nephrol* 12: 39-44, 1978.

65. **Robertson H, Wheeler J, and Morley AR.** Anti-glomerular basement membrane glomerulonephritis in the mouse: the role of macrophages. *Int J Exp Pathol* 76: 157-162, 1995.

66. **Ruan X, Chatziantoniou C, and Arendshorst WJ.** Impaired prostaglandin E(2)/prostaglandin I(2) receptor-G(s) protein interactions in isolated renal resistance arterioles of spontaneously hypertensive rats. *Hypertension* 34: 1134-1140, 1999.

67. **Sakairi Y, Jacobson HR, Noland TD, and Breyer MD.** Luminal prostaglandin E receptors regulate salt and water transport in rabbit cortical collecting duct. *Am J Physiol* 269: F257-265, 1995.

68. **Salama AD and Pusey CD.** Immunology of anti-glomerular basement membrane disease. *Curr Opin Nephrol Hypertens* 11: 279-286, 2002.

69. **Schneider A, Zhang Y, Guan Y, Davis LS, and Breyer MD.** Differential, inducible gene targeting in renal epithelia, vascular endothelium, and viscera of Mx1Cre mice. *Am J Physiol Renal Physiol* 284: F411-417, 2003.

70. **Scholkens BA, Jung W, Rascher W, Schomig A, and Ganten D.** Brain angiotensin II stimulates release of pituitary hormones, plasma catecholamines and increases blood pressure in dogs. *Clin Sci (Lond)* 59 Suppl 6: 53s-56s, 1980.

71. **Segi E, Sugimoto Y, Yamasaki A, Aze Y, Oida H, Nishimura T, Murata T, Matsuoka T, Ushikubi F, Hirose M, Tanaka T, Yoshida N, Narumiya S, and Ichikawa A.** Patent ductus arteriosus and neonatal death in prostaglandin receptor EP4-deficient mice. *Biochem Biophys Res Commun* 246: 7-12, 1998.

72. **Shearer GC, Stevenson FT, Atkinson DN, Jones H, Staprans I, and Kaysen GA.** Hypoalbuminemia and proteinuria contribute separately to reduced lipoprotein catabolism in the nephrotic syndrome. *Kidney Int* 59: 179-189, 2001.

73. **Silldorff EP, Yang S, and Pallone TL.** Prostaglandin E2 abrogates endothelin-induced vasoconstriction in renal outer medullary descending vasa recta of the rat. *J Clin Invest* 95: 2734-2740, 1995.

74. **Sonnenburg WK, Zhu JH, and Smith WL.** A prostaglandin E receptor coupled to a pertussis toxin-sensitive guanine nucleotide regulatory protein in rabbit cortical collecting tubule cells. *J Biol Chem* 265: 8479-8483, 1990.

75. **Steblay RW.** Glomerulonephritis induced in sheep by injections of heterologous glomerular basement membrane and Freund's complete adjuvant. *J Exp Med* 116: 253-272, 1962.

76. **Steinhauer HB, Batsford S, Schollmeyer P, and Kluthe R.** Studies on thromboxane B2 and prostaglandin E2 production in the course of murine autoimmune disease: inhibition by oral histidine and zinc supplementation. *Clin Nephrol* 24: 63-68, 1985.

77. **Stock JL, Shinjo K, Burkhardt J, Roach M, Taniguchi K, Ishikawa T, Kim HS, Flannery PJ, Coffman TM, McNeish JD, and Audoly LP.** The prostaglandin E2 EP1 receptor mediates pain perception and regulates blood pressure. *J Clin Invest* 107: 325-331, 2001.

78. **Stockand JD and Sansom SC.** Glomerular mesangial cells: electrophysiology and regulation of contraction. *Physiol Rev* 78: 723-744, 1998.

79. **Stokes JB and Kokko JP.** Inhibition of sodium transport by prostaglandin E2 across the isolated, perfused rabbit collecting tubule. *J Clin Invest* 59: 1099-1104, 1977.

80. **Suganami T, Mori K, Tanaka I, Mukoyama M, Sugawara A, Makino H, Muro S, Yahata K, Ohuchida S, Maruyama T, Narumiya S, and Nakao K.** Role of prostaglandin E receptor EP1 subtype in the development of renal injury in genetically hypertensive rats. *Hypertension* 42: 1183-1190, 2003.

81. **Ushikubi F, Segi E, Sugimoto Y, Murata T, Matsuoka T, Kobayashi T, Hizaki H, Tuboi K, Katsuyama M, Ichikawa A, Tanaka T, Yoshida N, and Narumiya S.** Impaired febrile response in mice lacking the prostaglandin E receptor subtype EP3. *Nature* 395: 281-284, 1998.

82. **Vaziri ND.** Molecular mechanisms of lipid disorders in nephrotic syndrome. *Kidney Int* 63: 1964-1976, 2003.

83. **Vinen CS and Oliveira DB.** Acute glomerulonephritis. *Postgrad Med J* 79: 206-213; quiz 212-203, 2003.

84. **Watabe A, Sugimoto Y, Honda A, Irie A, Namba T, Negishi M, Ito S, Narumiya S, and Ichikawa A.** Cloning and expression of cDNA for a mouse EP1 subtype of prostaglandin E receptor. *J Biol Chem* 268: 20175-20178, 1993.

85. **Wise H and Jones RL.** Characterization of prostanoid receptors on rat neutrophils. *Br J Pharmacol* 113: 581-587, 1994.

86. **Yang T, Singh I, Pham H, Sun D, Smart A, Schnermann JB, and Briggs JP.** Regulation of cyclooxygenase expression in the kidney by dietary salt intake. *Am J Physiol* 274: F481-489, 1998.